Doctor thesis

Electromagnetic instability in AdS/CFT

Akihiko Sonoda[♡*]

[♡] *Department of Physics, Osaka University, Toyonaka, Osaka 560-0043, Japan*

[*]Email: sonoda(at)het.phys.sci.osaka-u.ac.jp

Abstract

Vacuum instability, leading to pair creation or annihilation of charged particles, is one of the most interesting physical quantities in particle physics. Among various kinds of particle creation process, quark antiquark pair creation is particularly interesting. Quarks and gluons are described by quantum chromodynamics(QCD), which has a strong gauge coupling constant at low energy, popularly known as the asymptotic freedom. In QCD, perturbation is not a good approximation at low energy, thus it is essential to evaluate non-perturbative effects. To calculate QCD vacuum decay rates, we need to calculate non-perturbative effects about the QCD vacuum.

In 1951, Schwinger obtained a creation rate of an electron positron pair by evaluating an imaginary part of an effective Lagrangian of electromagnetism, after integrating out the electron positron fields. We expect that, in a similar manner, a creation rate of a quark antiquark pair is obtained by computing an imaginary part of an effective Lagrangian of QCD coupled to external electromagnetism. The Lagrangian includes quark fields, gluon fields and the electromagnetic fields as the external fields. The obstacle for the calculation for the quark case is that the gauge coupling of QCD is so strong that we have to evaluate quark antiquark 1-loop Feynman diagrams at all orders in gluon interaction, so any diagramatic calculations do not help at low energy. For this problem, recently developed notion known as a gauge/gravity duality, or equivalently AdS/CFT correspondence, can be applied, since the duality indeed enables us to calculate a strong coupling limit of quantum field theories.

In 1997, Maldacena conjectured that $\mathcal{N} = 4$ supersymmetric Yang-Mills theory is equivalent to type IIB superstring theory on $\mathrm{AdS}_5 \times S^5$. In particular, the large N_c limit and the strong coupling limit of the $\mathcal{N} = 4$ supersymmetric Yang-Mills theory is conjectured to be equivalent to classical type IIB supergravity on $\mathrm{AdS}_5 \times S^5$. The limits are a large N_c limit and a large 't Hooft coupling limit, $\lambda \equiv g^2 N_c \gg 1$. Non-perturbative quantum quantities of the large N_c strongly coupled gauge theory are derived from the classical gravity. However, how to calculate the creation rate of the quark antiquark have not been established yet in the AdS/CFT. In this doctor thesis, we study the vacuum instability in large N_c strongly coupled gauge theories.

Recently, research on the vacuum instability in strongly coupled gauge theories by the AdS/CFT have started. Semenoff and Zarembo derived the creation rate of the quark antiquark pair from a classical minimal surface of an open string world-

sheet with the AdS/CFT. With a different method, Hashimoto and Oka derived the creation rate of the quark antiquark pair from the imaginary part of a probe D-brane action in electric fields.

In our paper [arXiv:1403.6336 [hep-th]], by using the AdS/CFT, we obtained the creation rate of the quark antiquark pair in electromagnetic fields in the $\mathcal{N} = 4$ $SU(N_c)$ supersymmetric Yang-Mills theory with $\mathcal{N} = 2$ hypermulitiplets in the fundamental representation. By using the Hashimoto-Oka conjecture, we evaluated the imaginary part of the D7-brane DBI action in not only constant electric fields but also constant magnetic fields. We found that the creation rate of the massless quark antiquark diverges at zero temperature, while it becomes finite if we introduce a nonzero temperature. In the case of massive quarks, the creation rate of the quark antiquark in the $\mathcal{N} = 2$ SQCD was found to coincide with the creation rate of the hypermultiplets in the $\mathcal{N} = 2$ supersymmetric QED, in the massless limit.

In our paper [arXiv:1412.4254 [hep-th]], we worked on the decay rate in the Sakai-Sugimoto model. We evaluated the imaginary part of the D8-brane DBI action in the constant electromagnetic fields. We obtained the creation rate of the massless quark antiquark is non-zero at zero temperature, and also found a critical electric field in the confining phase of the strongly coupled large N_c gauge theory. The imaginary part of the D8-brane DBI action increases according to the increase of a magnetic field parallel to an electric field. On the other hand, the imaginary part decreases when we increase the magnetic field perpendicular to an electric field. We found that a critical electric field exists to have an imaginary part for the DBI action, and its value is identical to a QCD string tension between the quark and antiquark.

In our paper [arXiv:1504.07836 [hep-th]], we found that the energy distribution of the meson at highly excited modes is subject to a power law under a constant electric field or in a nonzero temperature. In general, any energy distribution is expected to obey a Maxwell-Boltzmann distribution. However, in our analysis using the AdS/CFT correspondence, at a critical electric field, we found that the energy distribution of the mesons at high excited modes is proportional to a power of the meson mass. The power is found to be equal to -4 in the case of the gravity dual of the D3-D5 brane system.

In this doctor thesis, we explain the contents explained above, with reviews on related subjects.

Contents

1 Introduction

In particle physics, creation of a particle antiparticle pair by vacuum decay is an important notion. Schwinger effect is one of the most interesting phenomena in particle physics. The phenomenon describes a pair creation of charged particles under an external field such as a strong electromagnetic field. Schwinger obtained the creation rate of an electron positron pair by evaluating the imaginary part of an effective Lagrangian of electromagnetism, after integrating out the electron positron fields [1, 2]. This rate Γ is derived as $\Gamma \sim \exp\left(-\pi m_e^2/eE\right)$ whose exponent has a negative power for the gauge coupling e. Thus, the Schwinger effect is a non-perturbative effect. Here, m_e is the electron mass and E is a constant electric field. A critical electric field is $E_{\rm cr} \sim m_e^2 c^3/e\hbar$, and the strength is about 10^{18} [V/m]. The phenomena occurs effectively only under a strong electromagnetic field.

Recently, we have seen advance in research on hadron physics of a strong electromagnetic field in both theoretical and experimental aspects. At the heavy ion collision in RHIC and LHC, it is expected that a strong magnetic field is generated by a collision of charged particles accelerated at about the speed of light. Another related topic is neutron stars and magnetors which carry a strong electromagnetic field. In such a strong electromagnetic field, it may be possible to create a pair charged particles. For example, we may think of a quark antiquark pair creation as well as the electron positron pair. Quarks

and gluons are described by quantum chromodynamics(QCD), which has a strong gauge coupling constant at low energy, popularly known as the asymptotic freedom. Thus, we cannot observe a single quark because quarks have a confining force. However, we expect that a quark antiquark pair creation occurs if a quark and an antiquark are separated by an electromagnetic field stronger than the confining force. In QCD, perturbation is not a good approximation at low energy, thus it is essential to evaluate non-perturbative effects. To calculate the creation rate of the quark antiquark pair, we need to calculate non-perturbative effects about the QCD vacuum. Recently developed notion known as a gauge/gravity duality, or equivalently AdS/CFT correspondence, can be applied, since the duality indeed enables us to calculate a strong coupling limit of quantum field theories [8–10].

The AdS/CFT correspondence states that the $\mathcal{N} = 4$ supersymmetric Yang-Mills theory is equivalent to type IIB superstring theory on $\mathrm{AdS}_5 \times S^5$. In particular, the large N_c limit and the strong coupling limit of the $\mathcal{N} = 4$ supersymmetric Yang-Mills theory is conjectured to be equivalent to classical type IIB supergravity on $\mathrm{AdS}_5 \times S^5$. The limits are a large N_c limit and a large 't Hooft coupling limit, $\lambda \equiv g^2 N_c \gg 1$. Non-perturbative quantum quantities of the large N_c strongly coupled gauge theory are derived from the classical gravity. It is not understood well how to calculate the creation rate of the quark antiquark in the AdS/CFT correspondence. In this thesis, We study the vacuum instability in the large N_c strongly coupled gauge theories.

The Schwinger effects have recently been studied by using the AdS/CFT correspondence. Within the AdS/CFT framework, the creation rate of the quark antiquark pair in the strongly coupled $\mathcal{N} = 4$ supersymmetric Yang-Mills theory was obtained in [19, 20]. Based on [19, 20], the holographic Schwinger effect were calculated in various systems [21–28]. On the other hand, K. Hashimoto and T. Oka obtained the vacuum decay rate, which can be identified as the creation rate of quark-antiquark pairs, in $\mathcal{N} = 2$ supersymmetric QCD(SQCD) by using a different method [16] in AdS/CFT correspondence: the imaginary part of the probe D-brane action.[1] The D3-D7 brane

[1]The method based on [19, 20] is a single instanton process for the creation of a pair and is valid for the electric field E smaller than the critical electric field, while the method in [16] is for E stronger than or comparable to the critical electric field. Both are basically a disc partition function in string theory, but evaluated in different regimes. The former is a semi-classical large disc, while the latter is a small disc giving the Dirac-Born-Infeld action. The boundary of the disc corresponds to the world line of the

system corresponds to $\mathcal{N}=4$ supersymmetric $SU(N_c)$ Yang-Mills theory accompanied by an $\mathcal{N}=2$ hypermultiplet in the fundamental representation of the $SU(N_c)$ gauge group [12]. They obtained the creation rate of the quarks and antiquarks in the $\mathcal{N}=2$ SQCD under a constant electric field by evaluating the imaginary part of the D7-brane action. In [17], we evaluated the imaginary part of the D7-brane action including not only a constant electric field but also a constant magnetic field and obtained the creation rate of the quark antiquark in the $\mathcal{N}=2$ SQCD.

In [18], we study the quark antiquark pair creation in non-supersymmetric QCD at large N_c at strong coupling, and the imaginary part of a D8-brane action in a constant electromagnetic field. The holographic models are the Sakai-Sugimoto model [14] and its deformed version [15].

As another topic of a vacuum instability, we are interested in a phase transition between a confining phase and a deconfining phase in strongly coupled gauge theories. At the phase transition, the energy distribution of meson at highly excited modes was found to obey a power-law, as studied K. Hashimoto, S. Kinoshita, K. Murata and T. Oka in [65, 67]. They named the phenomena a turbulent meson condensation. They speculated that the origin of the turbulence would be related to an AdS instability studied in [30]- [64]. The AdS instability was found under a perturbation in the time-depend system of Einstein-massless scalar theory. The authors of [65, 67] are interested in the universality of the AdS instability. Within the AdS/CFT correspondence, we can study a possible universality of the turbulent meson condensation. In [67], we explain that the turbulence power is universal, irrespective of how the transition is driven, by numerically calculating the power in various static brane setups at criticality. We also find that the power depends only on the cone-dimension of the probe D-brane.

The present doctor thesis is motivated by the following.

- The understanding of the vacuum instability in the large N_c strongly coupled gauge theories with the AdS/CFT correspondence
- The analysis about the vacuum instability induced by electromagnetic fields
- The universality of the turbulent meson condensation

created quark pair. A small E means a large disc , *i.e.* a larger separation of the created quark pair.

Firstly, although many papers about the AdS/CFT correspondence have been published, we haven't established the AdS/CFT dictionary about the vacuum instability such as the Schwinger effects. It is important to calculate the imaginary part of the effective action to evaluate the vacuum instability. The calculation of the imaginary part of the effective action in the gravity side gives us new idea about the vacuum instability from the AdS/CFT correspondence.

Secondly, many interesting results of the experiments about a strong magnetic field have recently been reported as we explained in the second paragraph. It is important to obtain the creation rate of the quark antiquark in not only an electric field but also a magnetic field. This is because there are some phenomena which depend on the direction of the electric fields and magnetic fields in high energy physics and condensed matter physics. For example, the quantum Hall effect occurs under a magnetic field which is not parallel to but perpendicular to an electric field. In this paper, we discuss the relationship between the vacuum instability and the directions of the electromagnetic fields in the AdS/CFT framework.

Thirdly, according to [65, 67], the meson's energy distribution at high excited modes obeys a turbulent power law in a D3-D7 brane system, which can be evaluated by a displacement of the probe D7-brane by an electric field. In particular, the shape of the D7-brane have a cusp. We are interested in the universality of the turbulent meson condensation in some other brane systems. In particular, it is worth examining the relation between the probe D-brane's cusp and the value of power about a meson's mass.

In the present doctor thesis, we summarize the electromagnetic instability and the universal turbulent meson. The content is based on the following three papers which have already been published.

1) K. Hashimoto, T. Oka and A. Sonoda, "Magnetic instability in AdS/CFT: Schwinger effect and Euler-Heisenberg Lagrangian of supersymmetric QCD," JHEP **1406**, 085 (2014) [arXiv:1403.6336 [hep-th]] [17].

2) K. Hashimoto, T. Oka and A. Sonoda, "Electromagnetic instability in holographic QCD," JHEP **1506**, 001 (2015) [arXiv:1412.4254 [hep-th]] [18].

3) K. Hashimoto, M. Nishida and A. Sonoda, "Universal Turbulence on Branes in Holography," JHEP **1508**, 135 (2015) [arXiv:1504.07836 [hep-th]] [67].

We discussed the quark antiquark pair creation in the $\mathcal{N} = 2$ large N SQCD. The creation rate of the quark antiquark pair is derived from the DBI action with the AdS/CFT correspondence in [17]. We derived the creation rate of the quark antiquark in a confining phase from the imaginary part of the DBI action with a Sakai-Sugimoto model in [18]. We found that the energy distribution of the mesons at high excited modes is a turbulent power law in the $\mathcal{N} = 2$ SQCD by using the AdS/CFT correspondence [67]. The results of the present doctor thesis are summarized as follows.

- We obtained the creation rate of the massless quark antiquark pair in the $\mathcal{N} = 2$ large N SQCD by evaluating the imaginary part of the DBI action in constant electromagnetic fields with the AdS/CFT correspondence. At zero temperature, an infrared divergence appears in the creation rate of the quark antiquark. We compared the the creation rate of the massless quark antiquark with the well-known results of QED. The massless quark antiquark divergence is similar to the results of the QED.

- We evaluated the creation rate of the massive quark antiquark pair in $\mathcal{N} = 2$ large N SQCD. This result is compared with the imaginary parts of the Euler-Heisenberg Lagrangian of $\mathcal{N} = 2$ supersymmetric QED(SQED) which has $2N_c$ scalar fields and N_c spinor fields. The creation rate of the massive quark antiquark is found to coincide with the creation rate of the massless quark antiquark at a finite temperature if we replace the quark mass with the temperature.

- The creation rate of the massless quark antiquark in a confining phase is obtained by the D8-brane DBI action in the Sakai-Sugimoto model. We found that the creation rate of the massless quark antiquark at zero temperature is finite, which is different from the result of the $\mathcal{N} = 2$ SQCD. The imaginary part of the D8-brane DBI action increases when we increase the magnetic field parallel to a fixed electric field. On the other hand, the imaginary part decreases when we increase the magnetic field perpendicular to the electric field. The critical electric field to have a non-zero imaginary part for the DBI action coincides with a QCD string tension between the quark and antiquark. The result was already mentioned in [23, 26] in a similar context.

- We found turbulent meson condensation in a D3-D5 brane system in the manner

similar to [65, 66]. The energy distribution of the highly excited meson modes is proportional to the power -4 of the meson mass in the D3-D5 brane system. At a finite temperature without a constant electric field, the power again found to be -4.

The organization of the doctor thesis is as follows. In section 2, we review the AdS/CFT correspondence [74]. We discuss various coordinates of the AdS space. Next, Maldacena's conjecture is explained in the idea of the AdS/CFT correspondence. Gubser, Klevanov, Polyakov and Witten introduced GKP-Witten prescription which is the external field-operator correspondence. Also, we introduce flavor to D3-branes to consider $\mathcal{N} = 2$ SQCD according to Karch and Katz [12]. In section 3, we consider the main topic, the quark antiquark pair creation. First, we derive the creation rate of an electron positron pair in external fields by evaluating the imaginary part of the Euler-Heisenberg Lagrangian which is the effective Lagrangian in QED. We introduce 't Hooft's idea, planar diagram and indicate that the quark antiquark 1-loop diagram becomes a disk amplitude in a strong coupling limit. With the Hashimoto-Oka's conjecture, we evaluate the imaginary part of the DBI action in constant electromagnetic fields. Also, the creation rate of the quark antiquark pair in a confining gauge theory is obtained by evaluating the imaginary part of the D8-brane DBI action in the Sakai-Sugimoto model. Then, we find that the critical electric field corresponds to the QCD string tension. In section 4, we consider the fluctuation of the probe D5-brane when we introduce a constant electric field or a temperature. Then, we find that the turbulent power law is -4 in the D3-D5 brane system when the shape of the probe D5-brane has a cusp by the external fields. This power of the turbulent power law depends only on a cone-dimension of the probe D-brane. In the last section, we summarize the doctor thesis.

2 The review of AdS/CFT correspondence

The goal which we would like to achieve is to introduce the AdS/CFT framework in order to obtain the creation of the quark antiquark pair in the electromagnetic fields. Since the quarks are strongly coupled to the gluons in QCD, the perturbation is not a good approximation. Recently, the AdS/CFT correspondence has been developed as a way to evaluate physical quantities in the strongly coupled gauge theory can be evaluated.

Maldacena suggested that strongly coupled gauge theories are related with gravity. According to the Maldacena's conjecture, GKP-Witten prescription gives us how concretely to calculate the physical quantities with an external field-operator correspondence. Also, we consider not only pure gauge theories but also including flavors. We need to introduce the flavors to gauge theories in order to examine the quark antiquark pair creation. If we add the flavor branes to the D3-branes, the $\mathcal{N} = 4$ supersymmetric Yang-Mills theory becomes $\mathcal{N} = 2$ supersymmetric QCD which includes gauge fields, Dirac fields and complex scalar fields. The theory is not a conformal field theory. But the Maldacena's conjecture is consistent in a probe limit. In next section, we will discuss the quark antiquark pair creation with the AdS/CFT framework.

2.1 AdS space

We review the AdS space. The (p+1)-dimensional Anti-de sitter space($\mathrm{AdS_{p+2}}$) is described by

$$X_0^2 + X_{p+2}^2 - \sum_{i=1}^{p+1} X_i^2 = R^2. \tag{2.1}$$

The flat metric of (p+3)-dimensional space is

$$ds^2 = -dX_0^2 - dX_{p+2}^2 + \sum_{i=1}^{p+1} dX_i^2. \tag{2.2}$$

Here, R is an AdS radius. This hyperbolic space clearly has $SO(2, p+1)$ symmetry. The $SO(2, p+1)$ symmetry becomes a strong evidence for the AdS/CFT correspondence. We define new coordinates of the AdS space.

- **Global coordinate**

  We take a new coordinate as

  $$X_0 = R\cosh\rho\cos\tau, \quad X_{p+2} = R\cosh\rho\sin\tau, \quad X_i = R\sinh\rho\,\Omega_i\ , \tag{2.3}$$

  where $i = 1, \cdots, p+1$ and $\sum_i \Omega_i^2 = 1$. Substituting (2.3) to (2.2), the metric is

  $$ds^2 = R^2(-\cosh^2\rho\, d\tau^2 + d\rho^2 + \sinh^2\rho\, d\Omega_{p+1}^2). \tag{2.4}$$

Here, the regions of τ, ρ are $0 \leq \tau < 2\pi, 0 \leq \rho < \infty$ respectively. In the neighborhood of $\rho = 0$, the above metric is

$$ds^2 \simeq R^2(-d\tau^2 + d\rho^2 + \rho^2 d\Omega_{p+1}^2). \tag{2.5}$$

The hyperbolic space is topologically $S^1 \times \mathbf{R}^{p+1}$. This coordinate has a closed timeline curve in order to be periodicity for τ. We should take universal cover, $-\infty < \tau < \infty$ since the causality is unbroken.

- **Conformal coordinate**

  We define $\sinh \rho$ as $\tan \theta \equiv \sinh \rho$. (2.3) is obtained by

$$ds^2 = \frac{R^2}{\cos^2 \theta}(-d\tau^2 + d\theta^2 + \sin^2 \theta \, d\Omega_{p+1}^2). \tag{2.6}$$

  The region of θ is $0 \leq \theta < 2\pi$. $\theta = \pi/2$ corresponds to the AdS boundary. If we rescale the metric, $ds'^2 = \cos^2 \theta ds^2 / R^2$, then we obtain $ds'^2 = -d\tau^2 + d\theta^2 + \sin^2 \theta \, d\Omega_{p+1}^2$. In $\theta = \pi/2$, the AdS boundary is S^{p+1}.

- **Poincare coordinate**

  Let us introduce a Poincare coordinate. We define the light-cone coordinate as

$$u \equiv \frac{X_0 - X_{p+1}}{R^2},$$
$$v \equiv \frac{X_0 + X_{p+1}}{R^2}.$$

  The parameters of $u, t, \vec{x}$ ($\vec{x} \in \mathbf{R}^p$) are introduced in the Poincare coordinate. t, x^i ($i = 1, \cdots, p$) are defined by

$$x^i \equiv \frac{X^i}{Ru},$$
$$t \equiv \frac{X_{p+2}}{Ru}.$$

  Also, with (2.1), we obtain

$$R^4 uv + R^2 u^2 (t^2 - \vec{x}^2) = R^2.$$

  From the above expressions, we vanish the parameter v and derive the following,

$$X_0 = \frac{1}{2u}(1 + u^2(R^2 + \vec{x}^2 - t^2)),$$
$$X^i = Rux^i, \;\; X_{p+2} = Rut, \tag{2.7}$$
$$X^{p+1} = \frac{1}{2u}(1 - u^2(R^2 - \vec{x}^2 + t^2)).$$

In this case, the metric becomes

$$ds^2 = R^2 \left(\frac{du^2}{u^2} + u^2(-dt^2 + d\vec{x}^2) \right). \tag{2.8}$$

u is changed to z which is defined by $z \equiv 1/u$. We obtain

$$ds^2 = \frac{R^2}{z^2} \left(dz^2 - dt^2 + d\vec{x}^2 \right). \tag{2.9}$$

The Poincare coordinate has two different Poincare charts [75]. In $z > 0$, the Poincare coordinate has the half hyperbolic surface, $X_0 > X_{p+1}$ in the AdS space. On the other hands, the Poincare coordinate in $z < 0$ has the half hyperbolic surface, $X_0 < X_{p+1}$ in the AdS space. We only cover the half AdS space with the Poincare coordinate(we usually cheese $z > 0$).

In this subsection, we explained the various coordinates. Note that we treat the Poincare coordinate because the coordinate doesn't cover the all AdS space. But, if we consider the Euclidean time with Wick rotation, we have no problem because the hyperbolic surface becomes topologically the ball which has a boundary. In the next subsection, we explain a Maldacena's conjecture.

2.2 Maldacena's conjecture

In [8], Maldacena conjectured that $\mathcal{N} = 4$ supersymmetric Yang-Mills theory is equivalent to type IIB superstring theory on $\mathrm{AdS}_5 \times S^5$. Recently, we have calculated the physical quantities in the strongly coupled gauge theories with the Maldacena's conjecture. The AdS/CFT correspondence gives us the non-perturbative effects in the strongly coupled theories.

Let us consider the type IIB superstring theory on the 10-dimensional Minkowski space-time. The type IIB theory has three kinds of Ramond-Ramond fields(R-R fields) such as R-R 0-form field, 2-form field and 4-form field(C_0, C_2 and C_4). These fields are coupled to D1-branes, D3-branes and D5-branes respectively.

We prepare the N D3-branes. The D3-branes localize on the position of $x^4 = x^5 = \cdots = x^9 = 0$. Then, the D3-branes solution is given by

$$ds^2 = H(r)^{-1/2} dx_{||}^2 + H(r)^{1/2}(dr^2 + r^2 d\Omega_5^2). \tag{2.10}$$

Here, $dx_{||}$ is the direction parallel to the D3-branes. $x_{||}$ is defined as $x_{||} = (-t, x^1, x^2, x^3)$. $d\Omega_5^2$ is the metric of S^5. r is the radius of the unit sphere. The function $H(r)$ is defined by

$$H(r) = 1 + \frac{4\pi g_s N \alpha'^2}{r^4}. \tag{2.11}$$

g_s is a string coupling. α' is defined as $\alpha' \equiv l_s^2$, where l_s is string length.

The parameter u is defined by $u \equiv r/\alpha'$. We take the following limit,

$$u : \text{fixed}, \quad \alpha' \to 0 \ . \tag{2.12}$$

This limit is called near horizon limit [8]. The metric of the D3-branes changes to the $AdS_5 \times S^5$ metric as

$$ds^2 = \alpha' \left[\frac{u^2}{\sqrt{4\pi g_s N}} dx_{||}^2 + \sqrt{4\pi g_s N} \frac{du^2}{u^2} + \sqrt{4\pi g_s N} d\Omega_5^2 \right]. \tag{2.13}$$

Compared with (2.8) in which we put $p = 3$, the first term and second term in (2.13) become the AdS_5 metric. Also, the AdS radius and the S^5 radius are same as $R^2 = \alpha' \sqrt{4\pi g_s N}$.

2.2.1 The relation between a temperature and a black hole metric

A gauge theory at a temperature is concerned with the black hole in the AdS/CFT framework. A temperature corresponds to the horizon of the black hole. We use Wick rotation in order to consider the finite temperature gauge theory such as Matsubara formalism. The Euclidean black hole metric is described by

$$ds^2 = +f(r) d\tau^2 + \frac{dr^2}{f(r)} + \cdots . \tag{2.14}$$

Expending the function $f(r)$ around $r = r_0$, we obtain

$$ds^2 \simeq (r - r_0) f'(r_0) d\tau^2 + \frac{dr^2}{(r - r_0) f'(r_0)}. \tag{2.15}$$

Here, r_0 is the horizon of the black hole. $f(r)$ is satisfied with $f(r_0) = 0$. If we define ρ as $\rho \equiv 2\sqrt{(r - r_0)/f'(r_0)}$, we obtain

$$ds^2 \simeq d\rho^2 + \rho^2 d\left(\frac{f'(r_0)}{2} \tau \right)^2 . \tag{2.16}$$

This metric is the sphere which has the radius ρ and the angle $f'(r_0)\tau/2$. The metric has the periodic boundary condition, $f'(r_0)\tau/2 \sim f'(r_0)\tau/2 + 2\pi$. In the Matsubara formalism, the imaginary time has the periodicity for β, where β is defined by $\beta = 1/T$. Here, we put Boltzmann constant $k_B = 1$. T is a temperature. Thus, the relation between the temperature and the horizon of the black hole is

$$T = \frac{f'(r_0)}{4\pi}. \tag{2.17}$$

For example, when we change (2.13) to the Euclidean black hole metric, we obtain

$$f(r) = \frac{r^2}{\alpha'\sqrt{4\pi g_s N}}\left(1 - \frac{r_0^4}{r^4}\right), \tag{2.18}$$

where $u = r/\alpha'$. Thus, the relation becomes $T = r_0/\pi R^2$. The zero temperature limit coincides with vanishing the horizon, $r_0 \to 0$

2.2.2 The low energy effective theory on the D3-branes

The low energy effective theory on the D3-branes is $\mathcal{N} = 4$ supersymmetric Yang-Miils theory. This theory has the 16 number of the supercharges and a superconformal field theory because the 1-loop beta function is zero. In the $\mathcal{N} = 4$ supersymmetric Yang-Miils theory, the field contents are gauge field A_μ, 6 real scalar fields ϕ^i $(i = 1, \cdots, 6)$, 4 positive chiral Weyl fermions λ_{L}^A and 4 negative chiral Weyl fermions $\lambda_{\mathrm{R}A}$ $(A = 1, \cdots, 4)$. These fields are derived from the Dirac-Born-Infeld action(DBI action) such as the D3-brane effective action. For simplicity, we only consider the boson part of a D3-brane action.

We consider the background is flat and put $g_{MN} = \eta_{MN}$ and $e^{\phi} = g_s$. Here, ϕ is a dilaton and g_s is a string coupling. The D3-brane DBI action is given by

$$S = -T_{\mathrm{D3}} \int d^4\sigma \sqrt{-\det(G_{\alpha\beta}[X] + 2\pi\alpha' F_{\alpha\beta})}, \tag{2.19}$$

where the D3-brane tension is $T_{\mathrm{D3}} = 1/(2\pi)^3 l_{\mathrm{s}}^4 g_{\mathrm{s}}$. The D3-brane flat spreads to the 0123-direction. we fix the target space coordinate X^α as $X^\alpha = \sigma^\alpha$ $(\alpha = 0, 1, \cdots, 3)$ when the D3-brane moves to the perpendicular to the D3-brane in infinitesimal. Thus, we obtain

$$G_{\alpha\beta}[X] = \eta_{\alpha\beta} + \partial_\alpha X^i \partial_\beta X^i, \tag{2.20}$$

where $i = 4, 5, \cdots, 9$. Substituting the metric to (2.19), when we take a decoupling limit $\alpha' \to 0$, we derive

$$S = \frac{1}{g_{\rm YM}^2} \int d^4\sigma \left(-\frac{1}{2} \partial_\mu \phi^i \partial^\mu \phi^i - \frac{1}{4} F_{\mu\nu} F^{\mu\nu} \right), \tag{2.21}$$

from the redefinition of $X^i \equiv 2\pi\alpha'\phi$. $g_{\rm YM}^2$ is a 4-dimensional Yang-Mills coupling. The relation between the Yang-Mills coupling and the string coupling is

$$g_{\rm YM}^2 = 2\pi g_{\rm s}. \tag{2.22}$$

The $O(l_s^{-4})$ term diverges in taking $\alpha' \to 0$, but we neglect the term because of the constant term. Similarly, we also discuss the fermionic terms in the $\mathcal{N} = 4$ supersymmetric Yang-Mills theory. In the case of the gauge theory, the gauge group is Abelian $U(1)$ because we consider a D3-brane. In order to enhance $U(N)$ non-Abelian gauge theories, we prepare the N number of the D3-branes and should introduce Chan-Paton factors. The n degrees of freedom for the fundamental strings coupled to the D3-branes at the endpoints, $\sigma = 0$ have $n = 1, 2, \cdots, N$. On the other hands, The $\bar{n}$ degrees of freedom at $\sigma = \pi$ have $\bar{n} = \bar{1}, \bar{2}, \cdots, \bar{N}$. Here, we consider the oriented fundamental strings. Thus, the fundamental strings have the N^2 degrees of freedom. The degrees of freedom correspond to the degrees of freedom of $U(N)$ gauge group.

2.2.3 The symmetries of gauge and gravity

In this part, we discuss the symmetries in the $\mathcal{N} = 4$ supersymmetric Yang-Mills theory and the $\mathrm{AdS}_5 \times S^5$ superstring theory. We have no the proof about the Maldacena's conjecture yet. But, almost superstring theory physicists have believed in the conjecture because the symmetries of the gauge theory side correspond to that of the gravity side. It is important to coincide with the symmetries of the two theories which have a duality such as the gauge/gravity dual, in order to regard the duality as consistent.

In the gravity side, we find that the D3-brane solution changes to the $\mathrm{AdS}_5 \times S^5$ metric when we take the near horizon limit. The AdS_5 metric has a $SO(2,4)$ symmetry from the review of the AdS space. Since S^5 has the symmetry of a $SO(6)$ rotation group, the $\mathrm{AdS}_5 \times S^5$ has $SO(2,4) \times SO(6)$.

On the other hands, the gauge theory has a Poincare symmetry, a scale symmetry and a R-symmetry associated with the supersymmetry. In general, Dp-branes($p \leq 8$)

make the Poincare symmetry $SO(1,9)$ broken to

$$SO(1,p) \times SO(9-p) \subset SO(1,9). \tag{2.23}$$

Thus, the Poincare symmetry in the 10-dimension is $SO(1,3) \times SO(6)$ in $p = 3$. The $SO(6)$ symmetry is the rotation symmetry in the 456789-directions to which the D3-branes is the perpendicular while the $SO(1,3)$ symmetry is the Lorentz symmetry in the 0123-directions. But, Polchinski mentioned that the $SO(1,3)$ symmetry is enhanced to a $SO(2,4)$ symmetry by the scale invariance in the $\mathcal{N} = 4$ supersymmetric Yang-Mills theory [11].

The gauge fields A_M $(M = 0, 1, \cdots, 9)$ on the D9-branes are reduced to the gauge fields A_μ $(\mu = 0, 1 \cdots, 3)$ and the six real scaler fields ϕ^i $(i = 1, 2, \cdots, 6)$ on the D3-branes. The scalar fields have the global symmetry of $SU(4) \simeq SO(6)$. This symmetry is the R-symmetry. The Majorana-Weyl spinor λ in the 10-dimension is reduced to the four positive chiral Weyl fermions $\lambda^A_{\rm L}$ $(A = 1, 2, \cdots, 4)$ and the four negative chiral Weyl fermions $\lambda_{{\rm R}A}$ on the D3-branes. These spinors are the spinor representations of $SO(6)$. Therefore, the $\mathcal{N} = 4$ supersymmetric Yang-Mills theory has the $SU(2,4) \times SO(6)$ symmetry, which corresponds to the symmetry of $\mathrm{AdS}_5 \times S^5$ superstring theory. We have the strong evidence for the consistency of the AdS/CFT correspondence.

2.2.4 The region of corresponding to gauge and gravity

The Maldacena's conjecture is mentioned to the equivalence between the $\mathcal{N} = 4$ supersymmetric Yang-Mills theory and the $\mathrm{AdS}_5 \times S^5$ superstring theory. In the previous part, we obtained the justification of the gauge/gravity dual from the symmetries. Next, we discuss the coupling region between the gauge theory and the gravity.

It is difficult to compete the stringy and quantum effects in the superstring theory. But we neglect the effects when we consider the following limits.

- $R \gg l_{\rm s}$ (use a supergravity and neglect the high excited modes of the string.)
- $R \gg l_p$ (treat a classical supergravity.)

Here, R is the AdS radius. l_s and l_p are a string length and Plank length respectively. The first condition means that the stringy effects are neglected. The limit corresponds to $g^2_{\rm YM} N \gg 1$ in the gauge theory side because the string coupling g_s is $g^2_{\rm YM} = 2\pi g_{\rm s}$. We

define 't Hooft coupling λ as $g^2_{\rm YM}N \equiv \lambda$. The second condition corresponds to a Large N limit such as $N \to \infty$ in the gauge theory side because the Planck length is $l_p = g_{\rm s}^{1/4} l_{\rm s}$. We take $N \to \infty$, fixing the large 't Hooft coupling. These limits obtain the following relation,

Large N strongly coupled $U(N)$ gauge theory $=$ $\mathrm{AdS}_5 \times \mathrm{S}^5$ classical supergravity.

The AdS/CFT correspondence means that the strongly coupled gauge theory is equivalent to the classical supergravity in the limits. In the next subsection, we discuss the quark antiquark pair creation in the strongly coupled large N gauge theory.

2.3 GKP-Witten relation

The AdS/CFT correspondence claims that $\mathcal{N} = 4$ supersymmetric Yang-Mills theory is equivalent to the $\mathrm{AdS}_5 \times S^5$ superstring theory. There is a expression of concrete correspondence called GKP-Witten relation [9, 10]. Maldacena didn't give us the concrete relation though he claimed the correspondence between the gauge and the gravity. Gubser, Klebanov, Polyakov and Witten gave

$$Z_{\rm AdS}[\phi|_{\rm bdy} = \phi_0(x)] = \langle e^{-\int d^d x \ O(x)\phi_0(x)} \rangle_{\rm CFT}. \tag{2.24}$$

GKP-Witten relation is defined by Euclidean metric. In $N \to \infty$, $\lambda \gg 1$, the left hand side corresponds to the on-shell classical gravity action for the AdS background. $\phi_0(x)$ is a field in the AdS boundary and corresponds to a source field in the gauge theory side. $O(x)$ is an operator for the source field. The source field corresponds to the operator one to one. We can obtain the correlation functions for the operator $O(x)$ by the generating function about $\phi_0(x)$ when we solve the the equation of motion about $\phi(x)$ and give the initial condition as $\phi|_{\rm bdy} = \phi_0(x)$ in the gravity side. For example, the relationships between a source and an operator are given by the following.

	A source	An operator
gravity	metric $g_{\mu\nu}$	stress tensor $T^{\mu\nu}$
Maxwell theory	gauge field A_μ	current j^μ

In the case of the quark antiquark pair creation, we should make the vacuum instability by an electromagnetic field. We derive the current between the quark and antiquark from

the effective action in the gravity by using the AdS/CFT correspondence. The vacuum instability occurs by putting the current on zero.

2.3.1 Massive scalar field case

Let us consider the example of the massive scalar field case by using the GKP-Witten prescription. In $d+1$-dimensional gravity, the massive scalar action is given by

$$I(\phi) = \frac{1}{2}\int_{\mathrm{AdS}_{d+1}} d^{d+1}x\sqrt{g}\,[g^{\mu\nu}\partial_\mu\phi\partial_\nu\phi + m^2\phi^2]. \tag{2.25}$$

Here, $g = \det g_{\mu\nu}$ $(\mu,\nu = 0,1,\cdots,d+1)$. We use the Poincare coordinate of the AdS background (2.9), where is Wick rotated as the following,

$$ds^2 = \frac{R^2}{z^2}[dz^2 + \eta^{mn}dx_m dx_n]. \tag{2.26}$$

Here, $m,n = 1,2,\cdots,d$ and $\eta_{mn} = \mathrm{daig}(+,\cdots,+)$. Then, the equation of motion becomes

$$[\Box - m^2]\phi(z,\boldsymbol{x}) = 0, \tag{2.27}$$

where $\Box$ is the d'Alembertian of the metric. We set the boundary condition as,

$$\lim_{z\to 0}\phi(z,\boldsymbol{x}) = \phi_0(\boldsymbol{x}). \tag{2.28}$$

To solve the equation of motion, it is convenient to use a Green function $K(z,\boldsymbol{x})$. The Green function is satisfied with

$$[\Box - m^2]K(z,\boldsymbol{x}) = 0, \quad \lim_{z\to 0}K(z,\boldsymbol{x}) = \delta(\boldsymbol{x}). \tag{2.29}$$

Thus, the solution is given by

$$\phi(z,\boldsymbol{x}) = \int d^d\boldsymbol{x}' K(z,\boldsymbol{x}-\boldsymbol{x}')\phi_0(\boldsymbol{x}'). \tag{2.30}$$

We reduce to evaluate the Green function $K(z,\boldsymbol{x})$.

Let us consider a Green function $\widetilde{K}(z,\boldsymbol{x})$ in the case of the source at infinity. Since the function $\widetilde{K}(z,\boldsymbol{x})$ has a translational invariance at the boundary $z=0$, we describe $\widetilde{K}(z,\boldsymbol{x}) = \widetilde{K}(z)$. Then, the equation of motion to which the Poincare coordinate (2.26) is substituted is described by

$$\left(z^{d+1}\frac{\partial}{\partial z}z^{1-d}\frac{\partial}{\partial z} - m^2R^2\right)\widetilde{K}(z) = 0. \tag{2.31}$$

When we put $\widetilde{K}(z) = z^{\Delta}$ in order to solve the equation, the characteristic equation for the differential equation is

$$\Delta(\Delta - 1) + (1 - d)\Delta - m^2 R^2 = 0. \tag{2.32}$$

If we regard two solutions as $\Delta = \Delta_{\pm}$ ($\Delta_+ \geq \Delta_-$), we obtain

$$\Delta_{\pm} = \frac{d \pm \sqrt{d^2 + 4m^2 R^2}}{2}. \tag{2.33}$$

We obtain $\tilde{K}(z) = cz^{\Delta_+}$ since $\Delta = \Delta_+$ is satisfied with $\lim_{z\to 0} \tilde{K}(z) = 0$. From now, we define Δ_+ as Δ.

The AdS metric has the inversion which is a symmetry such as,

$$\boldsymbol{x} \to \frac{\boldsymbol{x}}{z^2 + \boldsymbol{x}^2}, \quad z \to \frac{z}{z^2 + \boldsymbol{x}^2}. \tag{2.34}$$

By using this transformation, we move the source from the infinity point to the origin. Then, the Green function $K(z, \boldsymbol{x})$ is derived by

$$K(z, \boldsymbol{x}) = c \left(\frac{z}{z^2 + \boldsymbol{x}^2} \right)^{\Delta}. \tag{2.35}$$

Next, let us check this Green function by being a delta function at $z \to 0$. In $\boldsymbol{x} \neq 0$, the Green function becomes the delta function such as $\lim_{z\to 0} K(z, \boldsymbol{x}) = 0$. Also, the integral $\chi(z) = \int d^d \boldsymbol{x} K(z, \boldsymbol{x})$ is $\chi(z) = \lambda^{d-\Delta}\chi(\lambda z)$ by the scale transformation such as $z \to \lambda z$, $\boldsymbol{x} \to \lambda \boldsymbol{x}$. Thus, the Green function $K(z, \boldsymbol{x})$ is the delta function in $\boldsymbol{x} \to 0$ limit if we take $\lambda = 1/z$. The Green function $K(z, \boldsymbol{x})$ has the relation as $\lim_{z\to 0} K(z, \boldsymbol{x}) = z^{d-\Delta}\delta(\boldsymbol{x})$ in $\boldsymbol{x} \to 0$ limit. Therefore, the boundary condition for $\phi(z, \boldsymbol{x})$ becomes

$$\lim_{z\to 0} \phi(z, \boldsymbol{x}) = z^{d-\Delta}\phi_0(\boldsymbol{x}). \tag{2.36}$$

Substituting the solution of $\phi(z, \boldsymbol{x})$ to $I(\phi)$, we derive the following,

$$I(\phi) = \frac{c\Delta}{2} \int d^d \boldsymbol{x} d^d \boldsymbol{x}' \frac{1}{(\boldsymbol{x} - \boldsymbol{x}')^{2\Delta}} \phi_0(\boldsymbol{x})\phi_0(\boldsymbol{x}'), \tag{2.37}$$

from the total derivative term. Here, c is constant. It is determined by the normalization between the gauge theory and gravity. From the on-shell action, Δ is the conformal dimension of the operator $O(x)$ for the gauge theory.

2.4 Adding flavors

In this subsection, we explain the D3-D7 brane construction introduced by Karch-Katz [12]. The N_c D-branes describe $\mathcal{N} = 4$ supersymmetric Yang-Mills theory in the low energy limit $\alpha' \to 0$. When we introduce flavors, we need to add the degree of freedom about the flavors. Then, we introduce D7-branes to the D3-brane system. If we add the D7-branes, the $\mathcal{N} = 4$ supersymmetric Yang-Mills theory is broken to $\mathcal{N} = 2$ supersymmetric theory which includes the hypermultiplets such as Dirac spinor fields and complex scalar fields. When we introduce the N_f D7-branes, the oriented fundamental strings have the degree of freedom, $(\mathrm{N_c}, \mathrm{N_f})(\bar{\mathrm{N}}_\mathrm{c}, \bar{\mathrm{N}}_\mathrm{f})$ which is coupled to the N_c D3-branes with the N_f D7-branes. These are the degree of freedom about flavor symmetries and gauge symmetries for the quarks and antiquarks belonging to the fundamental representations respectively.

According to the Maldacena's conjecture, the solution of the $\mathrm{AdS}_5 \times S^5$ supergravity is derived from the D3-branes solution which imposes the near horizon limit. Since the AdS/CFT correspondence is important for the correspondence of the symmetries between the $\mathrm{AdS}_5 \times S^5$ metric and the supersymmetries in the gauge theory. We assume that the solution of the N_c D3-branes don't receive the backreaction of the N_f D7-branes. Then, we impose the limit of $N_f \ll N_c$. It is called a probe limit.

The D7-branes are probe branes in the D3-D7 brane construction. We consider the following brane construction about the D3-D7 brane system,

	0	1	2	3	4	5	6	7	8	9
D3	√	√	√	√						
D7	√	√	√	√	√	√	√	√		

The check marks represent Neumann boundary conditions. The D3-branes stretch to the 0123-directions, and the D7-branes stretch to the 01234567-directions. Also, the the D3-branes and the D7-branes separate to the 89-directions.

We review the $\mathcal{N} = 2$ supersymmetric QCD Lagrangian about the Karch-Katz model [68]. The model consists of the $\mathcal{N} = 4$ supersymmetric Yang-Mills theory with the $\mathcal{N} = 2$ hypermultiplets with the fundamental representation of the $SU(N_c)$ gauge group. With

$\mathcal{N}=1$ superspace formalism, the Lagrangian is described by

$$\mathcal{L} = \mathrm{Im}\left[\tau \int d^4\theta \left(\mathrm{tr}(\bar{\Phi}_I e^V \Phi_I e^{-V}) + Q_r^\dagger e^V Q^r + \tilde{Q}_r^\dagger e^{-V}\tilde{Q}^r\right)\right] + \mathrm{Im}\left[\tau \int d^2\theta \left(\mathrm{tr}(W^\alpha W_\alpha) + W\right) + \mathrm{c.c.}\right], \tag{2.38}$$

where the superpotential W becomes

$$W = \mathrm{tr}(\varepsilon_{IJK}\Phi_I\Phi_J\Phi_K) + \tilde{Q}_r(m_q + \Phi_3)Q^r. \tag{2.39}$$

τ is the complex gauge coupling. The $\mathcal{N}=4$ vector multiplet consists of the $\mathcal{N}=1$ vector multiplet W_α and the three $\mathcal{N}=1$ chiral superfields Φ_1, Φ_2 and Φ_3. The $\mathcal{N}=2$ hypermultiplets can be written down in the $\mathcal{N}=1$ chiral multiplets $Q^r, \tilde{Q}_r$ ($r = 1, 2, \cdots N_f$). The component fields of the $\mathcal{N}=4$ vector multiplet are the gauge field, the four Weyl spinor fields and the six real scalar fields with the adjoint representation of the $SU(N_c)$ gauge group. The component fields of the $\mathcal{N}=2$ hypermultiplets are the two Weyl spinor fields and the two complex scalar fields with the fundamental representation of the $SU(N_c)$ gauge group.

We discuss the quark antiquark pair creation about the $\mathcal{N}=4$ supersymmetric Yang-Mills theory with the flavors by using the Karch-Katz model in the next section.

3 Pair creations of quark-antiquark

In this section, we consider the quark antiquary pair creation in a constant electromagnetic field by using the AdS/CFT correspondence. Firstly, we review the electron positron pair creation by evaluating the imaginary part of the Euler-Heisenberg Lagrangian which is the effective Lagrangian in QED. Secondly, the quark antiquark 1-loop diagram is associated with a disk amplitude by introducing 't Hooft's idea. Thirdly, we derive the creation rate of the quark antiquark pair from the imaginary part of the DBI action with the AdS/CFT correspondence. Then, we obtain the creation rates in the $\mathcal{N}=2$ SQCD, the Sakai-Sugimoto model and the deformed Sakai-Sugimoto model.

3.1 The review of the electron-positron pair creations

Let us review the electron positron pair creation in quantum electrodynamics(QED). The vacuum polarization occurs in the QED vacuum. Photon creates a virtual electron

positron pair and the photon is created by the annihilation of the electron positron pair. But, the vacuum instability is caused by a strong electric field as an external field. Then, the on-shell electron positron pairs are created. The phenomena is called Schwinger effects.

We consider the electron positron pair creation in a constant electric field as a easy example. Since the rest mass of an electron and a positron are respectively $m_e c^2$, we need the energy more than $2m_e c^2$ in order to create an electron positron pair. If we introduce the strong electric field, the electron and the positron receive a Coulomb force for the opposite direction respectively. The total potential energy is profit for the electron positron pair to be created rather than for the electron and the positron to be separated more than x distance. In the distance between the electron and the positron, the potential energy by the electric field is $-eEx$. Thus, the total potential energy is

$$V(x) = 2m_e c^2 - eEx, \tag{3.1}$$

when we neglect the Coulomb potential between the electron and the positron. If the total potential energy $V(x)$ is zero, then the distance is $x = x_{\rm cr} = 2m_e c^2/eE$. In general, the virtual electron and positron are created and annihilated repeatedly in the vacuum. But, the electron positron pair are created rather than being annihilated in the distance more than $x_{\rm cr}$ between the electron and the positron. Then, the creation rate of the electron positron pair is

$$\Gamma_{\rm WKB} \sim \exp\left(-\frac{m_e^2 c^4}{e\hbar E}\right), \tag{3.2}$$

by using WKB approximation. Since the electric coupling constant appears in the denominator of (3.2), the Schwinger effects indicate non-perturbative behaviors. The creation rate is excluded when $E < m_e^2 c^4/e\hbar$. Then, the critical electric field becomes

$$E_{\rm cr} = \frac{m_e^2 c^4}{e\hbar} \sim 10^{16}\,[\mathrm{V/cm}], \tag{3.3}$$

where $E_{\rm cr}$ is the critical electric field.

Schwinger effects are the phenomenon which the vacuum instability causes by an external field. We consider the QED effective action without the dynamical gauge field. The effective Lagrangian is given by

$$\mathcal{L}_{\rm eff}^{\rm QED}(A_\mu^{\rm ex}) = -\frac{i}{\rm Vol}\int \mathcal{D}\bar{\psi}\mathcal{D}\psi\, \exp\left[i\int d^4x \bar{\psi}(i\not{D} - m)\psi\right], \tag{3.4}$$

where $\not{D} \equiv \gamma^\mu D_\mu = \gamma^\mu(\partial_\mu + ieA^{\rm ex}_\mu)$ and $A^{\rm ex}_\mu$ is an external field. In order to obtain the creation rate of the electron positron, we need to evaluate the effective action. We review the Euler-Heisenberg Lagrangian in the appendix according as Itzykson-Zuber [76].

It is important to consider the transition amplitude of the QED vacuum since the Schwinger effects are caused by the vacuum instability. The path integral of (3.4) indicates the transition amplitude of the vacuum $\mathcal{A}$. The vacuum decay rate is obtained by

$$\frac{dP}{dt} = -\Gamma P, \tag{3.5}$$

where P is the vacuum to vacuum transition probability by the external field. P is obtained by $P = |\mathcal{A}|^2$. Γ is the vacuum decay rate. The relation between the vacuum decay rate and the effective Lagrangian is the following,

$$\Gamma = \int d^3x \; 2\mathrm{Im}\, \mathcal{L}^{\rm QED}_{\rm eff}(A^{\rm ex}_\mu). \tag{3.6}$$

The vacuum decay rate is derived from the imaginary part of the effective Lagrangian. From now, we calculate the imaginary part of the effective Lagrangian.

Let us derive the creation rate of the electron positron pair from the Euler-Heisenberg Lagrangian which is the 1-loop electron positron effective Lagrangian. Euler, Heisenberg and Schwinger are evaluated by the 1-loop effective Lagrangian in the spinor QED [1] [2] as the following,

$$\mathcal{L}^{\rm QED}_{\rm eff} = \frac{\boldsymbol{E}^2 - \boldsymbol{B}^2}{2} + \frac{1}{8\pi^2}\int_0^\infty \frac{ds}{s} e^{-is(m^2-i\epsilon)} \left[e^2 ab \frac{\cosh(eas)\cos(ebs)}{\sinh(eas)\sin(ebs)} - \frac{1}{s^2} \right], \tag{3.7}$$

where a and b are defined as $a^2 - b^2 \equiv \boldsymbol{E}^2 - \boldsymbol{B}^2$, $ab \equiv \boldsymbol{E}\cdot\boldsymbol{B}$. $\boldsymbol{E}$ and $\boldsymbol{B}$ are respectively constant electric fields and constant magnetic fields. The s-integral is a proper time integral for the electron. The exponential includes $i\epsilon$-prescription to coverage of the integral in $s \to \infty$. The effective Lagrangian is called Euler-Heisenberg Lagrangian. We can obtain the creation rate of the electron positron pair by evaluating the imaginary part of the Lagrangian. When we only consider the constant electric field $A^3(x) = -Et$ in the z-direction, the Euler-Heisenberg Lagrangian is

$$\mathcal{L}^{\rm QED}_{\rm eff} = \frac{1}{2}E^2 + \frac{1}{8\pi^2}\int_0^\infty \frac{ds}{s^2} e^{-is(m^2-i\epsilon)} \left[eE\coth(eEs) - \frac{1}{s} \right]. \tag{3.8}$$

We explain the convergence of the integral at $s = 0$. In $s \to 0$, the integral coverages because $\mathrm{Im}(e^{-ism^2}) = -\sin(sm^2) \simeq -sm^2$ and the order in the above bracket is $O(s)$. Thus, the integral has no pole at $s = 0$. We consider the residual internal which expends the integral of (3.8) to complex integral. The first term of the integrand has $s_n = i\pi n/eE$, where n is a natural number. The region of the integral extends from $(0, \infty)$ to $(-\infty, \infty)$ and is taken as the integral path of the below semicircle. When we consider the residual integral at $s_n = i\pi n/eE, (n = 1, 2, \cdots)$ poles, the imaginary part of the Lagrangian is

$$\mathrm{Im}\,\mathcal{L}_{\mathrm{eff}}^{\mathrm{QED}} = \frac{(eE)^2}{8\pi^3}\sum_{n=1}^{\infty}\frac{1}{n^2}\exp\left(-\frac{\pi m_e^2}{|eE|}n\right). \tag{3.9}$$

In the bosonic case, Weisskipf calculated the creation rate of the charged scalar fields as the following,

$$\mathrm{Im}\,\mathcal{L}_{\mathrm{eff}}^{\mathrm{scalar\,QED}} = \frac{(eE)^2}{16\pi^3}\sum_{n=1}^{\infty}\frac{(-1)^{n+1}}{n^2}\exp\left(-\frac{\pi m^2}{|eE|}n\right), \tag{3.10}$$

in a scalar QED [3]. The factor which is common to the bosonic and fermionic cases is $\exp(-\pi m^2/|eE|)$. This factor indicates a non-perturbative effect. Now, we assume that the more than 2-loop Feynman diagrams such as the internal lines of the photon are neglected because the external electromagnetic fields are much larger than the dynamical electromagnetic fields.

The electron positron pair creation relates to a quantum tunneling through potential barrier in Fig.1. The electron has the bound state when the electron has a Coulomb potential. If this potential is added to a Coulomb force $-eEx$, then the quantum tunneling for the electron occurs by changing from the tiny lines to the fat lines in Fig.1. For the binding energy $-V_0$, the creation rate of the electron positron is proportional to

$$\exp\left[-2\int_0^{V_0/|eE|}dx\sqrt{2m(V_0 - |eE|x)}\right] = \exp\left(-\frac{4}{3}\sqrt{2mV_0}\frac{V_0}{|eE|}\right), \tag{3.11}$$

by using the WKP approximation. The binding energy is $|V_0| = 2m_e$ because the mass gap between the electron and the positron is $2m_e$. Thus, the creation rate is proportional to $\exp(-\mathrm{const.}\, m_e^2/|eE|)$. The results of the WKB approximation coincide with the case of the instant on number $n = 1$ in (3.9) except overall factor.

In the QED, we obtain the Euler-Heisenberg Lagrangian which is the 1-loop effective Lagrangian. Similarly, the creation rates of the charged particles can be derived from

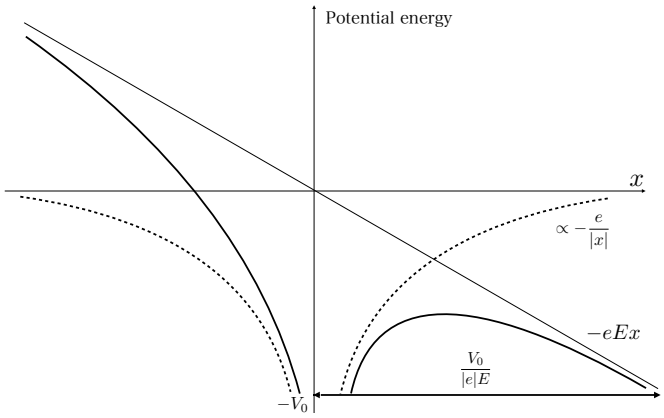

Figure 1: *The potential energy is the potential of the electron in an electric field. The dot lines means the Coulomb potential $\propto -e/|x|$. On the other hands, the linear line means the energy of the electron which receive the Coulomb force from the electric field as an external field. The bold line corresponds to the combination with the Coulomb potential and the the energy of the electron by the electric field.*

the 1-loop effective Lagrangian in electromagnetic fields except the QED. In QCD, we consider the quark antiquark pair creation in electromagnetic fields. But, we must evaluate the gluons loop effects because the gluon's coupling is strong. In next subsection, we introduce 't Hooft's idea.

3.2 Quark antiquark 1-loop Feynman diagram in large N QCD

In this subsection, we discuss the 1-loop quark antiquark diagram in quantum chromodynamics instead of the electron positron pair creation. The source term as an external field is $U(1)$ electromagnetic fields. The difference between the electron positron pair and the quark antiquark is for the quark antiquark to be coupled with gluons. Since the gluon coupling is strong, we must consider the all loop orders of the gluons and cannot use a perturbation. Then we introduce 't Hooft's idea and consider the large N gauge theory. The 't Hooft's idea is related to the AdS/CFT correspondence.

The Lagrangian which adds external $U(1)$ gauge fields to the QCD Lagrangian is

given by

$$\mathcal{L} = \mathcal{L}_{\rm QCD} - i\bar{\psi} e \not{A}^{\rm ex} \psi, \tag{3.12}$$

where,

$$\mathcal{L}_{\rm QCD} = -\frac{1}{4} F^a_{\mu\nu} F^{a\mu\nu} + \bar{\psi}(i\not{D} - m_q)\psi. \tag{3.13}$$

Here, $\not{D}$ is defined by $\not{D} \equiv \gamma^\mu D_\mu$. D_μ is $D_\mu = \partial_\mu - igA^a_\mu$. A^a_μ is the gluon fields. $A^{\rm ex}_\mu$ is the $U(1)$ gauge fields as external fields. ψ is a quark field and m_q is a quark mass. Also, $F^a_{\mu\nu}$ is field strength for the gluon fields and is defined as $F^a_{\mu\nu} = \partial_\mu A^a_\nu - \partial_\nu A^a_\mu + g f^{abc} A^b_\mu A^c_\nu$.

The 1-loop effective action in the QCD is given by

$$\mathcal{L}^{\rm QCD}_{\rm eff}(A^{\rm ex}_\mu) = -\frac{i}{\rm Vol} \ln \int \mathcal{D}\bar{\psi}\mathcal{D}\psi\mathcal{D}A^a_\mu \, \exp\left[i \int d^4x \, \mathcal{L} \right], \tag{3.14}$$

where Vol is 4-dimensional space-time volume.

In the QCD, the gluons are coupled to the 1-loop quark antiquark diagram. In particular, the Euler-Heisenberg Lagrangian receives the higher loop corrections for the gluons and is not good approximation for the perturbation since the QCD is a strongly coupled gauge theory. We introduce the 't Hooft's idea. When we consider the large N limit, planar diagrams are dominant in the Feynman diagrams.

3.2.1 't Hooft's idea

't Hooft introduced new Feynman diagrams which are called planar diagram [77]. The planar diagrams mean that we can describe the Feynman diagrams of the quarks and the gluons on the surface. If we take the large N limit, we find that the planar diagrams are dominant in the Feynman diagrams. Also, the large N strongly coupled gauge theory is compatible with the AdS/CFT correspondence. The physical quantities of the gauge theory is derived from the classical gravity more easily. Here, we introduce $1/N$ expanding according as the 't Hooft's discussion.

We review the 't Hooft's idea according to the Coleman's textbook [80]. We introduce the new indices for the $SU(N)$ gauge fields since the non-Abelian gauge fields are matrices. The gauge fields $A^a_{\mu b}$ are traceless Hermitian matrices. Then we obtain the condition as the following,

$$A^a_{\mu b} = A^{b\dagger}_{\mu a}, \quad A^a_{\mu a} = 0. \tag{3.15}$$

Thus, the field strength is

$$F^a_{\mu\nu b} = \partial_\mu A^a_{\nu b} - \partial_\nu A^a_{\mu b} + i[A_\mu, A_\nu]^a_{\ b}. \tag{3.16}$$

When we introduce the quark fields, quarks are the fundamental representation of the $SU(N)$ gauge group and have the index of the vector. Thus, the Lagrangian in the $SU(N)$ gauge theory is given by

$$\mathcal{L} = \frac{N}{g^2}\left[-\frac{1}{4}F^a_{\mu\nu b}F_a^{\mu\nu b} + \bar{\psi}_a(i\partial_\mu + A^a_{\mu b})\gamma^\mu\psi^a - m_q\bar{\psi}_a\psi^a\right], \tag{3.17}$$

where the Lagrangian doesn't include the $U(1)$ gauge fields as external fields. m_q is the quark mass. We determine that the gauge coupling is N/g^2 as the coupling of the quark and the gluons is unit. The propagator for the Dirac fields ψ^a becomes

$$\psi^a(x)\bar{\psi}_b(y) = \delta^a_{\ b}S(x-y). \tag{3.18}$$

$S(x-y)$ is the propagator for the single Dirac field. The propagator for the gluon fields $A^a_{\mu b}$ is

$$A^a_{\mu b}(x)A^c_{\nu d}(y) = \left(\delta^a_{\ d}\delta^c_{\ b} - \frac{1}{N}\delta^a_{\ b}\delta^c_{\ d}\right)D_{\mu\nu}(x-y). \tag{3.19}$$

$D_{\mu\nu}(x-y)$ is the propagator for the single gauge field. The second term in (3.19) becomes traceless condition.

Next, we introduce the new Feynman diagrams according as the 't Hooft's idea. The number of the lines is determined by the number of the indices of the fields. The fermion field ψ^a has a line and the gauge field $A^a_{\mu b}$ has two lines. Thus, the Dirac field coupled to the gauge field, the 3 point vertices and the 4 point vertices for the gauge fields are described in the different terms of the original Feynman diagrams. In particular, the loop diagrams are classified as the diagrams described on the surface or not. The former diagrams called planar diagrams, on the other hands, the latter diagrams called non-planar diagrams. It is important to treat the planar diagrams in the AdS/CFT correspondence.

Let us introduce the following rule before classifying the Feynman diagrams.

1) The propagators contribute the λ/N^2 factors.

2) The vertices contribute the N^2/λ factors.

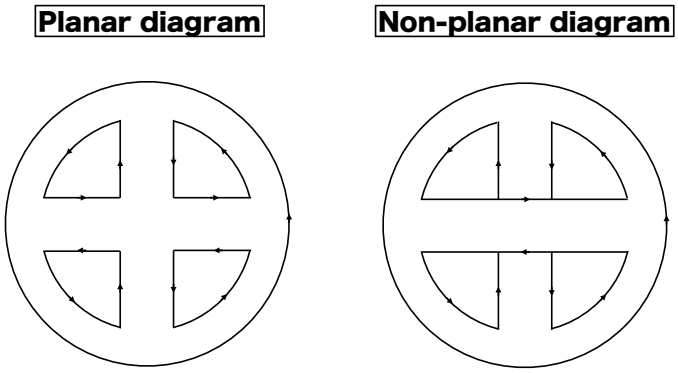

Figure 2: *The left figure is a planar diagram, while the right figure is a non-planar diagram. The left figure has five vertices, eight propagators and five loops, (V,E,F)=(5,8,5). On the other hands, the right figure has four vertices, six propagators and one loop, (V,E,F)=(4,6,1).*

3) The loop diagrams contribute the N factors.

Here, λ is a 't Hooft coupling which is defined as $\lambda = g^2 N$. For example, we see Fig.2. The left hand planar diagram has the five vertices, the eight propagators and the five loops. Thus, the planar diagram in Fig.2 is

$$(\text{The order of } \lambda, N) = \left(\frac{N^2}{\lambda}\right)^5 \left(\frac{\lambda}{N^2}\right)^8 N^5 = \lambda^3 N^{-1} \tag{3.20}$$

In general, the order of N in the planar diagrams is N^{-1}. The power of λ is large as the propagators increase. On the other hands, the right hand non-planar diagram has the four vertices, the six propagators and the one loop. Thus, the non-planar diagram in Fig. is

$$(\text{The order of } \lambda, N) = \left(\frac{N^2}{\lambda}\right)^4 \left(\frac{\lambda}{N^2}\right)^6 N^1 = \lambda^2 N^{-3}. \tag{3.21}$$

In general, the order of N in the non-planar diagram described on the surface of the torus is N^{-3}. The higher non-planar diagrams of $1/N$ expand can be described on the torus which has many genus. Thus, the planar and the non-planar diagrams are evaluated by

the following polynomial about λ, N,

$$(\text{ The diagram }) \propto g_0(\lambda)\frac{1}{N} + g_1(\lambda)\frac{1}{N^3} + g_2(\lambda)\frac{1}{N^5} + \cdots . \tag{3.22}$$

The planar diagram is contributed dominantly when we take the large N limit.

The $1/N$ expend method is not the summation of the Feynman diagrams for the gauge coupling expend such as the perturbation but the summation for the degree of freedom about the gauge group. It doesn't mean a perturbation. The method makes non-perturbative effects evaluated.

3.3 The massless quark antiquark pair creation in $\mathcal{N} = 2$ SQCD

In the previous subsection, we found that the planar diagram is dominant in the large N limit. In this subsection, the quark antiquark 1-loop amplitude becomes disk amplitude when we consider the strong coupling limit $\lambda \gg 1$. According to Hashimoto-Oka's conjecture, we derive the creation rate of the quark antiquark from evaluating the imaginary part of the DBI action in electromagnetic fields.

3.3.1 Hashimoto-Oka's conjecture

We discuss the relation between the Euler-Heisenberg Lagrangian in the $\mathcal{N} = 2$ SQCD and the DBI action in the electromagnetic fields according as the Hashimoto-Oka's conjecture [16]. Since QCD is the strongly coupled gauge theory, the vacuum amplitude for the quark antiquark pair creation contributes to the higher corrections for the gluons. We found that the planar diagram only contributes to the quark antiquark 1-loop diagrams with the 't Hooft's idea in the previous section. In this part, we discuss the quark antiquark 1-loop planar diagrams in the strong coupling limit $\lambda \gg 1$. The quark antiquark 1-loop planar diagram coincides with the disk amplitude such as Fig.3 in the strong coupling limit. The disk amplitude means that the fundamental open string propagates on the worldsheet in the string theory. It is well-known to derive the DBI action from the low energy effective action of the partition function for the open string in the flat target space background. The open string means the QCD string coupled to a quark and an antiquark in the QCD picture. Thus, according to the AdS/CFT correspondence, the Euler-Heisenberg Lagrangian in the $\mathcal{N} = 2$ large N supersymmetric gauge theory with

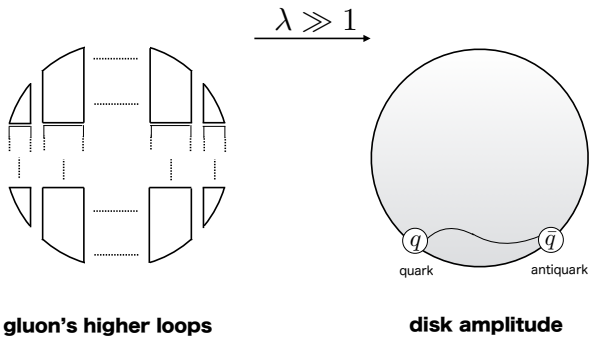

Figure 3: *In $\lambda \gg 1$, the 1-loop quark-antiquark diagram which has the gluon's higher loops corresponds to the disk amplitude. In QCD's picture, the disk regards the quark-antiquark pair as propagating on the worldsheet.*

flavors indicates the following relation in $\lambda \gg 1$,

$$\text{Euler-Heisenberg Lagramgian in } \mathcal{N} = 2 \text{ SQCD} = \text{DBI action in electromagnetic fields.} \quad (3.23)$$

Therefore, we need to evaluate the imaginary part of the DBI action in the electromagnetic fields in order to calculate the creation rate of the quark antiquark pair.

The vacuum instability corresponds to having the imaginary part of the DBI action. We consider the following condition in order to be vacuum unstable.

- We set $j = 0$ which is the current in the gauge theory from the gravity.
- We consider no fluctuation of the probe D-brane by the electromagnetic fields.

We assume that the above conditions indicate that the QCD vacuum is unstable.

Firstly, let us consider the example for the first condition. The positive charged particles and the negative charged particles cause the dielectric polarization by electric fields as external fields in the dielectric. Then, the current flows from the positive charged particles to the negative charged particles. This means that the stable system becomes unstable by the electric fields and the current flows in order to be stable for the system.

Thus, we examine that the current is zero when we introduce the electric fields, in order to know the quantities of the dielectric being unstable. Similarly, let us consider the QCD vacuum instability by the electromagnetic fields. If we introduce the electromagnetic fields to the vacuum, then the vacuum is unstable and the quark antiquark pair creation is caused by obtaining the energy for creating the quark antiquark pair. In fact, we can derive the current between the quark and the antiquark from the DBI action to which the D7 brane induced metric is substituted by using the GKP-Witten relation. When we consider the electric field in x-direction, the current j has the relation such as $j \propto \partial_z A_x$, where A_x is $U(1)$ gauge field in the gravity side. The current is substituted to the DBI action. In $j = 0$, the DBI action can have the imaginary part. On the other hands, the imaginary part of the DBI action is excluded in $j \neq 0$. That is, the unstable vacuum becomes stable because the current flows.

Secondly, the probe D-brane has the fluctuation fields when we introduce the the electromagnetic fields to the probe D-brane. Now, we consider the D3-D7 brane system in the subsection 2.4. The probe D7-brane fluctuates in the 89-directions. The background geometry is

$$ds^2 = \frac{u^2}{R^2}\eta_{\mu\nu}dx^\mu dx^\nu + \frac{R^2}{u^2}[d\rho^2 + \rho^2 d\Omega_3^2 + dw^2 + d\bar{w}^2], \tag{3.24}$$

from (2.8). The first term is 4-dimensional space-time. $\eta_{\mu\nu}$ is Minkowski metric which is defined as $\eta_{\mu\nu} = \mathrm{diag}(-1, 1, 1, 1)$. u is the parameter in the AdS direction. ρ is the radius of the 3-sphere and R is the AdS radius. w and $\bar{w}$ are the coordinate of the 89-directions respectively. u, ρ, w and $\bar{w}$ are associated with $u^2 = \rho^2 + w^2 + \bar{w}^2$. Since the $w, \bar{w}$ have the rotation symmetry, we fix $\bar{w}$ and consider the fluctuation of w. Thus, the induced metric on the D7-brane is given by

$$ds^2 = \frac{u^2}{R^2}\eta_{\mu\nu}dx^\mu dx^\nu + \frac{R^2}{u^2}[\{(\partial_\rho w)^2 + 1\}d\rho^2 + \rho^2 d\Omega_3^2]. \tag{3.25}$$

We consider the fluctuation of the probe D7-brane when we introduce the D7-brane to $U(1)$ gauge theory as F_{01}. Substituting the induced metric (3.25) to the D7-brane DBI action, the classical equation of motion is obtained by

$$\partial_\rho \left[\frac{\rho^3 \partial_\rho w \sqrt{1 - \frac{(2\pi\alpha')^2 R^4 F_{01}^2}{(\rho^2+w^2)^2}}}{\sqrt{(\partial_\rho w)^2 + 1}} \right] - \frac{2\rho^3 (2\pi\alpha')^2 R^4 F_{01}^2 w \sqrt{(\partial_\rho w)^2 + 1}}{(\rho^2 + w^2)^3 \sqrt{1 - \frac{(2\pi\alpha')^2 R^4 F_{01}^2}{(\rho^2+w^2)^2}}} = 0. \tag{3.26}$$

The solution w depends on ρ such as $w = w(\rho)$. In $F_{01} = 0$, w is a constant solution. According to the AdS/CFT dictionary, the constant coincides with a quark mass. In general, w doesn't become a constant solution because the D7-brane has the fluctuation by an external field. But, we are interested in vacuum instability when we add an external field to the stable vacuum without the external field. Therefore, we treat $w =$ const. when we examine the QCD vacuum instability by the electromagnetic fields.

3.3.2 The D7-brane DBI action in electromagnetic fields at a finite temperature

In this part, we evaluate the Euler-Heisenberg Lagrangian including constant electromagnetic fields in $\mathcal{N} = 2$ large N QCD according as [17]. It is difficult to evaluate the Schwinger effects in the strongly coupled QCD in order to be contribution of the gluon's loops. We calculate the creation rate of the quark antiquark pair in the $\mathcal{N} = 2$ SQCD with the gauge/gravity dual. In this part, we compute the Euler-Heisenberg Lagrangian in the case of the quark antiquark massless.

Let us consider the supersymmetric gauge theory on the boundary of an AdS space, which is $\mathcal{N} = 4$ supersymmetric Yang-Mills theory with a $\mathcal{N} = 2$ hypermultiplet with $SU(N_c)$ gauge group. The configuration of D-branes realizing the gauge theory is a D3-D7 brane system [12]. Taking a gravity dual, we use an AdS black hole metric as a background metric, in order to see the relation between the rate of quark antiquark creation and a temperature. The probe D7-brane in the AdS space has been well-studied to look at an electric conductivity, that is, an electric current determined by the external electric field [12, 70, 79]. The effective action (the D7-brane action in the AdS) is put to be real to determine the conductivity. Here on the other hand, we are interested in the instability caused by the external electromagnetic field, so the current j is put to zero (or takes some arbitrary value), giving an imaginary part in the effective action: this is how we obtain the Euler-Heisenberg Lagrangian [16].

The relation between a temperature and the AdS black hole is given by (2.14). Here, the function of $f(r)$ is $f(r) = r^2(1 - r_0^4/r^4)$. r_0 is the horizon of the AdS black hole. Also, the AdS radius R relates to the QCD coupling $g_{\rm QCD}$, the color N_c and α' as (2.13). Thus, we obtain

$$r_0 = \pi T, \qquad R^4 = 2g_{\rm QCD}^2 N_c \alpha'^2, \tag{3.27}$$

where α' is defined by $\alpha' = l_s^2$. As $r \equiv 1/z$, the AdS black hole metric is the following for (2.9),

$$ds^2 = \frac{R^2}{z^2}\left[-\left(1-\frac{z^4}{z_H^4}\right)dt^2 + \left(1-\frac{z^4}{z_H^4}\right)^{-1}dz^2 + d\vec{x}^2\right] + R^2 d\Omega_5^2, \tag{3.28}$$

where the coordinate z is the AdS radial direction, and $z = 0$ corresponds to the boundary of the AdS space, and $z = z_H$ is the horizon of the black hole. $d\vec{x}^2$ is defined by $d\vec{x}^2 = dx_1^2 + dx_2^2 + dx_3^2$. These parameters are given by the following relations between that of the gauge side and that of the gravity side:

$$z_H = \frac{1}{\pi T}, \qquad R^4 = 2\lambda\alpha'^2, \tag{3.29}$$

where $\lambda \equiv N_c g_{\rm QCD}^2$ is a 't Hooft coupling of the SQCD.

In the D3-D7 system, the D7-brane has the degree of freedom of the quark in the fundamental representation of the color $SU(N_c)$ gauge group by coupling to the D3-branes. Going to the gravity dual, the action in the gravity side is a D7-brane action in the AdS space. The D7-brane action is the following:

$$S_{D7} = -\mu_7 \int dt d^3\vec{x} dz d^3\Omega_3 \sqrt{-\det\left[P[g]_{ab} + 2\pi\alpha' F_{ab}\right]}, \tag{3.30}$$

where the factor μ_7 is the D7-brane tension, given by $\mu_7 \equiv 1/((2\pi)^7 g_s \alpha'^4)$. We need not consider the scalar fields on the D7-brane, since we are working for the massless SQCD.

The Euler-Heisenberg effective action is defined by

$$\mathcal{L} = -i \ln \langle e^{-i\int A_\mu^{\rm ext} j^\mu} \rangle_0, \tag{3.31}$$

which is a function of the external electric and magnetic fields represented by $A_\mu^{\rm ext}$. j^μ is the $U(1)$ current operator corresponding to the baryon charge, and the expectation value $\langle\ \rangle_0$ is taken with respect to the "false vacuum", i.e., the vacuum without the field which is now unstable. If the expectation value in (3.31) was taken with the true vacuum, the standard AdS/CFT dictionary [9, 10] states that the effective action is given by the D7-brane action evaluated with the reality condition for the action [12, 68, 79] and with the solution of the equation of motion. In ref. [16], Hashimoto and Oka proposed that the effective action (3.31) is given as the D7-brane action evaluated with the false-vacuum solution, i.e., the solution of the equation of motion without the electromagnetic fields.

Substituting the AdS black hole metric for the D7-brane action, the effective action becomes

$$\mathcal{L} = -2\pi^2 \mu_7 \int dz \frac{R^8}{z^5} \sqrt{\xi}, \tag{3.32}$$

where $d\Omega$-integral is $\mathrm{Vol}(S^3) = 2\pi^2$. The string coupling constant g_s is related to the gauge coupling constant of SQCD as $2\pi g_s = g^2_{\mathrm{QCD}}$. Without losing generality, we can choose the direction of the electromagnetic fields. Using the rotation symmetry, we fix the electric field to the x_1 direction. The magnetic fields are generic in x_1, x_2, x_3 directions. Then the ξ in the action is defined by the following:

$$\begin{aligned}\xi \equiv 1 &- \frac{(2\pi\alpha')^2 z^4}{R^4}\left[F_{0z}^2 + F_{01}^2 h(z)^{-1} - F_{1z}^2 h(z) - F_{12}^2 - F_{23}^2 - F_{13}^2\right] \\ &- \frac{(2\pi\alpha')^4 z^8}{R^8}[F_{23}^2\{F_{01}^2 h(z)^{-1} - F_{1z}^2 h(z)\} + F_{0z}^2\left\{F_{12}^2 + F_{23}^2 + F_{13}^2\right\}].\end{aligned} \tag{3.33}$$

The function $h(z)$ is defined as $h(z) = 1 - z^4/z_H^4$.

Consider rewriting the effective Lagrangian (3.33) in order to see the dependence on the charge density d and the current j. We derive the equations of motion from this action. Since we are interested in homogeneous phases, we simply put $\partial_i = 0$ $(i = 1, 2, 3)$. Then the equations of motion are the following:

$$\partial_z \left[\frac{F_{0z}}{z\sqrt{\xi}} + \frac{(2\pi\alpha')^2 z^3}{R^4\sqrt{\xi}} F_{0z}(F_{12}^2 + F_{23}^2 + F_{13}^2)\right] = 0, \tag{3.34}$$

$$\partial_0 \left[\frac{F_{0z}}{z\sqrt{\xi}} + \frac{(2\pi\alpha')^2 z^3}{R^4\sqrt{\xi}} F_{0z}(F_{12}^2 + F_{23}^2 + F_{13}^2)\right] = 0, \tag{3.35}$$

$$\partial_0 \left[\frac{F_{01}}{z\sqrt{\xi}} h(z)^{-1} + \frac{(2\pi\alpha')^2 z^3}{R^4\sqrt{\xi}} F_{01} F_{23}^2 h(z)^{-1}\right] + \partial_z \left[\frac{F_{1z}}{z\sqrt{\xi}} h(z) + \frac{(2\pi\alpha')^2 z^3}{R^4\sqrt{\xi}} F_{1z} F_{23}^2 h(z)\right] = 0. \tag{3.36}$$

In particular, the equations of motions in the case of time-independent field configurations are

$$\partial_z \left[\frac{F_{0z}}{z\sqrt{\xi}} + \frac{(2\pi\alpha')^2 z^3}{R^4\sqrt{\xi}} F_{0z}(F_{12}^2 + F_{23}^2 + F_{13}^2)\right] = 0, \tag{3.37}$$

$$\partial_z \left[\frac{F_{1z}}{z\sqrt{\xi}} h(z) + \frac{(2\pi\alpha')^2 z^3}{R^4\sqrt{\xi}} F_{1z} F_{23}^2 h(z)\right] = 0. \tag{3.38}$$

Next let us evaluate the charge density d and the current j in the gauge side. Using the dictionary of the AdS/CFT correspondence, they are respectively

$$d = \frac{2\pi\alpha' F_{0z}}{z\sqrt{\xi}} + \frac{(2\pi\alpha')^3 z^3}{R^4\sqrt{\xi}} F_{0z}(F_{12}^2 + F_{23}^2 + F_{13}^2), \tag{3.39}$$

$$j = \frac{2\pi\alpha' F_{1z}}{z\sqrt{\xi}} h(z) + \frac{(2\pi\alpha')^3 z^3}{R^4\sqrt{\xi}} F_{1z} F_{23}^2 h(z). \tag{3.40}$$

The solutions can be explicitly written as

$$A_0 = \mu - \int_0^z dz \frac{z R^4 d\sqrt{\xi}}{2\pi\alpha' R^4 + (2\pi\alpha')^3 z^4 (F_{12}^2 + F_{23}^2 + F_{13}^2)}, \tag{3.41}$$

$$A_1 = E_1 t - \int_0^z dz \frac{z R^4 j\sqrt{\xi}}{2\pi\alpha' R^4 h(z) + (2\pi\alpha')^3 z^4 F_{23}^2 h(z)}, \tag{3.42}$$

$$A_z = 0. \tag{3.43}$$

Here, μ is a constant and E_1 is a constant electric field. These charge density and current are substituted into ξ, to find

$$\xi = \frac{1 - \frac{(2\pi\alpha')^2 z^4}{R^4}(E_1^2 h(z)^{-1} - \vec{B}^2) - \frac{(2\pi\alpha')^4 z^8}{R^8}(E_1 B_1)^2 h(z)^{-1}}{1 + \frac{z^6 d^2}{R^4\left(1 + \frac{(2\pi\alpha')^2 z^4 \vec{B}^2}{R^4}\right)} - \frac{z^6 j^2 h(z)^{-1}}{R^4\left(1 + \frac{(2\pi\alpha')^2 z^4 B_1^2}{R^4}\right)}}, \tag{3.44}$$

where $F_{12} \equiv B_3$, $F_{23} \equiv B_1$, $F_{31} \equiv B_2$ are constant magnetic fields. Using this ξ, the effective Lagrangian with the constant electromagnetic fields is as follows:

$$\mathcal{L} = -2\pi^2 \mu_7 \int_0^{z_H} dz \frac{R^8}{z^5} \sqrt{\frac{1 - \frac{(2\pi\alpha')^2 z^4}{R^4}(E_1^2 h(z)^{-1} - \vec{B}^2) - \frac{(2\pi\alpha')^4 z^8}{R^8}(E_1 B_1)^2 h(z)^{-1}}{1 + \frac{z^6 d^2}{R^4\left(1 + \frac{(2\pi\alpha')^2 z^4 \vec{B}^2}{R^4}\right)} - \frac{z^6 j^2 h(z)^{-1}}{R^4\left(1 + \frac{(2\pi\alpha')^2 z^4 B_1^2}{R^4}\right)}}}. \tag{3.45}$$

When $j = 0$, the solution corresponds to the false vacuum, and (3.45) gives the Euler-Heisenberg effective action. This is our result from the AdS/CFT correspondence, and the basis for the following analyses. The imaginary part of the effective action gives half the inverse life time of the false vacuum.

When $j = 0$, using the spatial rotation symmetry, we can recover the full $\vec{E}$ and $\vec{B}$ dependence. The Euler-Heisenberg Lagrangian for a generic constant electromagnetic

field, at a finite temperature is

$$\mathcal{L} = -2\pi^2\mu_7 \int_0^{z_H} dz \frac{R^8}{z^5} \sqrt{\frac{1+\beta(z)\vec{B}^2 - \frac{\beta(z)}{h(z)}\vec{E}^2 - \frac{\beta(z)^2}{h(z)}\left(\vec{E}\cdot\vec{B}\right)^2}{1+\frac{z^2}{(2\pi\alpha')^2}\frac{\beta(z)}{1+\beta(z)\vec{B}^2}d^2}} \tag{3.46}$$

and $\beta(z) \equiv (2\pi\alpha')^2 z^4/R^4$. In particular, for the vanishing density $d = 0$, the Euler-Heisenberg Lagrangian is simplified as

$$\mathcal{L} = -2\pi^2\mu_7 \int_0^{z_H} dz \frac{R^8}{z^5} \sqrt{1+\beta(z)\vec{B}^2 - \frac{\beta(z)}{h(z)}\vec{E}^2 - \frac{\beta(z)^2}{h(z)}\left(\vec{E}\cdot\vec{B}\right)^2} \tag{3.47}$$

In the language of the massless $\mathcal{N} = 2$ SQCD, this Euler-Heisenberg Lagrangian (at a finite temperature and with $d = j = 0$) is written as

$$\mathcal{L} = -\frac{N_c\lambda}{2^3\pi^4} \int_0^{1/(\pi T)} \frac{dz}{z^5} \sqrt{1+\beta(z)\vec{B}^2 - \frac{\beta(z)}{h(z)}\vec{E}^2 - \frac{\beta(z)^2}{h(z)}\left(\vec{E}\cdot\vec{B}\right)^2} \tag{3.48}$$

where $\beta(z) = (2\pi^2/\lambda)z^4$ and $h(z) = 1 - (\pi T)^4 z^4$.

3.3.3 Imaginary part of Lagrangian in SQCD

We evaluate the imaginary part of the effective Lagrangian, and study the vacuum instability against not only the electric field but also the magnetic field in [17]. First, the imaginary part at zero temperature $T = 0$ and zero quark density diverges: The vacuum is not protected by a gap and thus extremely unstable. In a finite temperature case, the divergence is suppressed. In fact, assuming that the temperature provides a thermal mass for the quarks, the divergence of the imaginary part coincides with the result of a massive SQCD, and further with a supersymmetric QED, as we shall see in the next section.

In the previous subsection, we obtained the effective Lagrangian (3.45) with not only the constant electric field but also the constant magnetic field in the massless system. For simplicity, consider the case when the magnetic field is parallel to the electric field (E_1 and B_1 are nonzero). Then the effective Lagrangian is given by

$$\mathcal{L} = -2\pi^2\mu_7 \int_0^{z_H} dz \frac{R^8}{z^5} \sqrt{1 - \frac{(2\pi\alpha')^2 z^4}{R^4}(E_1^2 h(z)^{-1} - B_1^2) - \frac{(2\pi\alpha')^4 z^8}{R^8}(E_1 B_1)^2 h(z)^{-1}}. \tag{3.49}$$

We evaluate the imaginary part of the effective Lagrangian to derive the rate of the quark antiquark creation.

Consider the zero-temperature case, i.e., $z_H \to \infty$. Then the function $h(z)$ approaches unity. The z-integral of the imaginary part of the effective Lagrangian is dominated by the third term in the square root of the Lagrangian. Thus, this z-integral has a logarithmic divergence. Thus, in the presence of the magnetic field in addition to the electric field, the vacuum decay rate diverges for massless SQCD at strong coupling and at zero temperature. This is in sharp contrast with the zero magnetic field case in which $\mathrm{Im}\mathcal{L} = \frac{N_c}{32\pi}E^2$ is obtained [16]. In free Dirac systems, it is known that the divergence of the Euler-Heisenberg effective Lagrangian depends on dimensionality. In the pure electric field case (no magnetic field), for spatial dimension larger than two, the decay rate is finite, while for a (1+1)-dimensional system a divergence takes place. Our finding can be understood as an effective dimension reduction by the magnetic field. In a finite magnetic field, Landau levels are formed and the dispersion becomes flat in the two directions perpendicular to the field. Starting from three spatial dimensions, the magnetic field reduces the effective dimension to one. This may explain the divergence we obtain, although, it is unclear if the argument holds for a strongly interacting model.

In a finite temperature system, the divergence of the decay rate is suppressed. In order to evaluate the imaginary part of effective Lagrangian, we change the variable z of this integral to y defined by $y \equiv z/z_H$,

$$\mathcal{L} = -2\pi^2\mu_7(2\pi\alpha')^2R^4\chi\int_0^1\frac{dy}{y^5}\sqrt{1-\frac{y^4}{\chi}(E_1^2(1-y^4)^{-1}-B_1^2)-\frac{y^8}{\chi^2}(E_1B_1)^2(1-y^4)^{-1}}\,, \tag{3.50}$$

where χ is defined as $\chi \equiv R^4/(2\pi\alpha')^2z_H^4$. As mentioned above, we found that the imaginary part of the Lagrangian diverges in the limit $T \to 0$. In order to see the dependence on χ in the square root, we further change the variable y to $Y \equiv \chi^{-\frac{1}{4}}y$,

$$\mathcal{L} = -2\pi^2\mu_7(2\pi\alpha')^2R^4\int_0^{\chi^{-\frac{1}{4}}}dY\,\frac{\sqrt{1-(\chi+E_1^2-B_1^2)Y^4-\chi B_1^2Y^8-(E_1B_1)^2Y^8}}{Y^5\sqrt{1-\chi Y^4}}\,. \tag{3.51}$$

Let us look for the value of Y at which the integrand turns from real to imaginary. Since χ is small, we can ignore $\mathcal{O}(\chi)$ term in the numerator, to find the value as $Y = 1/\sqrt{E_1}$.

So the imaginary part of $\mathcal{L}$ is from the integral over the region $1/\sqrt{E_1} < Y < \chi^{-\frac{1}{4}}$. At the integration, the forth term in the square root of the numerator in the integrand becomes dominant for small χ, hence the imaginary part of the Lagrangian is approximately given by

$$\text{Im } \mathcal{L} \sim 2\pi^2 \mu_7 (2\pi\alpha')^2 R^4 (E_1 B_1) \int_{1/\sqrt{E_1}}^{\chi^{-\frac{1}{4}}} \frac{dY}{Y\sqrt{1-\chi Y^4}} \,. \tag{3.52}$$

Performing the integral for small χ leads to

$$\text{Im } \mathcal{L} \sim \frac{N_c}{4\pi^2} E_1 B_1 \log \frac{1}{T}, \tag{3.53}$$

where we find a logarithmic dependence on the temperature.

Let us evaluate the imaginary part of the Euler-Heisenberg Lagrangian for a generic constant electromagnetic field in a temperature. For small T, we obtain the following dominant term in the divergence,

$$\text{Im } \mathcal{L}_{T\neq 0} = \frac{N_c}{4\pi^2} \left| \vec{E} \cdot \vec{B} \right| \log \frac{b(E,B)}{T} + \mathcal{O}(T^0) \,, \tag{3.54}$$

where the constant b is defined as

$$b(E,B) \equiv \left[\frac{1}{2} \left(\vec{E}^2 - \vec{B}^2 + \sqrt{\left(\vec{E}^2 - \vec{B}^2 \right)^2 + 4 \left(\vec{E} \cdot \vec{B} \right)^2} \right) \right]^{1/4} . \tag{3.55}$$

In addition, in a finite density system, we find a density dependence ($d \neq 0$ but at $T = 0$),

$$\text{Im } \mathcal{L}_{d\neq 0} = \frac{N_c}{4\pi^2} \left| \vec{E} \cdot \vec{B} \right| \log \frac{1}{d} + \cdots \,. \tag{3.56}$$

This logarithmic dependence is quite similar to the finite temperature case (3.54). In fact, we see in the following that this form is quite common and has a physical interpretation, see (3.71).

3.4 The massive quark antiquark pair creation in $\mathcal{N} = 2$ SQCD

In this section, we evaluate the Euler-Heisenberg Lagrangian for the strongly coupled $\mathcal{N} = 2$ SQCD with a quark mass in constant electromagnetic fields. In zero temperature, the creation rate of the massive quark antiquark pair is finite unlike the case of the massless quark antiquark pair. The leading term coincides with that of a weakly coupled supersymmetric QED.

3.4.1 Critical electric field

In this section, for simplicity, we consider $T = 0$ and $d = 0$. First, let us take a D7-brane configuration of the SQCD with vanishing electromagnetic fields. The induced metric on the D7-brane is [12]

$$ds^2 = \frac{R^2}{z^2}\tilde{h}(z)\,(dx^\mu)^2 + \frac{R^2}{z^2\tilde{h}(z)}\left(dz^2 + d\Omega_3^2\right)\,, \tag{3.57}$$

where $\mu = 0, 1, 2, 3$ and $d\Omega_3^2$ is the metric of a unit 3-sphere, and

$$\tilde{h}(z) \equiv 1 + \frac{z^2\eta^2}{R^2}\,. \tag{3.58}$$

The constant η specifies the location of the D7-brane, which is physically related to the quark mass by

$$\frac{\eta}{2\pi\alpha'} = m_q\,. \tag{3.59}$$

Turning on the constant electromagnetic fields on the D7-brane, we obtain the Euler-Heisenberg Lagrangian for the strongly coupled $\mathcal{N} = 2$ SQCD

$$\mathcal{L} = -2\pi^2\mu_7\int_0^\infty dz\,\frac{R^8}{z^5}\sqrt{\xi} \tag{3.60}$$

with

$$\xi \equiv 1 + \beta(z)\tilde{h}(z)^{-2}\left(\vec{B}^2 - \vec{E}^2\right) - \beta(z)^2\tilde{h}(z)^{-4}\left(\vec{E}\cdot\vec{B}\right)^2\,. \tag{3.61}$$

The $\vec{B} = 0$ result agrees with [16], and when $\eta = 0$, it reproduces our massless SQCD result (3.47) at $T = 0$.

We can evaluate the critical electric field above which the effective Lagrangian acquires an imaginary part. Solving $\xi = 0$ for z results in and equation

$$\tilde{h}(z)^2 = \beta(z)b^4 \tag{3.62}$$

where the constant $b(E, B)$ is defined in (3.55). This equation is simplified as

$$1 = \left(\frac{2\pi\alpha'}{R^2}b^2 - \frac{\eta^2}{R^4}\right)z^2\,. \tag{3.63}$$

In order for this to have a solution, we need

$$b(E,B) > \frac{\eta}{\sqrt{2\pi\alpha'}R} = \left(\frac{2\pi^2}{\lambda}\right)^{1/4} m_q\,. \tag{3.64}$$

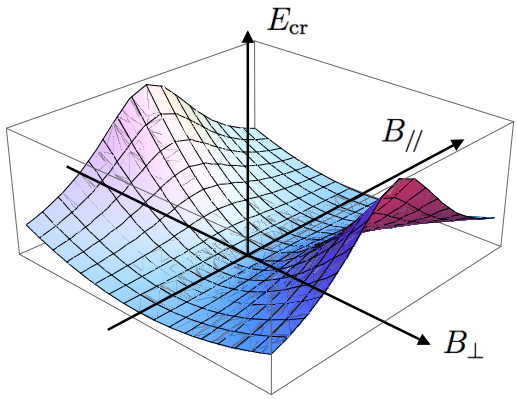

Figure 4: *A plot of the critical electric field $E_{\rm cr}$ as a function of the magnetic field $B_{//}$ and $B_\perp$, for nonzero m_q. We find that the magnetic field makes the critical electric field larger.*

This is the condition for having an imaginary part in the Euler-Heisenberg Lagrangian, a signal for vacuum instability. Without the magnetic field ($\vec{B} = 0$), this condition (3.64) reduces to the critical electric field found in [16],

$$|\vec{E}| > \left(\frac{2\pi^2}{\lambda}\right)^{1/2} m_q^2 \,. \tag{3.65}$$

Let us study magnetic field dependence of the critical electric field. The critical electric field $E_{\rm cr}$ is a solution of the equation

$$b(E_{\rm cr}, B) = \left(\frac{2\pi^2}{\lambda}\right)^{1/4} m_q \,. \tag{3.66}$$

Decomposing the magnetic field to two components $B_{//}$ and $B_\perp$ (parallel / perpendicular to the electric field), we can plot the value of the critical electric field as a function of the magnetic field $B_{//}$ and $B_\perp$, see Fig. 4. We find that the magnetic field does not lower the critical electric field. In fact, the critical electric field is minimized when the perpendicular magnetic field $B_\perp$ vanishes, and the minimized value is equal to the critical electric field in the absence of the magnetic field (3.65). In the zero magnetic field case, the critical field coincides with the confining force [16]. This is natural because the vacuum instability takes place when the quark-antiquarks are pulled apart with a force

stronger than the confining force. It is strange that the critical field has a $B_\perp$ dependence because the gluons mediating the confinement force is not affected by the magnetic field. We leave this puzzle for future consideration.

3.4.2 Vacuum decay rate in the small mass limit

When the quark mass is finite, the vacuum decay rate, i.e., the imaginary part of the effective action, is non-diverging, even above the critical field. Here, we evaluate the small mass asymptotic behavior of the vacuum decay rate. As shown in the previous section, the divergence of the decay rate originates from the integral at large z. With non-zero mass represented by the parameter $\eta \neq 0$, the function $\tilde{h}(z)$ has the following z dependence ($z_* \equiv R^2/\eta$)

$$\tilde{h}(z) \sim \begin{cases} 1 & (z \ll z_*), \\ \frac{\eta^2}{R^4} z^2 & (z \gg z_*). \end{cases} \tag{3.67}$$

This alters the divergent behavior of the integral: For $z \gg z_*$, the integrand of the effective Lagrangian behaves as

$$\frac{R^8}{z^5}\sqrt{\xi} \sim z^{-5}, \tag{3.68}$$

whose integral is convergent. The leading behavior of the imaginar part is given by

$$\text{Im } \mathcal{L} \sim 2\pi^2 \mu_7 \int_{z_0}^{z_*} dz \, \frac{R^8}{z^5} \frac{(2\pi\alpha')^2}{R^4} z^4 \left| \vec{E} \cdot \vec{B} \right|, \tag{3.69}$$

where the massless limit corresponds to $z_* \to \infty$. The lower bound of the integral z_0 is determined by the condition that the Lagrangian becomes imaginary, and is the solution of equation (3.63)

$$z_0 \equiv \left(\frac{2\pi\alpha'}{R^2} b^2 - \frac{\eta^2}{R^4} \right)^{-1/2}. \tag{3.70}$$

The divergence appears when $z_0 \ll z_*$, and the leading term is given by (3.69) which is evaluated as

$$\begin{aligned} \text{Im } \mathcal{L} &= \frac{N_c}{4\pi^2} \left| \vec{E} \cdot \vec{B} \right| \log \frac{z_*}{z_0} + \cdots \\ &= \frac{N_c}{4\pi^2} \left| \vec{E} \cdot \vec{B} \right| \log \frac{b(E,B)}{m_q} \ + \ \text{higher in } \ \frac{m_q}{b(E,B)}. \end{aligned} \tag{3.71}$$

Interestingly, this divergence coincides with (3.54) if we replace the temperature T with the quark mass m_q. The linear relation between the temperature and the quark mass is commonly found in thermal field theories at weak coupling, and our strongly coupled results are consistent with that. We shall see later that our asymptotic behavior (3.71), agrees with a weak coupling calculation of $\mathcal{N}=2$ supersymmetric QED.

3.4.3 Coincidence with $\mathcal{N}=2$ supersymmetric QED

In this part, we compare the Euler-Heisenberg Lagrangian of SQCD with the one-loop result of $\mathcal{N}=2$ supersymmetric QED. A priori, we expect no relation between them because our SQCD is with self-interacting gluons and is evaluated at strong coupling through the AdS/CFT correspondence, while the SQED is a weak coupling and photons are not interacting with each other at the one-loop level. However, unexpectedly, we find several coincidences: First is the small electric field asymptotic of the vacuum decay rate, and the second is the leading nonlinear electromagnetic response coefficients. This agreement may be attributed to the supersymmetries. It is known via AdS/CFT correspondence that in SQCD the gluon has a Coulombic potential, that is presumably why we find the agreement in the following. So, in one aspect, our report here should serve as a consistency check of our calculation of the imaginary D-brane action in the AdS/CFT correspondence.

First, let us check the divergence in the imaginary part. The one-loop QED [78] has the following expression for the effective Lagrangian when $\vec{E}$ is parallel to $\vec{B}$;

$$\text{Im}\,\mathcal{L}_{\text{scalar}} = \frac{EB}{8\pi^2}\sum_{l=1}^{\infty}\frac{(-1)^{l+1}}{l}\frac{\exp[-\pi l m^2/E]}{2\sinh(\pi lB/E)}\,, \tag{3.72}$$

$$\text{Im}\,\mathcal{L}_{\text{spinor}} = \frac{EB}{8\pi^2}\sum_{l=1}^{\infty}\frac{1}{l}\exp[-\pi l m^2/E]\coth(\pi lB/E)\,. \tag{3.73}$$

Here $\mathcal{L}_{\text{scalar}}$ denotes scalar QED (the charged particle is a scalar bosonic field) and $\mathcal{L}_{\text{spinor}}$ is for the ordinary QED. To have $\mathcal{N}=2$ supersymmetry, we need $2N_c$ scalars and N_c spinors, and thus

$$\begin{aligned}\text{Im}\,\mathcal{L}_{\mathcal{N}=2\text{ SQED}} &= N_c\,(\text{Im}\,\mathcal{L}_{\text{spinor}} + 2\,\text{Im}\,\mathcal{L}_{\text{scalar}}) \\ &= \frac{N_c EB}{8\pi^2}\sum_{l=1}^{\infty}\frac{1}{l}\exp[-\pi l m^2/E]\frac{\cosh(\pi lB/E)+(-1)^{l+1}}{\sinh(\pi lB/E)}\,.\end{aligned} \tag{3.74}$$

Let us consider a limit of electron mass m going to zero. In the expression above, the factor $\exp[-\pi l m^2/E]$ serves as a cut-off of the summation over l. Therefore we can approximate it as

$$\text{Im}\,\mathcal{L}_{\mathcal{N}=2\text{ SQED}} \sim \frac{N_c EB}{8\pi^2}\sum_{l=1}^{E/\pi m^2}\frac{1}{l}\frac{\cosh(\pi lB/E)+(-1)^{l+1}}{\sinh(\pi lB/E)}\,. \tag{3.75}$$

The divergence is due to $\cosh/\sinh \sim 1$ for large l, so, for large E/m^2 we can further approximate it as[2]

$$\begin{aligned}\text{Im}\,\mathcal{L}_{\mathcal{N}=2\text{ SQED}} &\sim \frac{N_c EB}{8\pi^2}\sum_{l=1}^{E/\pi m^2}\frac{1}{l} \sim \frac{N_c EB}{8\pi^2}\log\frac{E}{\pi m^2}\\ &\sim \frac{N_c}{4\pi^2}EB\log\frac{\sqrt{E}}{m}\,.\end{aligned} \tag{3.76}$$

We find that this SQED result is in agreement with our SQCD result (3.71).

3.5 The quark-antiquark pair creation in confining large N gauge theory

In this subsection, we study a quark antiquark pair creation in the confining phase [18]. The Sakai-Sugimoto model is the D-brane construction of the D4-D8 brane which has the $SU(N_f)_L \times SU(N_f)_R$ chiral symmetry and the confining phase [14]. We will obtain the creation rate of the quark antiquark in the confining non-supersymmetric gauge theory by evaluating the imaginary part of the D8-brane action with a constant electromagnetic field. Also, the critical electric field is obtained by a threshold at which the D8-brane action acquires a non-vanishing imaginary part.

3.5.1 Review of the Sakai-Sugimoto model

The D-brane contruction of the Sakai-Sugimoto model is with D4- and D8-branes. The D4-D8 brane constriction is given by the following.

[2] In literature, this expression for the dominant imaginary part in QED (non-supersymmetric) can be found in [5, 6].

	0	1	2	3	(4)	5	6	7	8	9
D4	√	√	√	√	√					
D8	√	√	√	√		√	√	√	√	√
anti-D8	√	√	√	√		√	√	√	√	√

A spatial coordinate x^4 of the spatial world-volume directions is compactified on S^1 with an anti-periodic boundary conditions for the fermions. The N_f D8-branes intersect $x^4 = 0$ with the D4-branes. Similarly, the N_c anti-D8-branes put parallel at $x^4 = \pi R$. Here, the R is the radius of S^1. We consider a flavor $N_f = 1$ for simplicity in this paper.[3]

The D4-branes metric is

$$ds^2_{D4} = \left(\frac{u}{R_{D4}}\right)^{3/2}(-dt^2 + \delta_{ij}dx^i dx^j + f(u)(dx^4)^2) + \left(\frac{R_{D4}}{u}\right)^{3/2}\left(\frac{du^2}{f(u)} + u^2 d\Omega_4^2\right). \tag{3.77}$$

The dilaton, the field strength of the Ramond-Ramond field, the function $f(u)$ and the AdS radius are defined as follows,

$$e^{\phi} = g_s\left(\frac{u}{R_{D4}}\right)^{3/4}, \quad F_4 \equiv dC_3 = \frac{2\pi N_c}{V_4}\epsilon_4, \quad f(u) \equiv 1 - \frac{u_{KK}^3}{u^3}, \quad R^3_{D4} \equiv \pi g_s N_c l_s^3, \tag{3.78}$$

where g_s is a string coupling and N_c is the number of colors gauge group. String length is l_s and is related to α' as $l_s^2 = \alpha'$. The coordinate u is the holographic radial direction, and $u = \infty$ corresponds to the boundary of the bulk space. The coordinate u is defined for the region $u_{KK} \leq u \leq \infty$. V_4 is the volume of the unit four sphere S^4. ϵ_4 is the volume form of the S^4. In order to avoid a possible singularity at $u = u_{KK}$, the coordinate u is follows a periodic boundary condition as follows,

$$x^4 \sim x^4 + \delta x^4, \quad \delta x^4 \equiv \frac{4\pi}{3}\frac{R_{D4}^{3/2}}{u_{KK}^{1/2}} = 2\pi R. \tag{3.79}$$

The Kaluza-Klein mass parameter is defined as follows,

$$M_{KK} \equiv \frac{2\pi}{\delta x^4} = \frac{3}{2}\frac{u_{KK}^{1/2}}{R_{D4}^{3/2}}. \tag{3.80}$$

[3]Since we consider the $N_f = 1$ D8-brane, the system does not have any charged mesons (which would have been created if they are lighter).

The gauge coupling g_{YM} at the cutoff scale M_{KK} in the 4-dimensional Yang-Mills theory is derived as $g_{YM}^2 = (2\pi)^2 g_s l_s/\delta x^4$ from the D4-brane action compactified on S^1. Thus, the AdS/CFT dictionary which is the relationship between the parameters R_{D4}, u_{KK}, g_s in the gravity side and the parameters $M_{KK}, g_{YM}N_c$ in the gauge side is the following,

$$R_{D4}^3 = \frac{1}{2}\frac{\lambda l_s^2}{M_{KK}}, \quad u_{KK} = \frac{2}{9}\lambda M_{KK} l_s^2, \quad g_s = \frac{1}{2\pi}\frac{\lambda}{M_{KK}N_c l_s}, \tag{3.81}$$

where a 't Hooft coupling λ is defined as $\lambda \equiv g_{YM}^2 N_c$.

Next, we consider a D8-brane embedded in the D4-brane background. The D8-brane and the anti-D8-brane are inserted respectively to $x^4 = 0$ and $x^4 = \pi R$. Under this boundary condition, the equation of motion requires $dx^4/du = 0$ which means that the coordinate x^4 of the D8-brane and anti-D8-brane is constant. Then, the induced metric on the D8-brane is

$$ds_{D8}^2 = \left(\frac{u}{R_{D4}}\right)^{3/2}(-dt^2 + \delta_{ij}dx^i dx^j) + \left(\frac{R_{D4}}{u}\right)^{3/2}\left(\frac{du^2}{f(u)} + u^2 d\Omega_4^2\right). \tag{3.82}$$

The D8-brane action is represented by

$$S_{D8} = S_{D8}^{\rm DBI} + S_{D8}^{\rm CS}. \tag{3.83}$$

The $S_{D8}^{\rm DBI}$ is the D8-brane Dirac-Born-Infeld(DBI) action and the $S_{D8}^{\rm CS}$ is the D8-brane Chern-Simons term. We do not consider the Chern-Simons term in this paper.

3.5.2 Euler-Heisenberg Lagrangian of the Sakai-Sugimoto model

We shall calculate the Euler-Heisenberg Lagrangian. It is simply the DBI action with a constant electromagnetic field. We substitute the D8-brane background and a constant electromagnetic field to the DBI action. The constant electromagnetic field on the S^4 is zero. We turn on only the electric field on the x^1 direction without losing generality due the spacial rotational symmetry. The magnetic fields are introduced in x^1, x^2, x^3 directions. The DBI action in the D8-brane background including a constant electromagnetic field is given by

$$S_{D8}^{\rm DBI} = -T_8 \int d^4x du d\Omega_4 e^{-\phi}\sqrt{-\det(P[g]_{ab} + 2\pi\alpha' F_{ab})}, \tag{3.84}$$

where T_8 is a D8-brane tension and defined as $T_8 = 1/(2\pi)^8 l_s^9$. Substituting the D8-brane background and the constant electromagnetic field to the D8-brane action, the effective Lagrangian is obtained by

$$\mathcal{L} = -\frac{8\pi^2}{3} T_8 \int_{u_{KK}}^{\infty} du\, e^{-\phi} \frac{u^4}{\sqrt{f(u)}} \left(\frac{R_{D4}}{u}\right)^{3/4} \sqrt{\xi}, \tag{3.85}$$

where the $d\Omega_4$ integral is Vol(S^4)=$8\pi^2/3$. Here ξ is defined by

$$\begin{aligned}\xi \equiv 1 &- \frac{(2\pi\alpha')^2 R_{D4}^3}{u^3}\left[F_{01}^2 - F_{12}^2 - F_{23}^2 - F_{13}^2 + f(u)\frac{u^3}{R_{D4}^3}(F_{0u}^2 - F_{1u}^2)\right] \\ &- \frac{(2\pi\alpha')^4 R_{D4}^6}{u^6}\left[F_{01}^2 F_{23}^2 + f(u)\frac{u^3}{R_{D4}^3}\{F_{0u}^2(F_{12}^2 + F_{23}^2 + F_{13}^2) - F_{1u}^2 F_{23}^2\}\right].\end{aligned} \tag{3.86}$$

Next, we derive the equations of motion from the DBI action. We put $\partial_i = 0$, $(i = 1, 2, 3)$ because we are interested in homogeneous phases. The equations of motion are given by [4]

$$\frac{(2\pi\alpha')^2 8\pi^2 T_8}{3g_s}\partial_u \left[\frac{(R_{D4}/u)^{3/2} u^4 \sqrt{f(u)} F_{0u}\left(1 + \frac{(2\pi\alpha')^2 R_{D4}^3}{u^3}\right)(F_{12}^2 + F_{23}^2 + F_{13}^2)}{\sqrt{\xi}}\right] = 0, \tag{3.87}$$

$$\frac{(2\pi\alpha')^2 8\pi^2 T_8}{3g_s}\partial_0 \left[\frac{(R_{D4}/u)^{3/2} u^4 \sqrt{f(u)} F_{0u}\left(1 + \frac{(2\pi\alpha')^2 R_{D4}^3}{u^3}\right)(F_{12}^2 + F_{23}^2 + F_{13}^2)}{\sqrt{\xi}}\right] = 0, \tag{3.88}$$

[4] When both the electric and the magnetic fields are nonzero, the Chern-Simons term comes into the equations of motion. Since the Chern-Simons term is of the form $\sim A_u EB$, the equations of motion for A_u acquire a new term, $\partial_0 A_u \sim EB$. This is nothing but the chiral anomaly. The field A_u grows in time for a constant E and B. We ignore this anomaly effect for simplicity, and interpret our outcome as the physical values measured at $t = 0$ at which A_u vanishes as an initial condition.

$$\frac{(2\pi\alpha')^2 8\pi^2 T_8}{3g_s}\partial_0\left[\frac{(R_{D4}/u)^{9/2}u^4 F_{01}\left(1+\frac{(2\pi\alpha')^2R_{D4}^3}{u^3}F_{23}^2\right)}{\sqrt{\xi f(u)}}\right]+$$
$$\frac{(2\pi\alpha')^2 8\pi^2 T_8}{3g_s}\partial_u\left[\frac{(R_{D4}/u)^{3/2}u^4\sqrt{f(u)}F_{1u}\left(1+\frac{(2\pi\alpha')^2R_{D4}^3}{u^3}F_{23}^2\right)}{\sqrt{\xi}}\right]=0. \tag{3.89}$$

In particular, the equations of motion for static configurations are derived as

$$\frac{(2\pi\alpha')^2 8\pi^2 T_8}{3g_s}\partial_u\left[\frac{(R_{D4}/u)^{3/2}u^4\sqrt{f(u)}F_{0u}\left(1+\frac{(2\pi\alpha')^2R_{D4}^3}{u^3}\right)(F_{12}^2+F_{23}^2+F_{13}^2)}{\sqrt{\xi}}\right]=0, \tag{3.90}$$

$$\frac{(2\pi\alpha')^2 8\pi^2 T_8}{3g_s}\partial_u\left[\frac{(R_{D4}/u)^{3/2}u^4\sqrt{f(u)}F_{1u}\left(1+\frac{(2\pi\alpha')^2R_{D4}^3}{u^3}F_{23}^2\right)}{\sqrt{\xi}}\right]=0. \tag{3.91}$$

By using the equations of motion, we can derive the charge density d and the current density j respectively as,

$$d\equiv\frac{(2\pi\alpha')^2 8\pi^2 T_8}{3g_s}\frac{(R_{D4}/u)^{3/2}u^4\sqrt{f(u)}F_{0u}\left(1+\frac{(2\pi\alpha')^2R_{D4}^3}{u^3}\right)(F_{12}^2+F_{23}^2+F_{13}^2)}{\sqrt{\xi}}, \tag{3.92}$$

$$j\equiv\frac{(2\pi\alpha')^2 8\pi^2 T_8}{3g_s}\frac{(R_{D4}/u)^{3/2}u^4\sqrt{f(u)}F_{1u}\left(1+\frac{(2\pi\alpha')^2R_{D4}^3}{u^3}F_{23}^2\right)}{\sqrt{\xi}}. \tag{3.93}$$

In this paper, we are not interested in the charge density and the current as we are looking at the vacuum instability. So we put $F_{0u}=0$ and $F_{1u}=0$ consistently.

Therefore, the D8-brane Lagrangian is derived as

$$\mathcal{L}=-\frac{8\pi^2 T_8}{3g_s}\int_{u_{KK}}^{\infty}du\,\frac{u^4(R_{D4}/u)^{3/2}}{\sqrt{1-\frac{u_{KK}^3}{u^3}}}\sqrt{1-\frac{(2\pi\alpha')^2R_{D4}^3}{u^3}\left[E_1^2-\vec{B}^2\right]-\frac{(2\pi\alpha')^4R_{D4}^6}{u^6}E_1^2B_1^2}, \tag{3.94}$$

where we define the constant electric field as $F_{01}\equiv E_1$ and the constant magnetic fields as $F_{12}\equiv B_3, F_{23}\equiv B_1, F_{13}\equiv B_2$, $\vec{B}^2\equiv B_1^2+B_2^2+B_3^2$. We change the variable u in this integral to a new coordinate y defined by $u=u_{KK}/y$. By using the dictionary

of the AdS/CFT correspondence, we reach the non-supersymmetric Euler-Heisenberg Lagrangian at large N_c,

$$\mathcal{L} = -\frac{M_{KK}^4 \lambda^3 N_c}{2 \cdot 3^8 \pi^5} \int_0^1 dy \frac{\sqrt{1 - \frac{3^6\pi^2}{4M_{KK}^4\lambda^2} y^3 (E_1^2 - \vec{B}^2) - \left(\frac{3^6\pi^2}{4M_{KK}^4\lambda^2}\right)^2 y^6 E_1^2 B_1^2}}{y^{9/2}\sqrt{1-y^3}}. \tag{3.95}$$

3.5.3 Imaginary part of the effective action in Sakai-Sugimoto model

In the previous part, we obtained the Euler-Heisenberg Lagrangian (3.94). Let us evaluate the imaginary part from the effective Lagrangian.

We look at the region of the u where the imaginary part of the Euler-Heisenberg Lagrangian (3.94) appears: the square root of the numerator in the integrand of (3.94) needs less than zero,

$$1 - \frac{(2\pi\alpha')^2 R_{D4}^3}{u^3}\left[E_1^2 - \vec{B}^2\right] - \frac{(2\pi\alpha')^4 R_{D4}^6}{u^6} E_1^2 B_1^2 < 0. \tag{3.96}$$

Note that the region of the original integral in (3.94) is from u_{KK} to ∞. The condition for the variable u such that the imaginary part of the Euler-Heisenberg Lagrangian is nonzero is given by

$$u_{KK} \leq u \leq \left[\frac{(2\pi\alpha')^2 R_{D4}^3}{2}\left\{E_1^2 - \vec{B}^2 + \sqrt{(E_1^2 - \vec{B}^2)^2 + 4E_1^2 B_1^2}\right\}\right]^{1/3}. \tag{3.97}$$

Thus, the imaginary part of the effective Lagrangian is obtained as

$$\mathrm{Im}\mathcal{L} = \frac{8\pi^2 T_8}{3g_s}\int_{u_{KK}}^{u_*} du \frac{u^4 (R_{D4}/u)^{3/2}}{\sqrt{1 - \frac{u_{KK}^3}{u^3}}}\sqrt{\frac{(2\pi\alpha')^4 R_{D4}^6}{u^6} E_1^2 B_1^2 + \frac{(2\pi\alpha')^2 R_{D4}^3}{u^3}\left[E_1^2 - \vec{B}^2\right] - 1}, \tag{3.98}$$

where the u_* is defined by

$$u_* \equiv \left[\frac{(2\pi\alpha')^2 R_{D4}^3}{2}\left\{E_1^2 - \vec{B}^2 + \sqrt{(E_1^2 - \vec{B}^2)^2 + 4E_1^2 B_1^2}\right\}\right]^{1/3}. \tag{3.99}$$

The region of the integral is shown in Fig.5.

In terms of the integral variable y, the imaginary part is

$$\mathrm{Im}\mathcal{L} = \frac{N_c \lambda^3 M_{KK}^4}{2 \cdot 3^8 \pi^5}\int_{y_*}^1 dy \frac{\sqrt{\left(\frac{3^6\pi^2}{4\lambda^2 M_{KK}^2}\right)^2 y^6 E_1^2 B_1^2 + \frac{3^6\pi^2}{4\lambda^2 M_{KK}^2} y^3\left[E_1^2 - \vec{B}^2\right] - 1}}{y^{9/2}\sqrt{1-y^3}}, \tag{3.100}$$

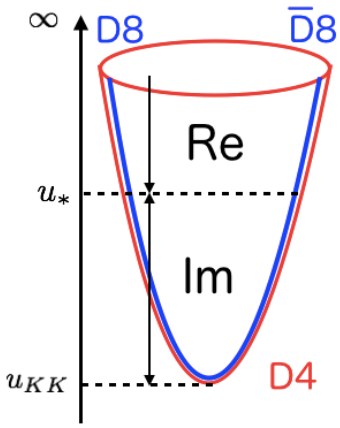

Figure 5: *When the region of u is $u_{KK} \leq u \leq u_*$, the Euler-Heisenberg Lagrangian has an imaginary part. It means that the pair creation of the quark antiquark occurs by the vacuum instability.*

where y_* is defined by

$$y_* \equiv \left[\frac{3^6\pi^2}{2^3\lambda^2 M_{KK}^4}\left\{E_1^2 - \vec{B}^2 + \sqrt{(E_1^2-\vec{B}^2)^2 + 4E_1^2B_1^2}\right\}\right]^{-1/3}. \tag{3.101}$$

Let us examine whether or not this creation rate of the quark antiquark diverges. We evaluate (3.5.3) by the neighborhood of u_{KK}. When we expand $u = u_{KK} + \epsilon$ ($\epsilon \ll u_{KK}$), the creation rate of the quark antiquark is

$$\begin{aligned}\mathrm{Im}\mathcal{L} &\simeq \frac{8\pi^2 T_8 R_{D4}^{3/2}}{3g_s} F(u_{KK}) \int_0^{u_*-u_{KK}} d\epsilon \frac{1}{\sqrt{(u_{KK}+\epsilon)^3 - u_{KK}^3}} \\ &\simeq \frac{8\pi^2 T_8 R_{D4}^{3/2} F(u_{KK})}{3\sqrt{3}g_s u_{KK}} \int_0^{u_*-u_{KK}} d\epsilon \frac{1}{\sqrt{\epsilon}} = (\text{finite}),\end{aligned} \tag{3.102}$$

where the function $F(u)$ is defined by

$$F(u) \equiv u^4 \sqrt{\frac{(2\pi\alpha')^4 R_{D4}^6}{u^6} E_1^2 B_1^2 + \frac{(2\pi\alpha')^2 R_{D4}^3}{u^3}\left[E_1^2 - \vec{B}^2\right] - 1}. \tag{3.103}$$

In the case of $\epsilon \ll u_{KK}$, we may approximate $F(u_{KK}+\epsilon) \simeq F(u_{KK})$ since it is not divergent. So, the creation rate does not diverge in the Sakai-Sugimoto model. Obviously, this is due to the confining scale u_{KK}.

We evaluate the critical electric field to break the vacuum by the creation of the quark antiquark. We derive the critical electric field from the condition that the effective Lagrangian starts to have the imaginary part. That is, from (3.97) we obtain

$$u_{KK} \leq \left[\frac{(2\pi\alpha')^2 R_{D4}^3}{2} \left\{ E_1^2 - \vec{B}^2 + \sqrt{(E_1^2 - \vec{B}^2)^2 + 4E_1^2 B_1^2} \right\} \right]^{1/3} . \tag{3.104}$$

Thus, the critical electric field $E_{\rm cr}$ is

$$E_{\rm cr} = \left[\frac{u_{KK}^3}{(2\pi\alpha')^2 R_{D4}^3} \cdot \frac{\left\{ \frac{u_{KK}^3}{(2\pi\alpha')^2 R_{D4}^3} + \vec{B}^2 \right\}}{\left\{ \frac{u_{KK}^3}{(2\pi\alpha')^2 R_{D4}^3} + B_1^2 \right\}} \right]^{1/2} . \tag{3.105}$$

As we can see from (3.105), for $B_2 = B_3 = 0$, the critical electric field is $E_{\rm cr} = [u_{KK}^3/(2\pi\alpha')^2 R_{D4}^3]^{1/2}$ and does not depend on B_1. By using the dictionary of the AdS/CFT correspondence, the critical electric field is obtained as

$$E_{\rm cr} = \frac{2}{27\pi} \lambda M_{KK}^2 \left[\frac{\frac{4}{3^6\pi^2}\lambda^2 M_{KK}^4 + \vec{B}^2}{\frac{4}{3^6\pi^2}\lambda^2 M_{KK}^4 + B_1^2} \right]^{1/2} . \tag{3.106}$$

The QCD string tension of the Sakai-Sugimoto model is $(2/27)\lambda M_{\rm KK}^2$. It coincides with the critical electric field in $B_2, B_3 = 0$. [5]

Let us evaluate the imaginary part of the Lagrangian (3.100). For a given electric field, the magnetic field can be decomposed into the parallel component and the perpendicular component. For numerical simplicity, we choose to measure the electric and magnetic fields in the unit of $2\lambda M_{\rm KK}^2/(3^3\pi)$ and denote those rescaled electromagnetic fields as $\tilde{E}$ and $\tilde{B}$. Our result (3.100) is written as

$$\mathrm{Im}\mathcal{L} = \frac{N_c \lambda^3 M_{KK}^4}{2 \cdot 3^8 \pi^5} \int_{y_*}^1 dy \frac{\sqrt{y^6 \tilde{E}^2 \tilde{B}_{//}^2 + y^3 \left(\tilde{E}^2 - \tilde{B}_\perp^2 - \tilde{B}_{//}^2 \right) - 1}}{y^{9/2}\sqrt{1-y^3}} . \tag{3.107}$$

This can be numerically evaluated, and the result is shown in Fig.6. For a fixed electric field, we plot $\mathrm{Im}\mathcal{L}$ as a function of the parallel magnetic field $B_{//}$ and the perpendicular magnetic field $B_\perp$.

[5] Note that we do not calculate the time-dependent process from the confining phase to the deconfining phase. We just evaluate the vacuum instability at the confined phase when we introduce the electromagnetic field. We follow the story in [16] and [18].

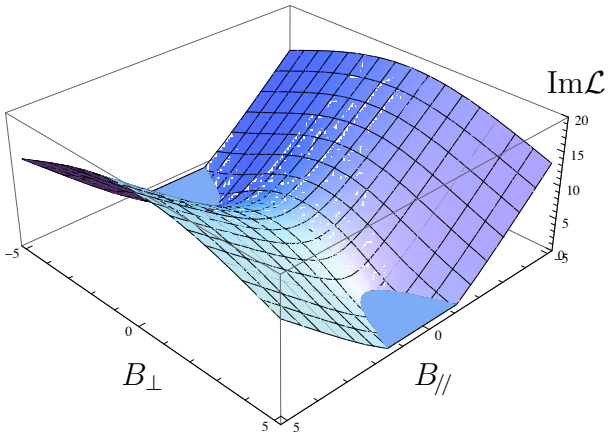

Figure 6: *The plot of the imaginary part of the Lagrangian for a fixed E, as a function of the magnetic field $B_{//}$ parallel to the electric field, and the magnetic field $B_\perp$ perpendicular to the electric field. For a large $|B_{//}|$, the imaginary part disappears. We took $\tilde{E} = 10$ in this figure.*

We find that the imaginary part Im$\mathcal{L}$ has a very different dependence on these parallel / perpendicular components of the magnetic field. When the magnetic field is parallel to the electric field, the imaginary part of the Lagrangian increases as the parallel magnetic field increases. On the other hand, when the magnetic field is perpendicular to the electric field, the situation is completely different. The evaluated imaginary part of the Lagrangian decreases when the perpendicular magnetic field increases. So, we conclude that the instability of the system is enhanced with the parallel magnetic field while is suppressed with the perpendicular magnetic field.

The creation rate of the quark antiquark pair is expected to increase with the parallel magnetic field because the magnetic field makes the (1+3)-dimensional system reduce effectively to a (1+1)-dimensional system by a Landau-level quantization. Our result is similar to [17] in SQCD.

Let us look more about the electric field dependence. For a parallel magnetic field, (3.107) is written as

$$\mathrm{Im}\mathcal{L}_{\text{para. B}} = \frac{N_c \lambda^3 M_{KK}^4}{2 \cdot 3^8 \pi^5} \int_{\tilde{E}^{-2/3}}^1 dy \frac{\sqrt{(y^3\tilde{E}^2 - 1)(y^3\tilde{B}_{//}^2 + 1)}}{y^{9/2}\sqrt{1-y^3}} \,. \tag{3.108}$$

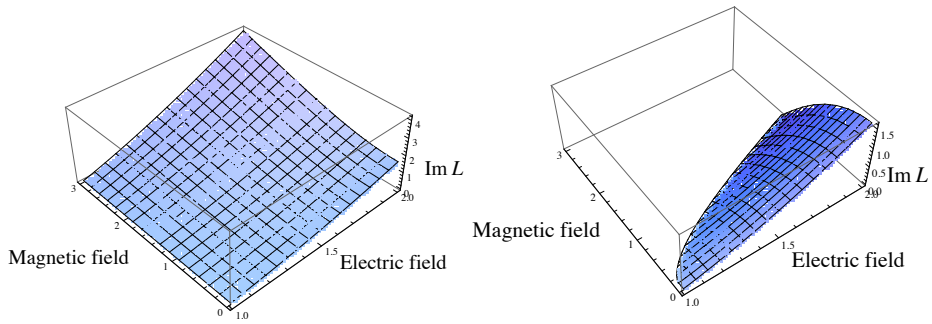

Figure 7: *The plot of the imaginary part of the Lagrangian. Left: The case with a magnetic field parallel to the electric field. Right: The case with a magnetic field perpendicular to the electric field.*

For a perpendicular magnetic field, it is written as

$$\mathrm{Im}\mathcal{L}_{\text{perp. B}} = \frac{N_c\lambda^3 M_{KK}^4}{2\cdot 3^8\pi^5}\int_{(\tilde{E}^2-\tilde{B}_\perp^2)^{-1/3}}^1 dy \frac{\sqrt{y^3(\tilde{E}^2-\tilde{B}_\perp^2)+1}}{y^{9/2}\sqrt{1-y^3}}\,. \tag{3.109}$$

The evaluation of our imaginary part of the Lagrangian (3.108) (3.109) is summarized in Fig.7.

If we look at only the critical value of the electric field as a function of the magnetic field, it shows a magnetic catalysis — the critical electric field only increases once one turns on the magnetic field. The imaginary part of the Lagrangian for the perpendicular magnetic field also follows the magnetic catalysis. However, the imaginary part of the Lagrangian increases for the parallel magnetic field, which can be interpreted as an inverse magnetic catalysis. In sum, the behavior of the instability of the system depends on the direction of the magnetic field relative to the electric field.

In the next subsection, we evaluate the imaginary part of the D8-brane action in the deformed Sakai-Sugimoto background.

3.6 Pair creation of quark antiquark in deformed D4-D8 brane system

In this subsection, in the deformed Sakai-Sugimoto model [15], we derive the creation rate of the quark antiquark pair from the imaginary part of the D-brane action with a constant electromagnetic field. We follow a procedure described in the previous subsection.

3.6.1 Euler-Heisenberg Lagrangian of deformed Sakai-Sugimoto model

In the Sakai-Sugimoto model, the D8-brane and the anti-D8-brane are inserted at the antipodal points of the compactified S^1, $x^4 = 0$ and $x^4 = \pi R$. However, generically x^4 coordinate for the inserted D-branes can depend on the coordinate u, and becomes a function of u. Accordingly, the region of u in which the D8-brane hangs down changes from $[u_{KK}, \infty)$ to $[u_0, \infty)$. The D4-brane background is given by (3.77). The coordinate x^4 of the anti-D8-brane is a function of u and moves in a sub-region of $0 < x^4(u) < \pi R$ $(u_{KK} < u < \infty)$. When $x^4 = \pi R$ $(u = u_{KK})$, the model corresponds to the Sakai-Sugimoto model in the previous section. For generic $x^4(u)$, the induced metric on the D8-brane is given by

$$ds^2_{D8} = \left(\frac{u}{R_{D4}}\right)^{3/2}(-dt^2 + \delta_{ij}dx^i dx^j) + \left(\frac{u}{R_{D4}}\right)^{3/2}\frac{du^2}{h(u)} + \left(\frac{R_{D4}}{u}\right)^{3/2}u^2 d\Omega_4^2, \quad (3.110)$$

where the region of u is $u_0 \leq u < \infty$ $(u_{KK} < u_0 < \infty)$ and the function of $h(u)$ is defined by

$$h(u) \equiv \left[f(u)\left(\frac{dx^4(u)}{du}\right)^2 + \left(\frac{R_{D4}}{u}\right)^3 \frac{1}{f(u)}\right]^{-1}. \quad (3.111)$$

Let us consider the D8-brane action including a constant electromagnetic field in the deformed Sakai-Sugimoto model. Substituting the induced metric on the D8-brane to (3.84), we obtain the following,

$$\mathcal{L} = -\frac{8\pi^2}{3}T_8 \int_{u_0}^{\infty} du \frac{u^4}{\sqrt{h(u)}}\left(\frac{u}{R_{D4}}\right)^{3/4} e^{-\phi}\sqrt{\xi}, \quad (3.112)$$

where the function of ξ is defined by

$$\begin{aligned}\xi \equiv 1 &- \frac{(2\pi\alpha')^2 R^3_{D4}}{u^3}\left[F^2_{01} - F^2_{12} - F^2_{23} - F^2_{13} + h(z)(F^2_{0u} - F^2_{1u})\right] \\ &- \frac{(2\pi\alpha')^4 R^6_{D4}}{u^6}\left[F^2_{01}F^2_{23} + h(u)\{F^2_{0u}(F^2_{12} + F^2_{23} + F^2_{13}) - F^2_{1u}F^2_{23}\}\right]. \end{aligned} \quad (3.113)$$

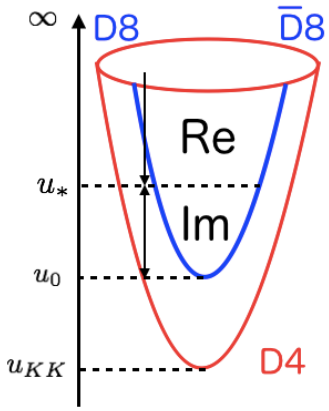

Figure 8: *The Euler-Heisenberg Lagrangian has an imaginary part in* $u_0 \leq u \leq u_*$. *Since the function of* x^4 *depends on* u *coordinate, the below region of the integral changes from* u_{KK} *to* u_0.

After a massage of the equations, we obtain

$$\mathcal{L} = -\frac{8\pi^2 T_8}{3g_s}\int_{u_0}^{\infty} du \frac{u^4}{\sqrt{h(u)}}\sqrt{1-\frac{(2\pi\alpha')^2 R_{D4}^3}{u^3}\left[E_1^2-\vec{B}^2\right]-\frac{(2\pi\alpha')^4 R_{D4}^6}{u^6}E_1^2 B_1^2}, \quad (3.114)$$

where the electromagnetic fields are defined by $F_{01} \equiv E_1, F_{12} \equiv B_3, F_{23} \equiv B_1, F_{13} \equiv B_2$ and $\vec{B}^2 \equiv B_1^2 + B_2^2 + B_3^2$.

3.6.2 Imaginary part of the effective action in deformed Sakai-Sugimoto model

In the previous part, the D8-brane action in the deformed Sakai-Sugimoto model was obtained as (3.114). In this subsection, we derive the creation rate of the massless quark antiquark from the imaginary part of the D8-brane action in a constant electromagnetic field.

From (3.114), we examine the case when the imaginary part of the effective Lagrangian appears. Since the function of $h(u)$ is positive, we should find a region of u such that the square root in the numerator of the integrand has an imaginary part. Although the coordinate of x^4 depends on u in the deformed Sakai-Sugimoto model, the dependence on u in the function of x^4 has no relation with the imaginary part of the effective Lagrangian. So, we may follow the same logic as given in the previous subsection. The condition that

this effective Lagrangian has an imaginary part is the same as (3.96). The integration region of u which gives an imaginary part is

$$u_0 \leq u < \left[\frac{(2\pi\alpha')^2 R^3}{2}\left\{E_1^2 - \vec{B}^2 + \sqrt{(E_1^2 - \vec{B}^2)^2 + 4E_1^2 B_1^2}\right\}\right]^{1/3}. \tag{3.115}$$

The imaginary part of the effective Lagrangian is evaluated as

$$\mathrm{Im}\mathcal{L} = \frac{8\pi^2 T_8}{3g_s}\int_{u_0}^{u_*} du \frac{u^4}{\sqrt{h(u)}}\sqrt{\frac{(2\pi\alpha')^4 R^6}{u^6}E_1^2 B_1^2 + \frac{(2\pi\alpha')^2 R^3}{u^3}\left[E_1^2 - \vec{B}^2\right] - 1}, \tag{3.116}$$

where u_* is defined by (3.99). The integral region of u is shown in Fig. 8

Next, we evaluate the critical electric field. The critical electric field is derived from the condition that the imaginary part of the effective Lagrangian starts to grow. From (3.115), we obtain

$$u_0 \leq \left[\frac{(2\pi\alpha')^2 R^3}{2}\left\{E_1^2 - \vec{B}^2 + \sqrt{(E_1^2 - \vec{B}^2)^2 + 4E_1^2 B_1^2}\right\}\right]^{1/3}. \tag{3.117}$$

The critical electric field E_{cr} is obtained by the following,

$$E_{\mathrm{cr}} = \left[\frac{u_0^3}{(2\pi\alpha')^2 R^3}\cdot\frac{\left\{\frac{u_0^3}{(2\pi\alpha')^2 R^3} + \vec{B}^2\right\}}{\left\{\frac{u_0^3}{(2\pi\alpha')^2 R^3} + B_1^2\right\}}\right]^{1/2}. \tag{3.118}$$

This critical electric field is of the same form as that for the critical electric field in the Sakai-Sugimoto model, if we change from u_{KK} to u_0 on (3.105). When $B_2, B_3 = 0$, the critical electric field is $E_{\mathrm{cr}} = [u_0^3/(2\pi\alpha')^2 R^3]^{1/2}$, which is the independent of B_1 as in the case of the Sakai-Sugimoto model.

In the summary of the section, According to the Hashimoto-Oka's conjecture, the Euler-Heisenberg Lagrangian in the strongly coupled large N gauge theory corresponds to the DBI action in the electromagnetic fields. We obtain the creation of the quark antiquark pair in the constant electromagnetic fields from imaginary part of the DBI action in the $\mathcal{N} = 2$ large N QCD, the Sakai-Sugimoto model and the deformed Sakai-Sugimoto model. The creation rate of the quark antiquark pair depends on the direction of the magnetic fields against the direction of the electric field. It indicates the magnetic catalysis which means that the increase of the creation rate depends on the increase of the magnetic fields in the electric field fixed.

4 Turbulent meson condensation

In this section, we analyze the turbulent behavior of the mesons at excited states in D3-D5 brane system by using the AdS/CFT correspondence before the Schwinger effects. The purpose is to find (1) whether we find the power-law behavior, and (2) whether the power is universal.

4.1 Brief introduction for turbulent meson condensation

Mesons are made from the bound state of the quark and the antiquark. If we introduce an electric field to the mesons, then the quark antiquark pair creation occurs. We are interested in the phase transition between the meson and the quark antiquark pair creation. The phenomena is well-known to be a meson melting.

Recently, K. Hashimoto, S. Kinoshita, K. Murata and T. Oka found that the energy distribution of the meson at the high excited modes is a power law such as

$$\varepsilon_n \propto (\omega_n)^{-5}, \tag{4.1}$$

where ε_n is the energy distribution of the meson at the n-th excited modes and ω_n is the meson mass at the n-th excited modes by using the AdS/CFT correspondence. In general, the meson energy distribution is suppressed by the exponential as the Maxwell-Boltzmann distribution. But, they found that the energy distribution of the meson conforms to the power law. The phenomena is called *turbulent meson condensation*. It means that they expect that the turbulent meson comes from *AdS instability*. The AdS instability conjecture by Bizon and Rostworowski [29] has attracted much attention on intrinsic turbulent nature of AdS spacetime. The importance of addressing the stability question of generic AdS spacetimes is obvious from the viewpoint of the renowned AdS/CFT correspondence. The issue of the AdS instability brings about various fruitful discussions on a possible universality of the instability (see for example [30]- [64]), while partially relies on details of numerical simulations.

In general, the turbulence relates to a power law in the phase transition. It is important to be the universality about the power law. It is worth examining the universality of the turbulent meson condensation. In [65, 66], they obtained the energy distribution of the meson at the high excited modes in the D3-D7 brane system. We are interested

in the other brane configuration. In this section, we evaluate the energy distribution of the meson in a D3-D5 brane system.

4.2 Review of the $\mathcal{N} = 2$ supersymmertic defect gauge theory in AdS/CFT

In this subsection, we review the derivation [72] of the spectrum of "mesons" from the fluctuation of a probe D5-brane at zero temperature and with no background electric field, by using the AdS/CFT correspondence. We are interested in the following D3-D5 brane configuration:

	0	1	2	3	4	5	6	7	8	9
D3	√	√	√	√						
D5	√	√	√		√	√	√			

The brane configuration preserves $\mathcal{N} = 2$ supersymmetries in total. The flavor probe D5-brane extends along the directions $x^0, x^1, x^2, x^4, x^5, x^6$, so it shares only x^0, x^1, x^2 directions with the gauge N_c D3-branes. Thus, the gluon $\mathcal{N} = 4$ multiplets live in the (3+1) dimensional spacetime while the quark hypermultiplets (and resultantly the mesons as their bound states) live only in a (2+1) dimensional domain wall, which is a defect.

It is known that meson states can be analyzed holographically by the D3-D5 brane system. The scalar meson field corresponds to a fluctuation of the probe D5-brane along the directions x^7, x^8, x^9, due to the AdS/CFT correspondence. For the fluctuation, the Laplace equation is classically solved by a Gauss hypergeometoric function [72], as we will see below.

The $\mathrm{AdS}_5 \times \mathrm{S}^5$ background metric is

$$ds^2 = \frac{r^2}{R^2}\eta_{\mu\nu}dx^\mu dx^\nu + \frac{R^2}{r^2}[d\rho^2 + \rho^2 d\Omega_2^2 + d\omega_4^2 + d\omega_5^2 + d\omega_6^2]. \tag{4.2}$$

The 5-sphere together with the AdS radial direction r is decided into a combination of ρ and 2-sphere Ω_2 and the remaining three directions x^7, x^8, x^9 which are parametrized by $\omega_4, \omega_5, \omega_6$. So the relation among these parameters is $r^2 = \rho^2 + \omega_4^2 + \omega_5^2 + \omega_6^2$. Since $(\omega_4, \omega_5, \omega_6)$ has a rotation symmetry, we may fix $\omega_5 = \omega_6 = 0$ for simplicity.

The D5-brane action is a Dirac-Born-Infeld(DBI) action given by

$$S_{\rm DBI} = -\tau_5 \int d^6\xi \; e^{-\phi}\sqrt{-\det(P[g]_{ab} + 2\pi l_s^2 F_{ab})}, \tag{4.3}$$

where τ_5 is the D5-brane tension and is defined by $\tau_5 = 1/(2\pi)^5 g_s l_s^6$. g_s is the string coupling. ϕ is the dilation field which is set to zero as the background.

The scalar mesons are eigen modes which are liberalized solutions for fluctuations of $\omega_4(x^i, \rho)$ of the D5-brane DBI action to which the background metric is substituted. Denoting the index i running $i = 0, 1, 2$ as the D5-brane does not extend along the direction x^3, we impose a boundary condition at the AdS boundary as

$$\omega_4(x^i, \rho = \infty) = R^2 m, \tag{4.4}$$

where m is related to the quark mass m_q as $m_q = (\lambda/2\pi^2)^{1/2} m$ due to the AdS/CFT dictionary. A static classical solution of the DBI equation of motion is

$$\omega_4(x^i, \rho) = R^2 m. \tag{4.5}$$

The solution roughly measures the distance between the D3-branes and the D5-brane.

Next, we consider the fluctuation χ around the static solution $R^2 m$, defined by $\chi \equiv R^{-2}\omega_4 - m$. We assume for simplicity that χ is independent of the coordinates x^1 and x^2. The action for χ obtained by just expanding (4.3) to the quadratic order is

$$S = \int d^3x \int_0^\infty d\rho \frac{\rho^2 R^2 m}{2(\rho^2 + R^4 m^2)^2} \left[(\partial_t \chi)^2 - \frac{(\rho^2 + R^4 m^2)^2}{R^4} (\partial_\rho \chi)^2 \right] + \mathcal{O}(\chi^3), \tag{4.6}$$

where the irrelevant overall factor is neglected. From (4.6), we derive the equation of motion as

$$\left[\frac{\partial^2}{\partial t^2} - \frac{(\rho^2 + R^4 m^2)^2}{\rho^2 R^2 m} \frac{\partial}{\partial \rho} \frac{\rho^2 m}{R^2} \frac{\partial}{\partial \rho} \right] \chi = 0, \tag{4.7}$$

Its normalizable solution is

$$\chi = \sum_{n=0}^{\infty} \mathrm{Re}\left[C_n \exp[i\Omega_n t] E_n(\rho) \right], \tag{4.8}$$

The basis functions are given by

$$E_n(\rho) \equiv \frac{4(n+1)}{\sqrt{\pi}} \left(\frac{R^4 m^2}{\rho^2 + R^4 m^2} \right)^{n+\frac{1}{2}} F\left(-n, -1/2 - n, 3/2; -\frac{\rho^2}{R^4 m^2} \right), \tag{4.9}$$

where F is the Gaussian hypergeometric function. The mass of the level n resonance meson is

$$\Omega_n \equiv 2\sqrt{(1/2+n)\,(3/2+n)}\,m. \tag{4.10}$$

For our later purpose we define the inner product in the ρ-space as

$$(F,G) \equiv \int_0^\infty d\rho \frac{\rho^2 R^2 m}{(\rho^2+R^4m^2)^2} F(\rho)G(\rho), \tag{4.11}$$

under which we have the orthonormality condition

$$(E_n, E_m) = \delta_{nm}. \tag{4.12}$$

Using the basis (4.9), we expand the fluctuation of the scalar field as

$$\chi = \sum_{n=0}^{\infty} c_n(t)E_n(\rho), \tag{4.13}$$

then with this we can define the linearlized meson energy at level n,

$$\varepsilon_n \equiv \frac{1}{2}(\dot{c}_n^2 + \Omega_n^2 c_n^2). \tag{4.14}$$

The linearlized total energy is given by the formula (**??**). All of these are analogous to what we have used in the case of the D3-D7 brane system in Sec. 2.

4.3 Turbulence with an electric field

We are ready for studying the turbulent meson behavior. The turbulence should show up in the meson energy distribution which is defined as (4.14). Note that the energy spectrum (4.14) is defined with no background electric field. Once the electric field is turned on, the meson spectrum changes compared to that with no electric field, since the probe D5-brane is affected by the electric field. It is well-known that the shape of the probe D-brane is deformed by the electric field [70]. We are interested in how the shape of the D5-brane changes and how the meson spectrum is affected accordingly.

To look at how the D5-brane shape is deformed, we solve the equation of motion from the DBI action (4.3). $AdS_5 \times S^5$ background is given by (4.2). From a simple

consideration of rotational symmetry, we can put $\omega_5, = \omega_6 = 0$ while ω_4 depends on the radial direction ρ as $w_4 = L(\rho)$. Then, the induced metric on the D5-brane is given by

$$ds^2 = \frac{r^2}{R^2}(-dt^2 + \delta_{ij}dx^i dx^j) + \frac{R^2}{r^2}[\{1 + (\partial_\rho L)^2\}d\rho^2 + \rho^2 d\Omega_2^2], \tag{4.15}$$

where $i, j = 1, 2$. Then we turn on a constant electromagnetic field. In (2+1) dimensions, Lorentz transformation can bring us to a frame on which only F_{01} component is nonzero. Denoting $E \equiv F_{01}$, we obtain the action with the electric field as[6]

$$S_{\rm DBI} = -4\pi\tau_5 \int d^3x \int_0^\infty d\rho\ \rho^2 \sqrt{1 + (\partial_\rho L)^2}\sqrt{1 - \frac{R^4(2\pi l_s^2)^2 E^2}{(\rho^2 + L^2)^2}}, \tag{4.16}$$

The equation of motion is obtained with a redefinition $\mathcal{E} \equiv 2\pi l_s^2 E$ as

$$\partial_\rho \left[\frac{\rho^2 \partial_\rho L\sqrt{1 - \frac{R^4\mathcal{E}^2}{(\rho^2+L^2)^2}}}{\sqrt{1 + (\partial_\rho L)^2}}\right] - \frac{2R^4\mathcal{E}^2\rho^2 L\sqrt{1 + (\partial_\rho L)^2}}{(\rho^2 + L^2)^3\sqrt{1 - \frac{R^4\mathcal{E}^2}{(\rho^2+L^2)^2}}} = 0. \tag{4.17}$$

We solve this equation numerically to obtain the shape of the probe D5-brane for a given value of $\mathcal{E}$. The results of the numerical calculations, with $R = 1$ and $m = 1$, are shown in Fig. 9. the shape of the D5-brane changes and the D5-brane has a cusp as the static electric field increases. With various chosen background electric field $\mathcal{E}$, the D5-brane changes its shape, and we find a conical D5-brane. It is the critical embedding, for which we expect the turbulent behavior of mesons.

Basically, as in the case of the D7-brane probe, for small $\mathcal{E}$ the D5-brane is at the Minkowski embedding (which has a smooth shape), while for a large enough $\mathcal{E}$ the D5-brane is at a black hole embedding where the induced metric on the D5-brane has an effective horizon. The critical embedding is in between those embeddings, and the D5-brane has a cone at the tip. The value of $\mathcal{E}$ with which the D5-brane can be in the critical embedding is called $\mathcal{E}_{\rm cr}$, and in Fig. 9 we plot various curves for various $\mathcal{E}/\mathcal{E}_{\rm cr}$.[7]

[6] The Chern-Simons terms in the D-brane effective actions does not contribute in our analysis. For D4-D8 setup, they may contribute. See a discussion in [18].

[7] Note again that the location of the tip of the D5-brane is not a monotonic function of $\mathcal{E}/\mathcal{E}_{\rm cr}$. In some region of the value of $\mathcal{E}/\mathcal{E}_{\rm cr}$, the D5-brane profile is found to be not unique. A fractal-like structure emerges, as in the case of the D3-D7 system.

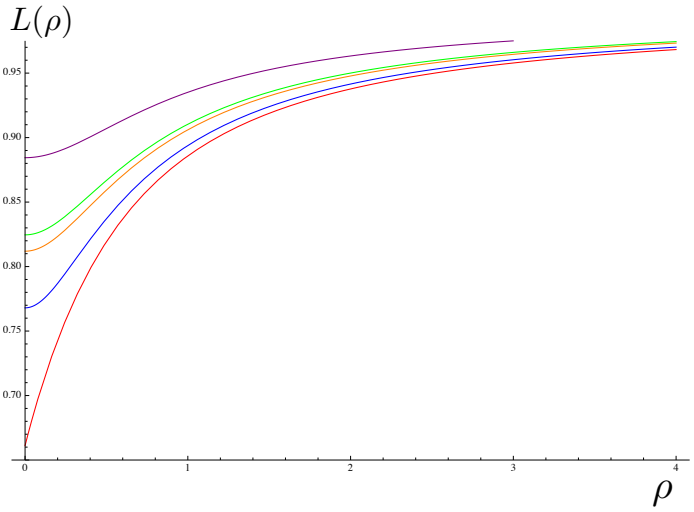

Figure 9: *The shape of the D5-brane in the AdS background. Each curve corresponds, from top to bottom, to* $\mathcal{E}/\mathcal{E}_{\rm cr} = 0.9, 0.99, 1, 1.017, 1$ *respectively. The D5-brane can have a cusp at* $\rho = 0$ *for* $\mathcal{E} = \mathcal{E}_{\rm cr} (\simeq 0.437)$ *(the red curve).*

From these numerical shape of the D5-branes in Fig. 9, we can calculate the meson energy spectrum, through the definitions given in the previous subsection. As the shape of the D5-brane changes by varying $\mathcal{E}/\mathcal{E}_{\rm cr}$, the decomposed meson energy spectrum changes. Our result for the energy distribution ε_n is presented in Fig. 10.

The energy distribution Fig. 10 shows that the critical embedding (the red dots) is distinctively different from other Minkowski embeddings. The red dots can be linearly fit as

$$\varepsilon_n \propto (\Omega_n)^{-3.97} \tag{4.18}$$

which is a power law. This is nothing but a weak turbulence, and is very similar to what we has been known in [65, 66] and what we found in the previous section. For the other Minkowski embeddings, there is a significant reduction of energy for higher excited mesons (large n region). So, the power law appears only at the critical embedding. The cusp of the D5-brane seems to be responsible for the power law of the meson energy distribution. We can conclude that the weak turbulence of the excited mesons is caused by the cusp of the D5-brane, which is realized and accompanied with the phase transition.

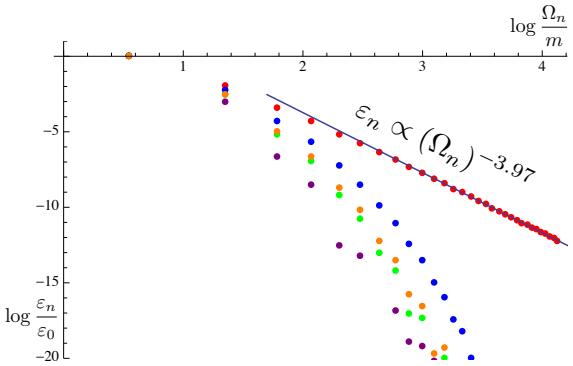

Figure 10: *The power law of the n-th meson mass including a static electric field. The vertical axis is the logarithm plots of the n-th meson energy divided by the lowest meson energy. The transverse axis describes the logarithm plots of the n-th meson mass.*

4.4 Turbulence at a finite temperature

In this subsection, we consider the energy spectrum of the highly excited meson states in a finite temperature D3-D5 system in the absence of the electric field, to study the universality of the power law (4.18). The basis of the analysis was given in [73] as we have reviewed. In the previous subsection, we studied the turbulent meson spectrum in the electric field. When the probe D5-brane has a cusp, the meson energy distribution obeys a power law: $\varepsilon_n \propto (\Omega_n)^{-3.97}$. It is of interest if the power law is universal or not. So, here we introduce a temperature to the AdS background, and examine the power law.

In AdS/CFT correspondence, the temperature is introduced by replacing the background AdS geometry (4.2) by an AdS black hole metric,

$$ds^2 = \frac{r^2}{R^2}[-f(r)dt^2 + d\vec{x}^2] + \frac{R^2}{r^2}\left[\frac{dr^2}{f(r)} + r^2 d\Omega_5^2\right], \tag{4.19}$$

where $d\vec{x}^2 \equiv dx_1^2 + dx_2^2 + dx_3^2$, and the function of $f(r)$ is defined by $f(r) \equiv 1 - (r_{\rm H}/r)^4$. The location of the black hole horizon $r_{\rm H}$ is related to the temperature as $T = r_{\rm H}/\pi R^2$ due to the AdS/CFT dictionary. Using a new coordinate $2u^2 = r^2 + \sqrt{r^4 - r_{\rm H}^4}$, the AdS

black hole metric is written as

$$ds^2 = \frac{u^2}{R^2}\left[-\frac{f(u)^2}{\tilde{f}(u)}dt^2 + \tilde{f}(u)d\vec{x}^2\right] + \frac{R^2}{u^2}\left[dv^2 + v^2 d\Omega_2^2 + d\tilde{\omega}_4^2 + d\tilde{\omega}_5^2 + d\tilde{\omega}_6^2\right], \tag{4.20}$$

where

$$f(u) \equiv 1 - \frac{r_{\rm H}^4}{4u^4}, \quad \tilde{f}(u) \equiv 1 + \frac{r_{\rm H}^4}{4u^4}. \tag{4.21}$$

The radial coordinates u and v parameterize the radii of S^5 and S^2 respectively, and they are related as $u^2 = v^2 + \tilde{\omega}_4^2 + \tilde{\omega}_5^2 + \tilde{\omega}_6^2$. As before, using the rotational symmetry, we can restrict ourselves to $\tilde{\omega}_5 = \tilde{\omega}_6 = 0$ and $\tilde{\omega}_4 \equiv \tilde{L}(v)$. Then, the induced metric on the D5-brane is given by

$$ds^2 = \frac{u^2}{R^2}\left[-\frac{f(u)^2}{\tilde{f}(u)}dt^2 + \tilde{f}(u)d\vec{x}^2\right] + \frac{R^2}{u^2}\left[\{1 + (\partial_v \tilde{L})^2\}dv^2 + v^2 d\Omega_2^2\right]. \tag{4.22}$$

Next, we determine the shape $\tilde{L}(v)$ of the probe D5-brane in this finite temperature system. The 1-flavor DBI action is defined by (4.3). By using the induced metric (4.22), the DBI action becomes

$$S_{\rm DBI} = -4\pi\tau_5 \int d^3x \int_0^\infty dv\ v^2 \left(1 - \frac{r_{\rm H}^4}{4(v^2+\tilde{L}^2)^2}\right)\sqrt{1 + \frac{r_{\rm H}^4}{4(v^2+\tilde{L}^2)^2}}\sqrt{1 + (\partial_v \tilde{L})^2}. \tag{4.23}$$

The Euler-Lagrange equation of the D5-brane is obtained as

$$\begin{aligned}\partial_v\left[\frac{v^2\partial_v\tilde{L}\left(4(v^2+\tilde{L}^2)^2 - r_{\rm H}^4\right)\sqrt{4(v^2+\tilde{L}^2)^2 + r_{\rm H}^4}}{(v^2+\tilde{L}^2)^3\sqrt{1+(\partial_v\tilde{L})^2}}\right] \\ -\frac{2r_{\rm H}^4 v^2\tilde{L}\left(4(v^2+\tilde{L}^2)^2 + 3r_{\rm H}^4\right)\sqrt{1+(\partial_v\tilde{L})^2}}{(v^2+\tilde{L}^2)^4\sqrt{4(v^2+\tilde{L}^2)^2 + r_{\rm H}^4}} = 0.\end{aligned} \tag{4.24}$$

We numerically calculate classical solutions $\tilde{L}(v)$ of the equation of motion. We chose the convention $R = 1$ and $m = 1$ which is the same as before. The theory has only two scales, the quark mass and the temperature. So the theory is determined only by the ratio of those. For fixed $m = 1$, we vary $r_{\rm H}$ and obtain various D5-brane shapes, as shown in Fig. 11.

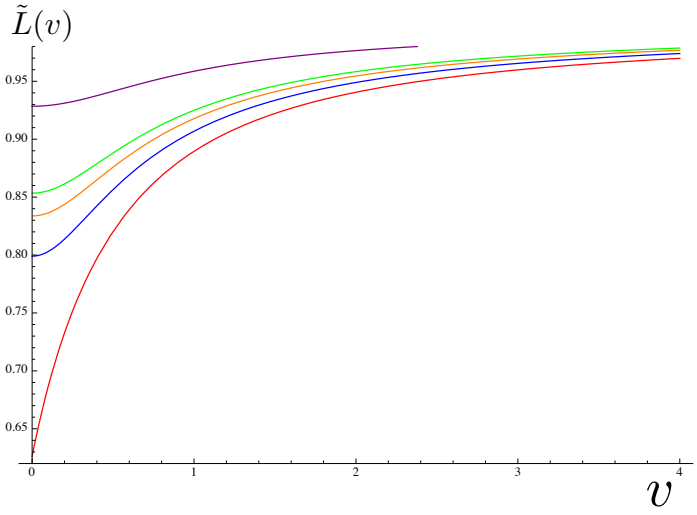

Figure 11: *The shape of the D5-brane in the AdS black hole background. Each curve is with* $r_{\rm H}/r_{\rm cr} = 0.9, 0.99, 1, 1.01, 1$ *respectively from top to bottom. The D5-brane of the red curve has a cusp at* $\rho = 0$*, which we call a critical embedding, for* $r_{\rm H} = r_{\rm cr} (\simeq 0.443)$*. The other curves are Minkowski embeddings.*

As the temperature changes, the amount of the gravity which the D5-brane feels changes, since the location of the horizon approaches the D5-brane. The red curve in Fig. 11 has a cusp of the D5-brane, and shows that the D5-brane is at the critical embedding.

We expect that a turbulent behavior of meson excited states causes the cusp of the D5-brane at $r_{\rm H}/r_{\rm cr} = 1$ shown by the red curve in Fig. 11. So let us present the results of the meson energy spectrum for the higher excitation modes: see Fig.12. As expected, the red dots which are the energy distribution of meson excitations corresponding to the cusp D5-brane (the red curve in Fig. 11) has a linear behavior. A linear fit of the red dots shows

$$\varepsilon_n \propto (\Omega_n)^{-3.95}. \tag{4.25}$$

Again, we have found that the critical embedding of the D5-brane shows a turbulent behavior of mesons. For other curves with the Minkowski embedding, we have no power law: the energy deposit at the higher meson resonance decreases rapidly for large n. So the weak turbulence, the power law behavior, is unique to the critical embedding of the D5-brane.

In conclusion, the turbulent behavior of the higher excited modes of mesons is observed when the shape of D5-brane has a cusp in the static electric field or at the finite

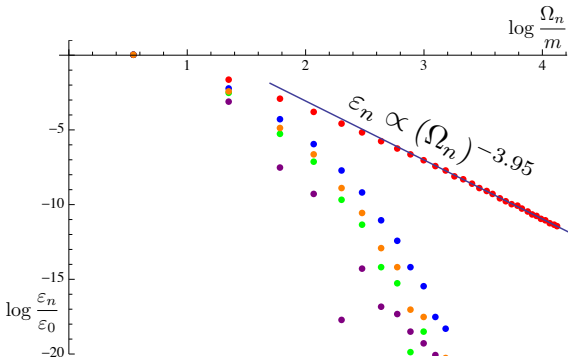

Figure 12: *The power law of the energy distribution ε_n for the n-th meson resonance, in the finite temperature system. The vertical axis is the logarithm of the n-th meson energy ε_n divided by the lowest meson energy ε_0. The horizontal axis is for the logarithm of the n-th meson mass Ω_n. The colors of the dots correspond to that of the curves in the previous figure.*

temperature. The meson energy distribution obeys the power law as a function of the meson mass, $\alpha \simeq -3.97$ or $\beta \simeq -3.95$ in the static electric field or at the finite temperature system, respectively. Since these powers are quite close to -4, we conclude that the turbulent behavior is a universal phenomenon irrespective of how the transition is made. We expect that the exact power may be $\varepsilon_n \propto (\Omega_n)^{-4}$, which may be confirmed with numerical simulations with higher accuracy.

4.5 Universal turbulence and a conjecture

In the previous subsections, we found that the power associated with the level distribution ε_n of the energy density for the meson level n has an integer power:

$$\varepsilon_n \propto (m_n)^{\alpha}\,, \tag{4.26}$$

where $\alpha = -5$ for the D3/D7 system (treated in section 2) and $\alpha = -4$ for the D3/D5 system (treated in section 3). Furthermore, the power in each case is found to be universal. The power does not change even though the external field to produce the phase transition is modified — the temperature and the magnetic field.

Therefore, it seems that the power α depends only on the dimensionality of the brane cone, and it does not depend on how the phase transition is driven. It is natural to make a generic conjecture on the power α: *The energy distribution for level n at the conical brane configuration for the phase transition is given by the power law as in (4.26), and the power is determined as*

$$\alpha = -(d_{\text{cone}} + 1) \tag{4.27}$$

where d_{cone} is the dimension of the cone. For the case of the D3/D7 (D3/D5) system, $d_{\text{cone}} = 4$ ($d_{\text{cone}} = 3$).

In this paper, we presented evidence for this conjecture for various situations associated with the D3/D7 and the D3/D5 holographic models, with various external fields, and all are consistent with the above conjecture.

To strengthen the plausibility of the conjecture, in the following part of this section we provide simple examples of decomposition of a conic brane configuration in flat space by eigen modes of harmonic functions. The examples are 1-dimensional and 2-dimensional cones, for simplicity. Both nontrivially can be worked out and are consistent with the conjectured relation (4.27).

Ex. 1-dimensional cone

Let us consider a one-dimensional cone in a flat space and calculate the power α when it is expanded in eigen modes. The one-dimensional cone is simply written as

$$L(\rho) = 1 - \frac{2}{\pi}|\rho| \tag{4.28}$$

which is defined on an interval $-\pi/2 < \rho < \pi/2$, at whose boundary the height function $L(\rho)$ is put to zero. We expand this cone by harmonic functions in one-dimensional flat space, *i.e.* Fourier modes. The eigen basis satisfying the Dirichlet boundary condition at the boundaries of the interval is

$$e_n(\rho) = \sqrt{\frac{2}{\pi}} \cos\left((2n+1)\rho\right) \tag{4.29}$$

where $n = 0, 1, 2, \cdots$ specifies the level of the modes. The magnitude of the eigenvalue of the Laplacian ∂_ρ^2 is just $m_n^2 = (2n+1)^2$. The expansion is easily done

as

$$L(\rho) = \sum_{n=0}^{\infty} c_n e_n(\rho) \quad \text{where} \quad c_n \equiv \frac{2^{5/2}}{\pi^{3/2}} \frac{1}{(2n+1)^2} \,. \tag{4.30}$$

So the meson energy for each level n is

$$\varepsilon_n \equiv \frac{1}{2} m_n^2 c_n^2 = \frac{2^4}{\pi^3} \frac{1}{(2n+1)^2} \tag{4.31}$$

So, for large n, we obtain the power

$$\varepsilon_n \sim n^\alpha \,, \quad \alpha = -2 \,. \tag{4.32}$$

From this simple example, we find that the possible power in the meson melting transition, if occurs in holography, would have $\alpha = -2$, if the cone of the probe brane is just one-dimensional.

Ex. 2-dimensional cone

Let us proceed to an example in 2 dimensions, to support our conjecture. The example is again a cone in a flat space. Let us consider a 2-dimensional cone

$$L(\rho) = 1 - \rho \tag{4.33}$$

where $\rho \equiv \sqrt{(x^1)^2 + (x^2)^2}$, and we consider $0 \leq \rho \leq 1$. The boundary $\rho = 1$ is a circle, and we impose a Dirichlet boundary condition for harmonic functions on the disk. The harmonic functions in 2 dimensions are Bessel functions $J_\nu(r)$,

$$\left[\frac{d^2}{dr^2} + \frac{1}{r} \frac{d}{dr} + \left(1 - \frac{\nu^2}{r^2} \right) \right] J_\nu(r) = 0 \,. \tag{4.34}$$

The subscript ν corresponds to the angular mode, so our cone configuration should be expanded only with $\nu = 0$. The Dirichlet boundary condition says $e_n(\rho = 1) = 0$, therefore, in terms of the Bessel functions, we have

$$e_n(\rho) = \frac{\sqrt{2}}{|J_0'(r_n)|} J_0(r_n \rho) \tag{4.35}$$

where $r_n (n = 0, 1, 2, 3, \cdots)$ label zeros of the Bessel function $J_0(r)$. The normalization is already fixed by using the following formula

$$\int_0^1 \rho \left(J_0(r_n \rho) \right)^2 d\rho = \frac{1}{2} \left(J_0'(r_n) \right)^2 \,. \tag{4.36}$$

The eigenvalue of the eigen mode function $e_n(\rho)$ is r_n^2, thus the "meson mass" of level n is $m_n = r_n$.

The expansion of the cone (4.33) is given by

$$L(\rho) = \sum_{n=0}^{\infty} c_n e_n(\rho), \quad c_n \equiv \int_0^1 \rho(1-\rho) e_n(\rho)\,. \tag{4.37}$$

We are interested in only the large n behavior, so we use the following expression for the large n asymptotic expansion of the Bessel functions,

$$J_0(r) = \sqrt{\frac{2}{\pi r}}\left(\cos(r-\pi/4) + \frac{1}{8r}\sin(r-\pi/4) + \mathcal{O}(1/r^2)\right)\,. \tag{4.38}$$

The zeros of this function at large n are given by

$$r_n \sim \frac{4n+3}{4}\pi + \frac{1}{(8n+6)\pi} \quad (n \gg 1) \tag{4.39}$$

So, at the leading order in the large n expansion, we have

$$e_n(\rho) \sim \sqrt{\frac{2}{\rho}}\cos\left(\frac{(4n+3)\pi}{4}\rho - \frac{\pi}{4}\right)\,. \tag{4.40}$$

Substituting this into (4.37), we obtain the large n behavior of the coefficient c_n,

$$c_n = \frac{3\sqrt{2}}{4\pi^2} n^{-5/2} + \mathcal{O}(n^{-3})\,. \tag{4.41}$$

The meson condensation c_n is found to scale as $\sim n^{-5/2}$. Therefore the energy distribution is obtained as

$$\varepsilon_n = \frac{1}{2} m_n^2 c_n^2 \sim \frac{9}{16\pi^2} n^{-3}\,, \tag{4.42}$$

which shows the power

$$\alpha = -3 \tag{4.43}$$

for the case of the 2-dimensional cone in a flat space.

These simple examples are consistent with our conjecture (4.27), so it is expected that the brane turbulence (4.26) with the power (4.27) is universal, not only in AdS-like geometries but also in a box of flat geometries.

In summary, if we introduce the constant electric field or a temperature to the D5-brane, the shape of the D5-brane has the cusp by the external fields. Then, we obtain the energy distribution of the meson at the high excited modes which is the turbulent power law, $\varepsilon_n \propto (\omega)^{-4}$. It means that this power of the turbulent power law depends on a cone-dimension of the probe D-brane from some examples.

5 Conclusion

The electromagnetic instability was examined by the imaginary part of the DBI action in the electromagnetic fields. We obtained the creation rate of the quark antiquark pair in the large N_c $\mathcal{N} = 2$ supersymmeric QCD and the large N_c strongly coupled gauge theories in a confining phase.

Before the Schwinger effects occurs, there are mesons which are bound states of the quark and the antiquark. We found that the energy distribution of the meson at the high excited modes obeys the turbulent power law in the D3-D5 brane system. The turbulent power is -4. We found that the power depends only on the cone-dimension of the probe D-brane.

The results of the doctor thesis are summarized as follows.

- We obtained the creation rate of the massless quark antiquark pair in the $\mathcal{N} = 2$ large N SQCD by evaluating the imaginary part of the DBI action in constant electromagnetic fields with the AdS/CFT correspondence. At zero temperature, an infrared divergence appears in the creation rate of the quark antiquark. We compared the the creation rate of the massless quark antiquark with the well-known results of QED. The massless quark antiquark divergence is similar to the results of the QED.

- We evaluated the creation rate of the massive quark antiquark pair in $\mathcal{N} = 2$ large N SQCD. This result is compared with the imaginary parts of the Euler-Heisenberg Lagrangian of $\mathcal{N} = 2$ supersymmetric QED(SQED) which has $2N_c$ scalar fields and N_c spinor fields. The creation rate of the massive quark antiquark is found to coincide with the creation rate of the massless quark antiquark at a finite temperature if we replace the quark mass with the temperature.

- The creation rate of the massless quark antiquark in a confining phase is obtained by the D8-brane DBI action in the Sakai-Sugimoto model. We found that the creation rate of the massless quark antiquark at zero temperature is finite, which is different from the result of the $\mathcal{N} = 2$ SQCD. The imaginary part of the D8-brane DBI action increases when we increase the magnetic field parallel to a fixed electric field. On the other hand, the imaginary part decreases when we increase the magnetic field perpendicular to the electric field. The critical electric field to have

a non-zero imaginary part for the DBI action coincides with a QCD string tension between the quark and antiquark. The result was already mentioned in [23, 26] in a similar context.

- We found turbulent meson condensation in a D3-D5 brane system in the manner similar to [65, 66]. The energy distribution of the highly excited meson modes is proportional to the power -4 of the meson mass in the D3-D5 brane system. At a finite temperature without a constant electric field, the power again found to be -4.

There are several issues concerning the vacuum instability with the AdS/CFT correspondence. The vacuum instability in the AdS/CFT correspondence is derived from the evaluation of the imaginary part of the DBI action. For that, we assumed that the Euler-Heisenberg Lagrangian in the $\mathcal{N} = 2$ large N_c SQCD coincides with the D-brane DBI action in the electromagnetic fields. In particular, there remains ambiguity about the correctness of the Hashimoto-Oka's conjecture . The conjecture was obtained by the relationship between the quark antiquark 1-loop diagram in the strongly coupled large N gauge theory and the disk amplitude. The disk amplitude means that the fundamental openstring moves on the worldsheets. In the low energy limit, the partition function of the open string is the DBI action in the flat target space. We need to discuss the relationship between the Euler-Heisenberg Lagrangian in the strongly coupled large N gauge theory and the DBI action in the electromagnetic fields.

We considered the imaginary part of the 1-flavor DBI actions in the strongly coupled gauge theory. It is important to calculate the creation rate of the quark-antiquark pairs with multi-flavors. We haven't known the non-abelian DBI action formalism. If we can treat the non-abelian DBI action formalism, we consider the charged mesons pair creations.

Acknowledgments

I would like to appreciate my supervisor Prof. Koji Hashimoto for continuing encouragement and support, and thank to Masayuki Asakawa, Takahiro Kubota, Norihiro Iizuka and Satoshi Yamaguchi for reading this thesis carefully, and Takashi Oka and Mitsuhiro Nishida for the collaborators, and Ryo Yamamura for some discussions.

A Euler-Heisenberg Lagrangian in QED

In this appendix, we derive the Euler-Heisenberg Lagrangian (3.8) in the QED from the Itzykson-Zuber textbook [76]. Let us consider the Dirac equation with the external gauge field $A_\mu(x)$ in order to obtain the creation rate of the electron positron pair. The Dirac equation is given by

$$[i\not{\partial} - e\not{A}(x) - m]\,\psi(x) = 0, \tag{A.1}$$

where $\not{\partial}$ is defined as $\not{\partial} \equiv \gamma^\mu \partial_\mu$ and m is a electron mass. The Lagrangian interaction term for the gauge field becomes

$$\mathcal{L}_{\rm int} = -\mathcal{H}_{\rm int} = -e\bar{\psi}_{\rm in}(x)\gamma^\mu \psi_{\rm in}(x) A_\mu(x). \tag{A.2}$$

It is convenient to use the S-matrix with the time-evolution operator in order to consider the vacuum amplitude for the interaction. The S-matrix is defined as the following,

$$S = T\exp\left[-ie\int d^4x\ \bar{\psi}_{\rm in}(x)\gamma^\mu\psi_{\rm in}(x)A_\mu(x)\right], \tag{A.3}$$

where T is the time-ordered product.

The vacuum amplitude inducing the interaction is

$$\begin{aligned} S_0(A) &= \langle 0\ {\rm in}|S|0\ {\rm in}\rangle \\ &= \sum_{n=0}^{\infty}\frac{(-ie)^n}{n!}\int dx_1\cdots dx_n \langle 0|T\left[\bar{\psi}(x_1)\not{A}\psi(x_1)\cdots\bar{\psi}(x_n)\not{A}\psi(x_n)\right], \end{aligned} \tag{A.4}$$

where "in" is neglected. By using Wick theorem, we define the matrix as

$$C(\alpha_k, x_k; \alpha_l, x_l) = -ie\sum_\alpha \langle 0|T\left[\not{A}_{\alpha_k,\alpha}\psi_\alpha(x_k)\bar{\psi}_{\alpha_l}(x_l)\right]|0\rangle. \tag{A.5}$$

Thus, S_0 can be described by

$$S_0(A) = \sum_{n=0}^{\infty}\frac{1}{n!}\int dx_1\cdots dx_n \sum_P \varepsilon_P \sum_{\alpha_1\cdots\alpha_n} C(\alpha_1,x_1;\alpha_{P_1},x_{P_1})\cdots C(\alpha_n,x_n;\alpha_{P_n},x_{P_n}). \tag{A.6}$$

ε_P is a sign function which needs to contract ψ with $\bar{\psi}$. The matrix C is redefined as a bracket. Since the matrix C has the index of the spinor and the argument of the space-time, we define the following,

$$C(\alpha, x; \beta, y) = \langle x, \alpha|\Pi|y, \beta\rangle. \tag{A.7}$$

Here, Π is the operator which acts on the bracket. Substituting (A.7) to (A.6), $S_0(A)$ becomes

$$S_0(A) = \mathrm{Det}(I - \Pi) = \exp\left[\mathrm{Tr}\ \ln(I - \Pi)\right]. \tag{A.8}$$

Det and Tr are the determinant and the trace for the spinor including the integral about the continuous parameters respectively.

Π can be evaluated by the following,

$$\Pi = \frac{e\not{A}}{\not{P} - m + i\epsilon}. \tag{A.9}$$

Thus, $S_0(A)$ is

$$S_0(A) = \exp\left\{-\mathrm{Tr}\ \ln\left[(\not{P} - m)\frac{1}{\not{P} - e\not{A} - m + i\epsilon}\right]\right\}. \tag{A.10}$$

Here, the one-body scattering operator $\mathcal{T}(A)$ is defined as

$$\begin{aligned}\mathcal{T}(A) &= e\not{A} + e\not{A}\frac{1}{\not{P} - m + i\epsilon}\mathcal{T}(A) \\ &= e\not{A} + e\not{A}\frac{1}{\not{P} - m + i\epsilon}e\not{A} + e\not{A}\frac{1}{\not{P} - m + i\epsilon}e\not{A}\frac{1}{\not{P} - m + i\epsilon}e\not{A} + \cdots.\end{aligned} \tag{A.11}$$

The hermitian conjugate for the operator B which acts on the Hilbert space $|x, \alpha\rangle$ is defined as

$$\bar{B} = \gamma^0 B^\dagger \gamma^0. \tag{A.12}$$

The hermitian conjugate for the operator $\mathcal{T}$ is

$$\bar{\mathcal{T}} = e\not{A} + \bar{\mathcal{T}}\frac{1}{\not{P} - m - i\epsilon}e\not{A}, \tag{A.13}$$

and the sign of $i\epsilon$ changes. Thus, we obtain

$$e\not{A} = \bar{\mathcal{T}} - \bar{\mathcal{T}}\frac{1}{\not{P} - m - i\epsilon}e\not{A}. \tag{A.14}$$

When we substitute the above equation to (A.12), the $\mathcal{T}(A)$ becomes

$$\mathcal{T}(A) = \bar{\mathcal{T}}(A)\left[\frac{1}{\not{P} - m + i\epsilon} - \frac{1}{\not{P} - m - i\epsilon}\right]\mathcal{T}(A) + \bar{\mathcal{T}}(A), \tag{A.15}$$

That is,

$$\begin{aligned}\mathcal{T}(A) - \bar{\mathcal{T}}(A) &= \bar{\mathcal{T}}(A)\left[\frac{1}{\not{P} - m + i\epsilon} - \frac{1}{\not{P} - m - i\epsilon}\right]\mathcal{T}(A) \\ &= \mathcal{T}(A)\left[\frac{1}{\not{P} - m + i\epsilon} - \frac{1}{\not{P} - m - i\epsilon}\right]\bar{\mathcal{T}}(A) \\ &= \bar{\mathcal{T}}(A)\left[\frac{2\pi}{i}(\not{P} + m)\delta(P^2 - m^2)\right]\mathcal{T}(A). \end{aligned} \tag{A.16}$$

Here, the operator $2\pi(\not{P} + m)\delta(P^2 - m^2)$ is made from the positive energy state and the negative energy state,

$$2\pi(\not{P} + m)\delta(P^2 - m^2) = \rho^{(+)} + \rho^{(-)}, \tag{A.17}$$

with

$$\rho^{(\pm)} \equiv 2\pi(\not{P} + m)\theta(\pm P^0)\delta(P^2 - m^2). \tag{A.18}$$

Now, we consider the following loop contraction about (A.6),

$$C(\alpha_1, x_1; \alpha_2, x_2)C(\alpha_2, x_2; \alpha_3, x_3)\cdots C(\alpha_k, x_k; \alpha_1, x_1). \tag{A.19}$$

The retarded propagator propagates from a past to a future such as,

$$\frac{\not{P} + m}{(P + i\epsilon)^2 - m^2} = \frac{1}{\not{P} - m + i\not{\epsilon}}. \tag{A.20}$$

$\not{\epsilon}$ is the infinitesimal time-like 4-dimensional vector. In the loop contraction, the retarded propagator is zero when the propagator propagates from the past to the future. Thus, we obtain the following condition,

$$\mathrm{Det}\left[I - e\not{A}\frac{1}{\not{P} - m + i\not{\epsilon}}\right] = 1. \tag{A.21}$$

The retarded propagator becomes

$$\frac{1}{\not{P} - m + i\not{\epsilon}} = (\not{P} + m)\left[\mathbf{P}\left(\frac{1}{P^2 - m^2}\right) - i\pi\varepsilon(P^0)\delta(P^2 - m^2)\right]. \tag{A.22}$$

Here, $\varepsilon(P^0)$ is the sign function and $\mathbf{P}$ means the principal integral. The difference between the Feynman propagator and the retarded propagator is

$$\frac{1}{\not{P} - m + i\epsilon} - \frac{1}{\not{P} - m + i\not{\epsilon}} = -i\rho^{(-)}. \tag{A.23}$$

By using (A.21) and (A.22), we obtain the following equation,

$$1 = \mathrm{Det}\left[I - e\not{A}\frac{1}{\not{P} - m + i\epsilon}\right] \mathrm{Det}\left[I - i\mathcal{T}(A)\rho^{(-)}\right]. \tag{A.24}$$

Since the first determinant corresponds to S_0, we can derive the following equation from (A.24),

$$\begin{aligned}
[S_0(A)]^{-1} &= \mathrm{Det}\left[I - i\mathcal{T}(A)\rho^{(-)}\right], \\
|S_0(A)|^{-2} &= \exp\left\{\mathrm{Tr}\ \ln\left[I - \mathcal{T}(A)\rho^{(+)}\bar{\mathcal{T}}(A)\rho^{(-)}\right]\right\}.
\end{aligned} \tag{A.25}$$

The bracket in the exponential is defined as,

$$\Gamma(x) = \mathrm{tr}\langle x|\ \ln\left[I - \mathcal{T}(A)\rho^{(+)}\bar{T}(A)\rho^{(-)}\right]|x\rangle. \tag{A.26}$$

$\Gamma(x)$ is the probability density of the electron positron pair. Thus, the relation between S_0 and $\Gamma(x)$ is

$$|S_0(A)|^2 = \exp\left[-\int d^4x\ \Gamma(x)\right]. \tag{A.27}$$

Let us evaluate the probability density of the the electron positron pair $\Gamma(x)$. If we remember (A.10), we obtain the following equation,

$$\ln\ S_0(A) = \mathrm{Tr}\ \ln\left\{[\not{P} - e\not{A}(X) - m + i\epsilon]\frac{1}{\not{P} - m + i\epsilon}\right\}. \tag{A.28}$$

Since the trace of the operator is invariant for the transposition, we take the charge conjugation,

$$C\gamma C^{-1} = -\gamma_\mu^T, \tag{A.29}$$

and (A.28) changes to the following,

$$\ln\ S_0(A) = \mathrm{Tr}\ \ln\left\{[\not{P} - e\not{A}(X) + m - i\epsilon]\frac{1}{\not{P} + m - i\epsilon}\right\}. \tag{A.30}$$

By using (A.28) and (A.30), we obtain

$$2\ \ln\ S_0(A) = \mathrm{Tr}\ \ln\left(\left\{[\not{P} - e\not{A}(X)]^2 - m^2 + i\epsilon\right\}\frac{1}{P^2 - m^2 + i\epsilon}\right). \tag{A.31}$$

Now, we introduce Schwinger parameter formula,

$$\ln \frac{a}{b} = \mathrm{Re} \int_0^\infty \frac{ds}{s}(e^{is(b+i\epsilon)} - e^{is(a+i\epsilon)}). \tag{A.32}$$

In order to be good to converge the integral, we use the $i\epsilon$-prescription and the divergence at $s = 0$ is neglected. Thus, we derive the following creation rate from the Schwinger parameter formula,

$$\begin{aligned}
\Gamma(x) &= \mathrm{Re} \int_0^\infty \frac{ds}{s} e^{-is(m^2-i\epsilon)} \mathrm{tr} \left(\langle x| \exp\left\{ is \left(\not{P} - e\not{A}(x) \right)^2 \right\} |x\rangle - \langle x| e^{isP^2} |x\rangle \right) \\
&= \mathrm{Re} \int_0^\infty \frac{ds}{s} e^{-is(m^2-i\epsilon)} \\
&\qquad \times \langle x| \left(\exp\left\{ is \left[(P - eA(x))^2 + \frac{e}{2}\sigma_{\mu\nu} F^{\mu\nu}(x) \right] \right\} - e^{isP^2} \right) |x\rangle.
\end{aligned} \tag{A.33}$$

If we consider the constant electromagnetic fields, the creation rate $\Gamma(x)$ doesn't depend on x. To simplify this, we treat the constant purely electric field which is $A^3(x) = -Et, (t = x^0)$ in z-direction. Then,

$$\mathrm{tr}\ e^{ise\sigma_{\mu\nu}F^{\mu\nu}/2} = 4\cosh(seE). \tag{A.34}$$

Also, with $[X_0, P_0] = -i$,

$$\begin{aligned}
(P - eA)^2 &= P_0^2 - \boldsymbol{P}_T^2 (P^3 + eEX^0)^2 \\
&= e^{-iP^0P^3/eE} \left\{ P_0^2 - \boldsymbol{P}_T^2 - e^2E^2(X^0)^2 \right\} e^{iP^0P^3/eE},
\end{aligned} \tag{A.35}$$

where we use the Baker-Campbell-Hausdorff formula,

$$e^A B e^{-A} = B + [A, B] + \frac{1}{2!}[A, [A, B]] + \cdots . \tag{A.36}$$

$\boldsymbol{P}_T$ is the transverse momentum for the z-direction. When we integral the part of (A.33), we obtain

$$\begin{aligned}
&\mathrm{tr} \langle x| e^{is[(P-eA)^2 + e\sigma_{\mu\nu}F^{\mu\nu}/2]} |x\rangle \\
&\quad = 4\cosh(seE) \int \frac{d^3p}{(2\pi)^4} d\omega d\omega'\ e^{i(\omega'-\omega)(t+p^3/eE) - isp_T^2} \langle \omega| e^{is(P_0^2 - e^2E^2X_0^2)} |\omega'\rangle \\
&\quad = \frac{2eE}{(2\pi)^2 is} \cosh(seE) \int_{-\infty}^{\infty} d\omega\ \langle \omega| e^{is(P_0^2 - e^2E^2X_0^2)} |\omega\rangle.
\end{aligned} \tag{A.37}$$

The integral in (A.37) means the integral of the trace for the time-evolution operator of the harmonic oscillators. When we replace $P_0 \to P$, $X_0 \to Q$, $2ieE \to \omega_0$ and $1/2 \to m_0$ respectively, we obtain

$$\begin{aligned} \mathrm{Tr}\ \exp\left[is\left(\frac{P^2}{2m_0}+\frac{m_0\omega_0^2}{2}Q^2\right)\right] &= \sum_{n=0}^{\infty}\exp\left[is\left(n+\frac{1}{2}\right)\omega_0\right] \\ &= \frac{i}{2\sin(s\omega_0/2)}. \end{aligned} \tag{A.38}$$

Thus, the *omega*-integral is evaluated by

$$\int_{-\infty}^{\infty} d\omega\ \langle\omega|e^{is(P_0^2-e^2E^2X_0^2)}|\omega\rangle = \frac{1}{2\sinh(seE)}. \tag{A.39}$$

Therefore, the creation rate of the electron positron pair becomes

$$\Gamma = -\frac{1}{(2\pi)^2}\int_0^{\infty}\frac{ds}{s^2}\left[eE\coth(seE)-\frac{1}{s}\right]\mathrm{Re}(ie^{-is(m^2-i\epsilon)}). \tag{A.40}$$

The $1/s$ term coincides with the case of $e=0$ in (A.33). The convergence of the s-integral is discussed by the Euler-Heisenberg Lagrangian in the subsection 3.1.

Next, let us derive the effective Lagrangian called by the Euler-Heisenberg Lagrangian from the creation rate of the electron positron pair. The Lagrangian which receives the quantum corrections can be written as,

$$\begin{aligned} \mathcal{L}_{\mathrm{eff}}^{\mathrm{QED}} &= \mathcal{L}_0 + \delta\mathcal{L}, \\ \mathcal{L}_0 &= -\frac{1}{4}F_{\mu\nu}F^{\mu\nu} = \frac{1}{2}(\boldsymbol{E}^2-\boldsymbol{B}^2), \\ \delta\mathcal{L} &\equiv \delta\mathcal{L}[(\boldsymbol{E}^2-\boldsymbol{B}^2),(\boldsymbol{E}\cdot\boldsymbol{B})^2]. \end{aligned} \tag{A.41}$$

$\delta\mathcal{L}$ means that the Lagrangian has the quantum correction. Since a Lagrangian is Lorentz invariant, the Lagrangian depends on $\boldsymbol{E}^2-\boldsymbol{B}^2$ and $(\boldsymbol{E}\cdot\boldsymbol{B})^2$. The vacuum decay amplitude and the quantum Lagrangian are associated with

$$\langle 0|S|0\rangle = S_0(A) = \exp\left[i\int d^4x\,\delta\mathcal{L}\right]. \tag{A.42}$$

Thus, we derive the following relation between the creation rate of the electron positron pair and the quantum Lagrangian from the above expression and (A.27),

$$\Gamma = \int d^3x\ 2\mathrm{Im}\,\delta\mathcal{L}. \tag{A.43}$$

Therefore, the quantum Lagrangian in the constant electric field is evaluated by

$$\delta\mathcal{L}(E) = \frac{1}{8\pi^2}\int_0^\infty \frac{ds}{s^2}\left[eE\coth(seE) - \frac{1}{s}\right] e^{-is(m^2-i\epsilon)} \ . \tag{A.44}$$

The quantum Lagrangian coincides with the second term in (3.8). On the other hands, in the case of the full electromagnetic fields, the quantum Euler-Heisenberg Lagrangian is obtained by

$$\delta\mathcal{L} = \frac{1}{8\pi^2}\int_0^\infty \frac{ds}{s}e^{-ism^2}\left[e^2ab\frac{\cosh(eas)\cos(ebs)}{\sinh(eas)\sin(ebs)} - \frac{1}{s^2}\right], \tag{A.45}$$

where a and b are defined as $a^2 - b^2 \equiv \boldsymbol{E}^2 - \boldsymbol{B}^2$, $ab \equiv \boldsymbol{E}\cdot\boldsymbol{B}$. $\boldsymbol{E}$ and $\boldsymbol{B}$ are respectively constant electric fields and constant magnetic fields. The quantum Lagrangian in the full constant electromagnetic fields coincides with the second term in (3.7).

In the QED, we obtain the Euler-Heisenberg Lagrangian which is the 1-loop electron positron pair effective Lagrangian. The creation rate of the electron positron pair is derived from the imaginary part of the Euler-Heisenberg Lagrangian.

References

[1] J. S. Schwinger, "On gauge invariance and vacuum polarization," Phys. Rev. **82**, 664 (1951).

[2] W. Heisenberg and H. Euler, "Consequences of Dirac's theory of positrons," Z. Phys. **98**, 714 (1936)

[3] V. Weisskipf, "The electrodynamics of the vacuum based on the quantum theory of the electron, "Kong. Dans. Vid. Selsk. Math-fys. Medd. XIV No. 6 (1936); English translation in: Early Quantum Electrodynamics: A Source Book, A. I. Miller, (Cambridge University Press, 1994). (1936).

[4] G. V. Dunne, "Heisenberg-Euler effective Lagrangians: Basics and extensions," In *Shifman, M. (ed.) et al.: From fields to strings, vol. 1* 445-522 [hep-th/0406216].

[5] Y. Hidaka, T. Iritani and H. Suganuma, "Fast Vacuum Decay into Quark Pairs in Strong Color Electric and Magnetic Fields," AIP Conf. Proc. **1388**, 516 (2011) [arXiv:1103.3097 [hep-ph]].

[6] Y. Hidaka, T. Iritani and H. Suganuma, "Fast vacuum decay into particle pairs in strong electric and magnetic fields," arXiv:1102.0050 [hep-ph].

[7] I. K. Affleck, O. Alvarez and N. S. Manton, "Pair Production at Strong Coupling in Weak External Fields," Nucl. Phys. B **197**, 509 (1982).

[8] J. M. Maldacena, "The Large N limit of superconformal field theories and supergravity," Adv. Theor. Math. Phys. **2**, 231 (1998) [hep-th/9711200].

[9] S. S. Gubser, I. R. Klebanov and A. M. Polyakov, "Gauge theory correlators from noncritical string theory," Phys. Lett. B **428**, 105 (1998) [hep-th/9802109].

[10] E. Witten, "Anti-de Sitter space and holography," Adv. Theor. Math. Phys. **2**, 253 (1998) [hep-th/9802150].

[11] J. Polchinski, Nucl. Phys. B **303**, 226 (1988).

[12] A. Karch and E. Katz, "Adding flavor to AdS / CFT," JHEP **0206**, 043 (2002) [hep-th/0205236].

[13] E. Witten, "Anti-de Sitter space, thermal phase transition, and confinement in gauge theories," Adv. Theor. Math. Phys. **2**, 505 (1998) [hep-th/9803131].

[14] T. Sakai and S. Sugimoto, "Low energy hadron physics in holographic QCD," Prog. Theor. Phys. **113**, 843 (2005) [hep-th/0412141].

[15] O. Aharony, J. Sonnenschein and S. Yankielowicz, "A Holographic model of deconfinement and chiral symmetry restoration," Annals Phys. **322** (2007) 1420 [hep-th/0604161].

[16] K. Hashimoto and T. Oka, "Vacuum Instability in Electric Fields via AdS/CFT: Euler-Heisenberg Lagrangian and Planckian Thermalization," JHEP **1310**, 116 (2013) [arXiv:1307.7423].

[17] K. Hashimoto, T. Oka and A. Sonoda, "Magnetic instability in AdS/CFT: Schwinger effect and Euler-Heisenberg Lagrangian of supersymmetric QCD," JHEP **1406**, 085 (2014) [arXiv:1403.6336 [hep-th]].

[18] K. Hashimoto, T. Oka and A. Sonoda, "Electromagnetic instability in holographic QCD," JHEP **1506**, 001 (2015) [arXiv:1412.4254 [hep-th]].

[19] A. S. Gorsky, K. A. Saraikin and K. G. Selivanov, "Schwinger type processes via branes and their gravity duals," Nucl. Phys. B **628** (2002) 270 [hep-th/0110178].

[20] G. W. Semenoff and K. Zarembo, "Holographic Schwinger Effect," Phys. Rev. Lett. **107** (2011) 171601 [arXiv:1109.2920 [hep-th]].

[21] J. Ambjorn and Y. Makeenko, "Remarks on Holographic Wilson Loops and the Schwinger Effect," Phys. Rev. D **85**, 061901 (2012) [arXiv:1112.5606 [hep-th]].

[22] S. Bolognesi, F. Kiefer and E. Rabinovici, "Comments on Critical Electric and Magnetic Fields from Holography," JHEP **1301**, 174 (2013) [arXiv:1210.4170 [hep-th]].

[23] Y. Sato and K. Yoshida, "Holographic description of the Schwinger effect in electric and magnetic fields," JHEP **1304**, 111 (2013) [arXiv:1303.0112 [hep-th]].

[24] Y. Sato and K. Yoshida, "Potential Analysis in Holographic Schwinger Effect," JHEP **1308**, 002 (2013) [arXiv:1304.7917, arXiv:1304.7917 [hep-th]].

[25] Y. Sato and K. Yoshida, "Holographic Schwinger effect in confining phase," JHEP **1309**, 134 (2013) [arXiv:1306.5512 [hep-th]].

[26] Y. Sato and K. Yoshida, "Universal aspects of holographic Schwinger effect in general backgrounds," JHEP **1312**, 051 (2013) [arXiv:1309.4629 [hep-th]].

[27] D. Kawai, Y. Sato and K. Yoshida, "The Schwinger pair production rate in confining theories via holography," arXiv:1312.4341 [hep-th].

[28] M. Sakaguchi, H. Shin and K. Yoshida, "No pair production of open strings in a plane-wave background," arXiv:1402.2048 [hep-th].

[29] P. Bizon and A. Rostworowski, "On weakly turbulent instability of anti-de Sitter space," Phys. Rev. Lett. **107**, 031102 (2011) [arXiv:1104.3702 [gr-qc]].

[30] H. P. de Oliveira, L. A. Pando Zayas and E. L. Rodrigues, "A Kolmogorov-Zakharov Spectrum in AdS Gravitational Collapse," Phys. Rev. Lett. **111**, no. 5, 051101 (2013) [arXiv:1209.2369 [hep-th]].

[31] S. L. Liebling, "Nonlinear collapse in the semilinear wave equation in AdS space," Phys. Rev. D **87**, no. 8, 081501 (2013) [arXiv:1212.6970 [gr-qc]].

[32] O. J. C. Dias, G. T. Horowitz, D. Marolf and J. E. Santos, "On the Nonlinear Stability of Asymptotically Anti-de Sitter Solutions," Class. Quant. Grav. **29**, 235019 (2012) [arXiv:1208.5772 [gr-qc]].

[33] M. Maliborski, "Instability of Flat Space Enclosed in a Cavity," Phys. Rev. Lett. **109**, 221101 (2012) [arXiv:1208.2934 [gr-qc]].

[34] A. Buchel, L. Lehner and S. L. Liebling, "Scalar Collapse in AdS," Phys. Rev. D **86**, 123011 (2012) [arXiv:1210.0890 [gr-qc]].

[35] A. Buchel, S. L. Liebling and L. Lehner, "Boson stars in AdS spacetime," Phys. Rev. D **87**, no. 12, 123006 (2013) [arXiv:1304.4166 [gr-qc]].

[36] P. Bizo, "Is AdS stable?," Gen. Rel. Grav. **46**, no. 5, 1724 (2014) [arXiv:1312.5544 [gr-qc]].

[37] M. Maliborski and A. Rostworowski, "Lecture Notes on Turbulent Instability of Anti-de Sitter Spacetime," Int. J. Mod. Phys. A **28**, 1340020 (2013) [arXiv:1308.1235 [gr-qc]].

[38] M. Maliborski and A. Rostworowski, "Time-Periodic Solutions in an Einstein AdS?Massless-Scalar-Field System," Phys. Rev. Lett. **111**, 051102 (2013) [arXiv:1303.3186 [gr-qc]].

[39] V. Balasubramanian, A. Buchel, S. R. Green, L. Lehner and S. L. Liebling, "Holographic Thermalization, Stability of Anti?de Sitter Space, and the Fermi-Pasta-Ulam Paradox," Phys. Rev. Lett. **113**, no. 7, 071601 (2014) [arXiv:1403.6471 [hep-th]].

[40] M. Maliborski and A. Rostworowski, "What drives AdS spacetime unstable?," Phys. Rev. D **89**, no. 12, 124006 (2014) [arXiv:1403.5434 [gr-qc]].

[41] B. Craps, O. Evnin and J. Vanhoof, "Renormalization group, secular term resummation and AdS (in)stability," JHEP **1410**, 48 (2014) [arXiv:1407.6273 [gr-qc]].

[42] G. T. Horowitz and J. E. Santos, "Geons and the Instability of Anti-de Sitter Spacetime," arXiv:1408.5906 [gr-qc].

[43] O. J. C. Dias, G. T. Horowitz and J. E. Santos, "Gravitational Turbulent Instability of Anti-de Sitter Space," Class. Quant. Grav. **29**, 194002 (2012) [arXiv:1109.1825 [hep-th]].

[44] F. V. Dimitrakopoulos, B. Freivogel, M. Lippert and I. S. Yang, "Instability corners in AdS space," arXiv:1410.1880 [hep-th].

[45] E. Caceres, A. Kundu, J. F. Pedraza and D. L. Yang, "Weak Field Collapse in AdS: Introducing a Charge Density," arXiv:1411.1744 [hep-th].

[46] B. Craps, O. Evnin and J. Vanhoof, "Renormalization, averaging, conservation laws and AdS (in)stability," JHEP **1501**, 108 (2015) [arXiv:1412.3249 [gr-qc]].

[47] A. Buchel, S. R. Green, L. Lehner and S. L. Liebling, "Conserved quantities and dual turbulent cascades in anti?de Sitter spacetime," Phys. Rev. D **91**, no. 6, 064026 (2015) [arXiv:1412.4761 [gr-qc]].

[48] O. J. C. Dias, G. T. Horowitz and J. E. Santos, "Gravitational Turbulent Instability of Anti-de Sitter Space," Class. Quant. Grav. **29** (2012) 194002 [arXiv:1109.1825 [hep-th]].

[49] M. P. Heller, R. A. Janik and P. Witaszczyk, "A numerical relativity approach to the initial value problem in asymptotically Anti-de Sitter spacetime for plasma thermalization - an ADM formulation," Phys. Rev. D **85** (2012) 126002 [arXiv:1203.0755 [hep-th]].

[50] O. J. C. Dias, G. T. Horowitz, D. Marolf and J. E. Santos, "On the Nonlinear Stability of Asymptotically Anti-de Sitter Solutions," Class. Quant. Grav. **29** (2012) 235019 [arXiv:1208.5772 [gr-qc]].

[51] D. Garfinkle, L. A. Pando Zayas and D. Reichmann, "On Field Theory Thermalization from Gravitational Collapse," JHEP **1202** (2012) 119 [arXiv:1110.5823 [hep-th]].

[52] M. P. Heller, D. Mateos, W. van der Schee and D. Trancanelli, Phys. Rev. Lett. **108** (2012) 191601 [arXiv:1202.0981 [hep-th]].

[53] S. W. Hawking, "Information Preservation and Weather Forecasting for Black Holes," arXiv:1401.5761 [hep-th].

[54] A. Buchel, S. L. Liebling and L. Lehner, "Boson stars in AdS spacetime," Phys. Rev. D **87** (2013) 12, 123006 [arXiv:1304.4166 [gr-qc]].

[55] H. Bantilan, F. Pretorius and S. S. Gubser, "Simulation of Asymptotically AdS5 Spacetimes with a Generalized Harmonic Evolution Scheme," Phys. Rev. D **85** (2012) 084038 [arXiv:1201.2132 [hep-th]].

[56] V. Cardoso, L. Gualtieri, C. Herdeiro, U. Sperhake, P. M. Chesler, L. Lehner, S. C. Park and H. S. Reall *et al.*, "NR/HEP: roadmap for the future," Class. Quant. Grav. **29** (2012) 244001 [arXiv:1201.5118 [hep-th]].

[57] J. Jalmuzna, A. Rostworowski and P. Bizon, "A Comment on AdS collapse of a scalar field in higher dimensions," Phys. Rev. D **84** (2011) 085021 [arXiv:1108.4539 [gr-qc]].

[58] M. J. Bhaseen, J. P. Gauntlett, B. D. Simons, J. Sonner and T. Wiseman, "Holographic Superfluids and the Dynamics of Symmetry Breaking," Phys. Rev. Lett. **110** (2013) 1, 015301 [arXiv:1207.4194 [hep-th]].

[59] S. L. Liebling and C. Palenzuela, "Dynamical Boson Stars," Living Rev. Rel. **15** (2012) 6 [arXiv:1202.5809 [gr-qc]].

[60] J. Garcia-Bellido, J. Rubio, M. Shaposhnikov and D. Zenhausern, "Higgs-Dilaton Cosmology: From the Early to the Late Universe," Phys. Rev. D **84** (2011) 123504 [arXiv:1107.2163 [hep-ph]].

[61] M. Maliborski and A. Rostworowski, "Time-Periodic Solutions in an Einstein AdS?Massless-Scalar-Field System," Phys. Rev. Lett. **111** (2013) 051102 [arXiv:1303.3186 [gr-qc]].

[62] A. Buchel, L. Lehner and S. L. Liebling, "Scalar Collapse in AdS," Phys. Rev. D **86** (2012) 123011 [arXiv:1210.0890 [gr-qc]].

[63] H. K. Kunduri and J. Lucietti, "Classification of near-horizon geometries of extremal black holes," Living Rev. Rel. **16** (2013) 8 [arXiv:1306.2517 [hep-th]].

[64] B. Wu, "On holographic thermalization and gravitational collapse of massless scalar fields," JHEP **1210** (2012) 133 [arXiv:1208.1393 [hep-th]].

[65] K. Hashimoto, S. Kinoshita, K. Murata and T. Oka, "Turbulent meson condensation in quark deconfinement," arXiv:1408.6293 [hep-th].

[66] K. Hashimoto, S. Kinoshita, K. Murata and T. Oka, "Meson turbulence at quark deconfinement from AdS/CFT," arXiv:1412.4964 [hep-th].

[67] K. Hashimoto, M. Nishida and A. Sonoda, "Universal Turbulence on Branes in Holography," JHEP **1508**, 135 (2015) doi:10.1007/JHEP08(2015)135 [arXiv:1504.07836 [hep-th]].

[68] J. Erdmenger, N. Evans, I. Kirsch and E. Threlfall, "Mesons in Gauge/Gravity Duals - A Review," Eur. Phys. J. A **35**, 81 (2008) [arXiv:0711.4467 [hep-th]].

[69] M. Kruczenski, D. Mateos, R. C. Myers and D. J. Winters, "Meson spectroscopy in AdS / CFT with flavor," JHEP **0307**, 049 (2003) [hep-th/0304032].

[70] J. Erdmenger, R. Meyer and J. P. Shock, "AdS/CFT with flavour in electric and magnetic Kalb-Ramond fields," JHEP **0712**, 091 (2007) [arXiv:0709.1551 [hep-th]].

[71] D. Mateos, R. C. Myers and R. M. Thomson, "Holographic phase transitions with fundamental matter," Phys. Rev. Lett. **97**, 091601 (2006) [hep-th/0605046].

[72] R. C. Myers and R. M. Thomson, "Holographic mesons in various dimensions," JHEP **0609**, 066 (2006) [hep-th/0605017].

[73] D. Mateos, R. C. Myers and R. M. Thomson, "Thermodynamics of the brane," JHEP **0705**, 067 (2007) [hep-th/0701132].

[74] O. Aharony, S. S. Gubser, J. M. Maldacena, H. Ooguri and Y. Oz, Phys. Rept. **323**, 183 (2000) [hep-th/9905111].

[75] C. A. Bayona and N. R. F. Braga, Gen. Rel. Grav. **39**, 1367 (2007) [hep-th/0512182].

[76] C. Itzykson and J. B. Zuber, New York, Usa: Mcgraw-hill (1980) 705 P.(International Series In Pure and Applied Physics)

[77] G. 't Hooft, Nucl. Phys. B **72**, 461 (1974). doi:10.1016/0550-3213(74)90154-0

[78] N. Tanji, "Dynamical view of pair creation in uniform electric and magnetic fields," Annals Phys. **324**, 1691 (2009) [arXiv:0810.4429 [hep-ph]].

[79] A. Karch and A. O'Bannon, "Holographic thermodynamics at finite baryon density: Some exact results," JHEP **0711**, 074 (2007) [arXiv:0709.0570 [hep-th]].

[80] S. Coleman, Cambridge University Press